STEFANO
CURTAROLO

LATTICE THINGS

- DIRECT
- RECIPROCAL

NEED AM BOOK!

LATTICE

chap 4, 7 A/M read

PERIODICITY

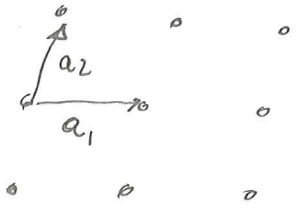

a) BRAVAIS LATTICE
infinite array of discrete points, exact images.
translated with a BRAVAIS LATICE

b) $\bar{R} = n_1 \bar{a}_1 + n_2 \bar{a}_2 + n_3 \bar{a}_3$

primitive vectors

PRIMITIVE UNIT CELL ⇓ CONTAINS 1 POINT

Linear combinations of $\bar{a}_1, \bar{a}_2, \bar{a}_3 \Rightarrow$ other primitive vectors

CUBIC, a

BCC = $a_1 = a\hat{x}$ $\bar{a}_2 = a\hat{y}$ $\bar{a}_3 = \frac{a}{2}(\hat{x}+\hat{y}+\hat{z})$

$\bar{a}_1 = \frac{a}{2}(-\hat{x}+\hat{y}+\hat{z})$ $\bar{a}_2 = \frac{a}{2}(\hat{x}-\hat{y}+\hat{z})$ $\bar{a}_3 = \frac{a}{2}(\hat{x}+\hat{y}-\hat{z})$

FCC $a_1 = \frac{a}{2}(\hat{y}+\hat{z})$ $a_2 = \frac{a}{2}(\hat{x}+\hat{z})$ $a_3 = \frac{a}{2}(\hat{x}+\hat{y})$

COORDINATION NUMBER # nearest neighbours

CUB = 6
BCC = 8
FCC = 12

PRIMITIVE & CONVENTIONAL

WIGNER & SEITZ — CONNECT TO NEIGHBOURS
— DRAW ⊥ PLANE IN MEDIAN POINT

CRYSTAL WITH BASIS:

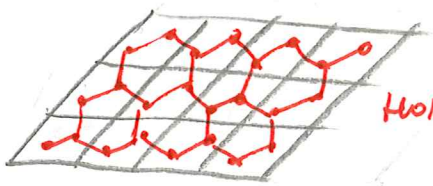

HONEY COMB

BCC CUBIC +
$0, -\frac{a}{2}(\hat{x}+\hat{y}+\hat{z})$

FCC
0 $\frac{a}{2}(\hat{x}+\hat{y})$ $\frac{a}{2}(\hat{y}+\hat{z})$ $\frac{a}{2}(\hat{z}+\hat{x})$

DIAMOND

HEXAGONAL c $c = \sqrt{\frac{8}{3}}a = 1.63\,a$

DIRECTIONS
[100]

RECIPROCAL.

chap 5 / 6

VON LAUE construction

DIFFRACTION

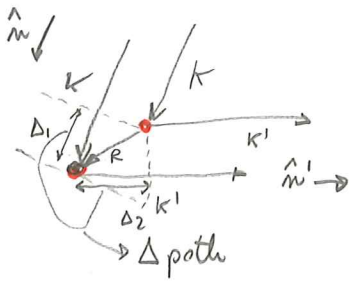

K = incident wave
K' = diffracted
do they interfere CONSTRUCTIVELY ?
if Δ path ~ m λ

Δ_1 = projection R over K ⇒ $\frac{\bar{R}\cdot\bar{K}}{|K|}$ R

Δ_2 = projection R over K' ⇒ $-\frac{\bar{R}\cdot\bar{K}'}{|K'|} =$

↑ because it is in the opposite direction

$$\Delta = \frac{\bar{R}\cdot(K-K')}{|K|} = m\lambda \qquad \text{but } K = \frac{2\pi}{\lambda}$$

$$\Rightarrow \boxed{\bar{R}\cdot(\bar{K}-\bar{K}') = 2\pi m}$$

$$\bar{R}\cdot\Delta\bar{K} = 2\pi m \Rightarrow \boxed{e^{i\bar{R}\cdot\Delta\bar{K}} = 1}$$

if $\bar{R} = n_1\bar{a}_1 + n_2\bar{a}_2 + n_3\bar{a}_3$ (integers)

$\Rightarrow \bar{K} \in \{\bar{G}\} = k_1\bar{b}_1 + k_2\bar{b}_2 + k_3\bar{b}_3$ RECIPROCAL

$$\boxed{b_i = \frac{2\pi\, a_j \times a_k}{a_1\cdot(a_2\times a_3)}} = \det\begin{pmatrix}\vec{a_1}\\ a_2\\ a_3\end{pmatrix} = \text{Volume PRIMITIVE CELL}$$

— $\bar{b}_i \cdot \bar{a}_j = \delta_{ij}$

— $\bar{K}\cdot\bar{R} = 2\pi(k_1n_1 + k_2n_2 + k_3n_3)$ ⇒ (integer)

$V_R = \bar{a}_1\cdot(\bar{a}_2\times\bar{a}_3)$

$V_K = \frac{(2\pi)^3}{V_R}$

Reciprocal [Reciprocal] = Identity !

R1 | WIGNER SEITZ OF RECIPROCAL is BRILLOUIN ZONE

MILLER INDICES (h, k, ℓ)

Plane with Miller indices (h, k, ℓ) is $\perp$ to Reciprocal vector $(h\bar{b}_1 + k\bar{b}_2 + \ell\bar{b}_3)$

but where.

Miller: set of INTEGERS with NO COMMON FACTOR (?) inversely proportional to intercepts of crystal plane along crystal axes. $(h; k; \ell) = \frac{1}{\tau_1} : \frac{1}{\tau_2} : \frac{1}{\tau_3}$

EXAMPLES BOOK AM 93.

LAVE construction equivalent to BRAGG

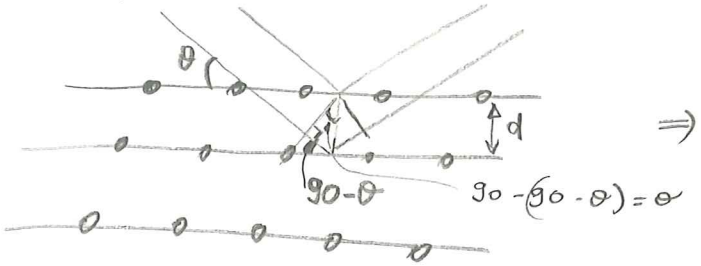

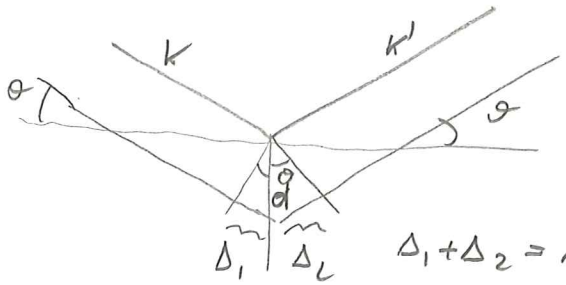

$\Delta_1 + \Delta_2 = n\lambda$

$\Rightarrow 2d \sin\theta = n\lambda$

in CUBIC depends on orientation

$$d = \frac{a}{\sqrt{h^2 + k^2 + \ell^2}}$$

in general $\frac{d(2H)^2}{d_{hkl}^2} = |\bar{g}|^2$ ↓ vector of reciprocal lattice

R2

STRUCTURE FACTOR

FOR CRYSTAL WITH n-basis

BRAGG reach is present when Δk is in reciprocal space lattice.

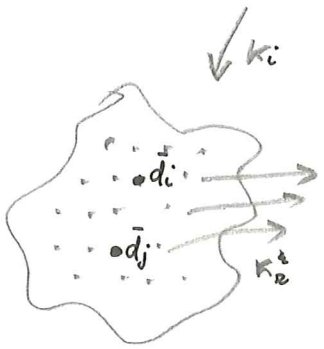

for a solid $e^{i(k'-k)\vec{R}} = 1 \quad \forall \vec{R} \in$ BRAVAIS

$k_2' - k_i = \vec{K}$ ~~$d_i - d_j$~~ distance

$\vec{K}(\vec{d}_i - \vec{d}_j)$ path difference } in phase total is $e^{i\vec{k}(d_i - d_j)}$ ⇒

⇒ each point carries a phase

point(i) ⇒ $e^{i\vec{K}\cdot\vec{d}_i}$ phase

⇒ SUM OF ALL ~~PHASES~~ will decode Amplitude diffraction

basis → $S_K = \sum_i^n e^{i\vec{k}\cdot\vec{d}_i}$ geometrical structure factor

SUM OVER BASIS ATOMS WITHIN UNIT CELLS.

$I_k \propto |S_K|^2$

~~$\vec{d}_i + \vec{R}$ and $\vec{d}_i$ are not~~ electrical

⇒ ~~$S_K =$~~

BCC ⇒ ~~Bravais~~ Reciprocal [BCC] = FCC ⇒ too pair to analiti (we want cubic)

BCC = CUBIC + 2 · base $\left[0, \frac{a}{2}(\hat{x}+\hat{y}+\hat{z})\right]$

Reciprocal [CUB] = CUB $b = \frac{a\,2\pi}{a}$ $\vec{K} = (h\hat{x}+k\hat{y}+l\hat{z})\left(\frac{2\pi}{a}\right)$

$$S_K = \left[1 + e^{i\vec{K}\cdot\frac{1}{2}a(\hat{x}+\hat{y}+\hat{z})}\right]$$

$$= \begin{cases} 2 & h+k+l = \text{even} \\ 0 & h+k+l = \text{odd} \end{cases}$$

get S Factor FOR FCC, MONO OM HEX

DIFF FROM A POLYATOMIC CRYSTAL

$$S_K = \sum_i^n f_i(\vec{k}) e^{i\vec{K}\cdot\vec{d}}$$ depends on density of electrons of atom i

then

R3

Those who have not wandered amidst the mineralogical departments of natural history museums are often surprised to learn that metals, like most other solids, are crystalline, for although one is used to the very obvious crystalline features of quartz, diamond, and rock salt, the characteristic plane faces at sharp angles with one another are absent from metals in their most commonly encountered forms. However, those metals that occur naturally in the metallic state are quite often found in crystalline forms, which are completely disguised in finished metal products by the great malleability of metals, which permits them to be fashioned into whatever macroscopic shape one wishes.

The true test of crystallinity is not the superficial appearance of a large specimen, but whether on the microscopic level the ions are arranged in a periodic array.[1] This underlying microscopic regularity of crystalline matter was long hypothesized as the obvious way to account for the simple geometric regularities of macroscopic crystals, in which plane faces make only certain definite angles with each other. It received direct experimental confirmation in 1913 through the work of W. and L. Bragg, who founded the subject of X-ray crystallography and began the investigation of how atoms are arranged in solids.

Before we describe how the microscopic structure of solids is determined by X-ray diffraction and how the periodic structures so revealed affect fundamental physical properties, it is useful to survey some of the most important geometrical properties of periodic arrays in three-dimensional space. These purely geometrical considerations are implicit in almost all the analysis one encounters throughout solid state physics, and shall be pursued in this chapter and in Chapters 5 and 7. The first of many applications of these concepts will be made to X-ray diffraction in Chapter 6.

BRAVAIS LATTICE

A fundamental concept in the description of any crystalline solid is that of the *Bravais lattice*, which specifies the periodic array in which the repeated units of the crystal are arranged. The units themselves may be single atoms, groups of atoms, molecules, ions, etc., but the Bravais lattice summarizes only the geometry of the underlying periodic structure, regardless of what the actual units may be. We give two equivalent definitions of a Bravais lattice[2]:

(a) A Bravais lattice is an infinite array of discrete points with an arrangement and orientation that appears *exactly* the same, from whichever of the points the array is viewed.

(b) A (three-dimensional) Bravais lattice consists of all points with position vectors $\mathbf{R}$ of the form

$$\mathbf{R} = n_1\mathbf{a}_1 + n_2\mathbf{a}_2 + n_3\mathbf{a}_3, \tag{4.1}$$

[1] Often a specimen is made up of many small pieces, each large on the microscopic scale and containing large numbers of periodically arranged ions. This "polycrystalline" state is more commonly encountered than a single macroscopic crystal, in which the periodicity is perfect, extending through the entire specimen.

[2] Why the name Bravais appears is explained in Chapter 7.

where $\mathbf{a}_1$, $\mathbf{a}_2$, and $\mathbf{a}_3$ are any three vectors not all in the same plane, and n_1, n_2, and n_3 range through all integral values.[3] Thus the point $\Sigma n_i \mathbf{a}_i$ is reached by moving n_i steps[4] of length a_i in the direction of $\mathbf{a}_i$ for $i = 1, 2$, and 3.

The vectors $\mathbf{a}_i$ appearing in definition (b) of a Bravais lattice are called *primitive vectors* and are said to *generate* or *span* the lattice.

It takes some thought to see that the two definitions of a Bravais lattice are equivalent. That any array satisfying (b) also satisfies (a) becomes evident as soon as both definitions are understood. The argument that *any* array satisfying definition (a) can be generated by an appropriate set of three vectors is not as obvious. The proof consists of an explicit recipe for constructing three primitive vectors. The construction is given in Problem 8a.

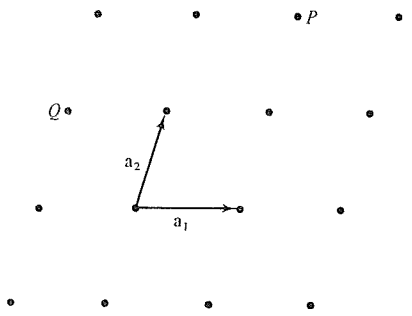

Figure 4.1
A general two-dimensional Bravais lattice of no particular symmetry: the oblique net. Primitive vectors $\mathbf{a}_1$ and $\mathbf{a}_2$ are shown. All points in the net are linear combinations of these with integral coefficients; for example, $P = \mathbf{a}_1 + 2\mathbf{a}_2$, and $Q = -\mathbf{a}_1 + \mathbf{a}_2$.

Figure 4.1 shows a portion of a two-dimensional Bravais lattice.[5] Clearly definition (a) is satisfied, and the primitive vectors $\mathbf{a}_1$ and $\mathbf{a}_2$ required by definition (b) are indicated in the figure. Figure 4.2 shows one of the most familiar of three-dimensional Bravais lattices, the simple cubic. It owes its special structure to the fact that it can be spanned by three mutually perpendicular primitive vectors of equal length.

Figure 4.2
A simple cubic three-dimensional Bravais lattice. The three primitive vectors can be taken to be mutually perpendicular, and with a common magnitude.

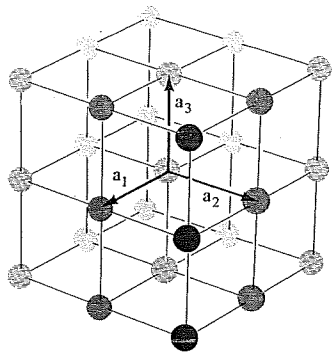

[3] We continue with the convention that "integer" means a negative integer or zero, as well as a positive integer.

[4] When n is negative, n steps in a direction means n steps in the opposite direction. The point reached does not, of course, depend on the order in which the $n_1 + n_2 + n_3$ steps are taken.

[5] A two-dimensional Bravais lattice is also known as a *net*.

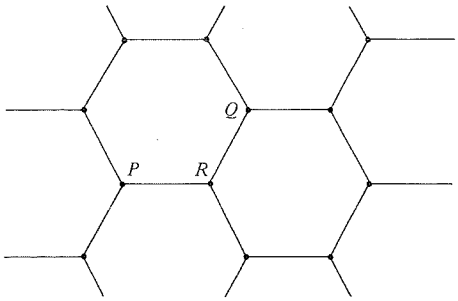

Figure 4.3
The vertices of a two-dimensional honeycomb do *not* form a Bravais lattice. The array of points has the same appearance whether viewed from point P or point Q. However, the view from point R is rotated through 180°.

It is important that not only the arrangement, but also the orientation must appear the same from every point in a Bravais lattice. Consider the vertices of a two-dimensional honeycomb (Figure 4.3). The array of points looks the same when viewed from adjacent points only if the page is rotated through 180° each time one moves from one point to the next. Structural relations are clearly identical, but *not* orientational relations, so the vertices of a honeycomb do not form a Bravais lattice. A case of more practical interest, satisfying the structural but not the orientational requirements of definition (a), is the three-dimensional hexagonal close-packed lattice, described below.

INFINITE LATTICES AND FINITE CRYSTALS

Since all points are equivalent, the Bravais lattice must be infinite in extent. Actual crystals are, of course, finite, but if they are large enough the vast majority of points will be so far from the surface as to be unaffected by its existence. The fiction of an infinite system is thus a very useful idealization. If surface effects are of interest the notion of a Bravais lattice is still relevant, but now one must think of the physical crystal as filling up only a finite portion of the ideal Bravais lattice.

Frequently one considers finite crystals, not because surface effects are important, but simply for conceptual convenience, just as in Chapter 2 we placed the electron gas in a cubical box of volume $V = L^3$. One then generally picks the finite region of the Bravais lattice to have the simplest possible form. Given three primitive vectors $\mathbf{a}_1$, $\mathbf{a}_2$, and $\mathbf{a}_3$, one usually considers the finite lattice of N sites to be the set of points of the form $\mathbf{R} = n_1\mathbf{a}_1 + n_2\mathbf{a}_2 + n_3\mathbf{a}_3$, where $0 \leqslant n_1 < N_1$, $0 \leqslant n_2 < N_2$, $0 \leqslant n_3 < N_3$, and $N = N_1N_2N_3$. This artifact is closely connected with the generalization to the description of crystalline systems[6] of the periodic boundary condition we used in Chapter 2.

FURTHER ILLUSTRATIONS AND IMPORTANT EXAMPLES

Of the two definitions of a Bravais lattice, definition (b) is mathematically more precise and is the obvious starting point for any analytic work. It has, however, two

[6] We shall make particular use of it in Chapters 8 and 22.

minor shortcomings. First, for any given Bravais lattice the set of primitive vectors is not unique—indeed, there are infinitely many nonequivalent choices (see Figure 4.4)—and it is distasteful (and sometimes misleading) to rely too heavily on a definition that emphasizes a particular choice. Second, when presented with a particular array of points one usually can tell at a glance whether the first definition is satisfied, although the existence of a set of primitive vectors or a proof that there is no such set can be rather more difficult to perceive immediately.

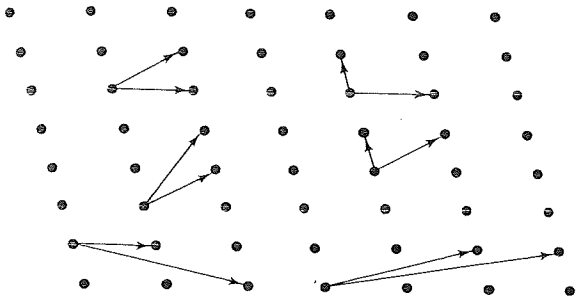

Figure 4.4
Several possible choices of pairs of primitive vectors for a two-dimensional Bravais lattice. They are drawn, for clarity, from different origins.

Consider, for example, the *body-centered cubic* (bcc) lattice, formed by adding to the simple cubic lattice of Figure 4.2 (whose sites we now label A) an additional point, B, at the center of each little cube (Figure 4.5). One might at first feel that the center points B bear a different relation to the whole than the corner points A. However, the center point B can be thought of as corner points of a second simple cubic array.

Figure 4.5
A few sites from a body-centered cubic Bravais lattice. Note that it can be regarded either as a simple cubic lattice formed from the points A with the points B at the cube centers, or as a simple cubic lattice formed from the points B with the points A at the cube centers. This observation establishes that it is indeed a Bravais lattice.

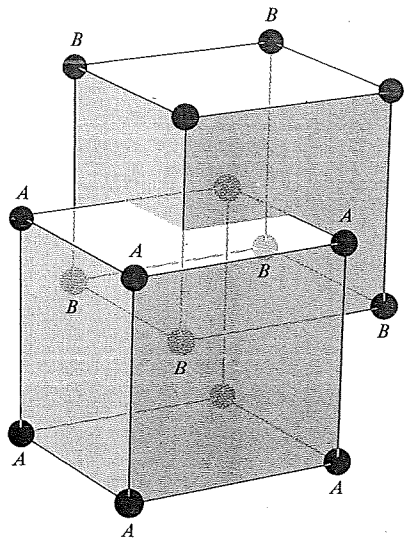

In this new array the corner points A of the original cubic array are center points. Thus all points do have identical surroundings, and the body-centered cubic lattice is a Bravais lattice. If the original simple cubic lattice is generated by primitive vectors

$$a\hat{\mathbf{x}}, \quad a\hat{\mathbf{y}}, \quad a\hat{\mathbf{z}}, \tag{4.2}$$

where $\hat{\mathbf{x}}$, $\hat{\mathbf{y}}$, and $\hat{\mathbf{z}}$ are three orthogonal unit vectors, then a set of primitive vectors for the body-centered cubic lattice could be (Figure 4.6)

$$\mathbf{a}_1 = a\hat{\mathbf{x}}, \quad \mathbf{a}_2 = a\hat{\mathbf{y}}, \quad \mathbf{a}_3 = \frac{a}{2}(\hat{\mathbf{x}} + \hat{\mathbf{y}} + \hat{\mathbf{z}}). \tag{4.3}$$

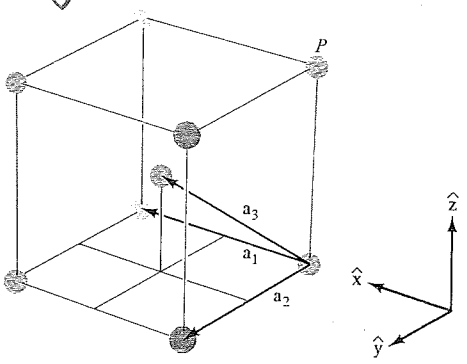

Figure 4.6
Three primitive vectors, specified in Eq. (4.3), for the body-centered cubic Bravais lattice. The lattice is formed by taking all linear combinations of the primitive vectors with integral coefficients. The point P, for example, is $P = -\mathbf{a}_1 - \mathbf{a}_2 + 2\mathbf{a}_3$.

A more symmetric set (see Figure 4.7) is

$$\mathbf{a}_1 = \frac{a}{2}(\hat{\mathbf{y}} + \hat{\mathbf{z}} - \hat{\mathbf{x}}), \quad \mathbf{a}_2 = \frac{a}{2}(\hat{\mathbf{z}} + \hat{\mathbf{x}} - \hat{\mathbf{y}}), \quad \mathbf{a}_3 = \frac{a}{2}(\hat{\mathbf{x}} + \hat{\mathbf{y}} - \hat{\mathbf{z}}). \tag{4.4}$$

It is important to convince oneself both geometrically and analytically that these sets do indeed generate the bcc Bravais lattice.

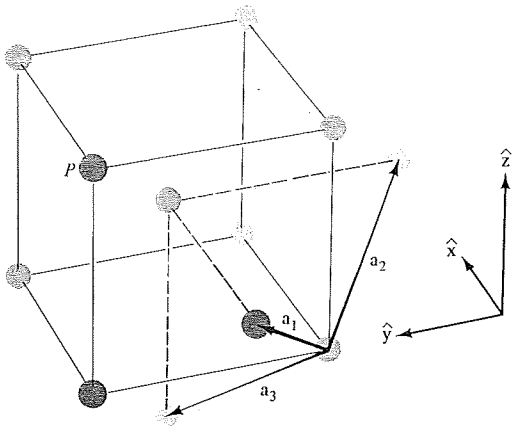

Figure 4.7
A more symmetric set of primitive vectors, specified in Eq. (4.4), for the body-centered cubic Bravais lattice. The point P, for example, has the form $P = 2\mathbf{a}_1 + \mathbf{a}_2 + \mathbf{a}_3$.

Another equally important example is the *face-centered cubic* (fcc) Bravais lattice. To construct the face-centered cubic Bravais lattice add to the simple cubic lattice of Figure 4.2 an additional point in the center of each square face (Figure 4.8). For ease in description think of each cube in the simple cubic lattice as having horizontal bottom and top faces, and four vertical side faces facing north, south, east, and west. It may sound as if all points in this new array are not equivalent, but in fact they are. One can, for example, consider the *new* simple cubic lattice formed by the points added

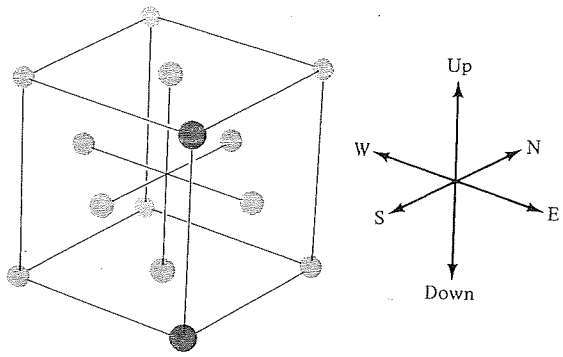

Figure 4.8
Some points from a face-centered cubic Bravais lattice.

to the centers of all the horizontal faces. The original simple cubic lattice points are now centering points on the horizontal faces of the new simple cubic lattice, whereas the points that were added to the centers of the north-south faces of the original cubic lattice are in the centers of the east-west faces of the new one, and vice versa.

In the same way one can also regard the simple cubic lattice as being composed of all points centering the north-south faces of the original simple cubic lattice, or all points centering the east-west faces of the original cubic lattice. In either case the remaining points will be found centered on the faces of the new simple cubic framework. Thus any point can be thought of either as a corner point or as a face-centering point for any of the three kinds of faces, and the face-centered cubic lattice is indeed a Bravais lattice.

A symmetric set of primitive vectors for the face-centered cubic lattice (see Figure 4.9) is

$$\mathbf{a}_1 = \frac{a}{2}(\hat{\mathbf{y}} + \hat{\mathbf{z}}), \quad \mathbf{a}_2 = \frac{a}{2}(\hat{\mathbf{z}} + \hat{\mathbf{x}}), \quad \mathbf{a}_3 = \frac{a}{2}(\hat{\mathbf{x}} + \hat{\mathbf{y}}). \tag{4.5}$$

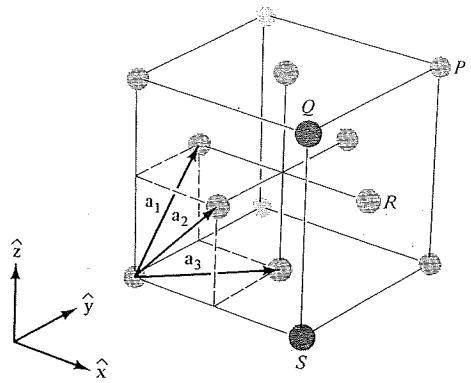

Figure 4.9
A set of primitive vectors, as given in Eq. (4.5), for the face-centered cubic Bravais lattice. The labeled points are $P = \mathbf{a}_1 + \mathbf{a}_2 + \mathbf{a}_3$, $Q = 2\mathbf{a}_2$, $R = \mathbf{a}_2 + \mathbf{a}_3$, and $S = -\mathbf{a}_1 + \mathbf{a}_2 + \mathbf{a}_3$.

The face-centered cubic and body-centered cubic Bravais lattices are of great importance, since an enormous variety of solids crystallize in these forms with an atom (or ion) at each lattice site (see Tables 4.1 and 4.2). (The corresponding simple cubic form, however, is very rare, the alpha phase of polonium being the only known example among the elements under normal conditions.)

Table 4.1
ELEMENTS WITH THE MONATOMIC FACE-CENTERED CUBIC CRYSTAL STRUCTURE

ELEMENT	a (Å)	ELEMENT	a (Å)	ELEMENT	a (Å)
Ar	5.26 (4.2 K)	Ir	3.84	Pt	3.92
Ag	4.09	Kr	5.72 (58 K)	δ-Pu	4.64
Al	4.05	La	5.30	Rh	3.80
Au	4.08	Ne	4.43 (4.2 K)	Sc	4.54
Ca	5.58	Ni	3.52	Sr	6.08
Ce	5.16	Pb	4.95	Th	5.08
β-Co	3.55	Pd	3.89	Xe (58 K)	6.20
Cu	3.61	Pr	5.16	Yb	5.49

Data in Tables 4.1 to 4.7 are from R. W. G. Wyckoff, *Crystal Structures*, 2nd ed., Interscience, New York, 1963. In most cases, the data are taken at about room temperature and normal atmospheric pressure. For elements that exist in many forms the stable room temperature form (or forms) is given. For more detailed information, more precise lattice constants, and references, the Wyckoff work should be consulted.

Table 4.2
ELEMENTS WITH THE MONATOMIC BODY-CENTERED CUBIC CRYSTAL STRUCTURE

ELEMENT	a (Å)	ELEMENT	a (Å)	ELEMENT	a (Å)
Ba	5.02	Li	3.49 (78 K)	Ta	3.31
Cr	2.88	Mo	3.15	Tl	3.88
Cs	6.05 (78 K)	Na	4.23 (5 K)	V	3.02
Fe	2.87	Nb	3.30	W	3.16
K	5.23 (5 K)	Rb	5.59 (5 K)		

A NOTE ON USAGE

Although we have defined the term "Bravais lattice" to apply to a set of points, it is also generally used to refer to the set of vectors joining any one of these points to all the others. (Because the points *are* a Bravais lattice, this set of vectors does not depend on which point is singled out as the origin.) Yet another usage comes from the fact that any vector **R** determines a *translation* or *displacement*, in which everything is moved bodily through space by a distance R in the direction of **R**. The term "Bravais lattice" is also used to refer to the set of translations determined by the vectors, rather than the vectors themselves. In practice it is always clear from the context whether it is the points, the vectors, or the translations that are being referred to.[7]

[7] The more general use of the term provides an elegant definition of a Bravais lattice with the precision of definition (b) and the nonprejudicial nature of definition (a): A Bravais lattice is a discrete set of vectors not all in a plane, closed under vector addition and subtraction (i.e., the sum and difference of any two vectors in the set are also in the set).

COORDINATION NUMBER

The points in a Bravais lattice that are closest to a given point are called its *nearest neighbors*. Because of the periodic nature of a Bravais lattice, each point has the same number of nearest neighbors. This number is thus a property of the lattice, and is referred to as the *coordination number* of the lattice. A simple cubic lattice has coordination number 6; a body-centered cubic lattice, 8; and a face-centered cubic lattice, 12. The notion of a coordination number can be extended in the obvious way to some simple arrays of points that are not Bravais lattices, provided that each point in the array has the same number of nearest neighbors.

PRIMITIVE UNIT CELL

A volume of space that, when translated through all the vectors in a Bravais lattice, just fills all of space without either overlapping itself or leaving voids is called a *primitive cell* or *primitive unit cell* of the lattice.[8] There is no unique way of choosing a primitive cell for a given Bravais lattice. Several possible choices of primitive cells for a two-dimensional Bravais lattice are illustrated in Figure 4.10.

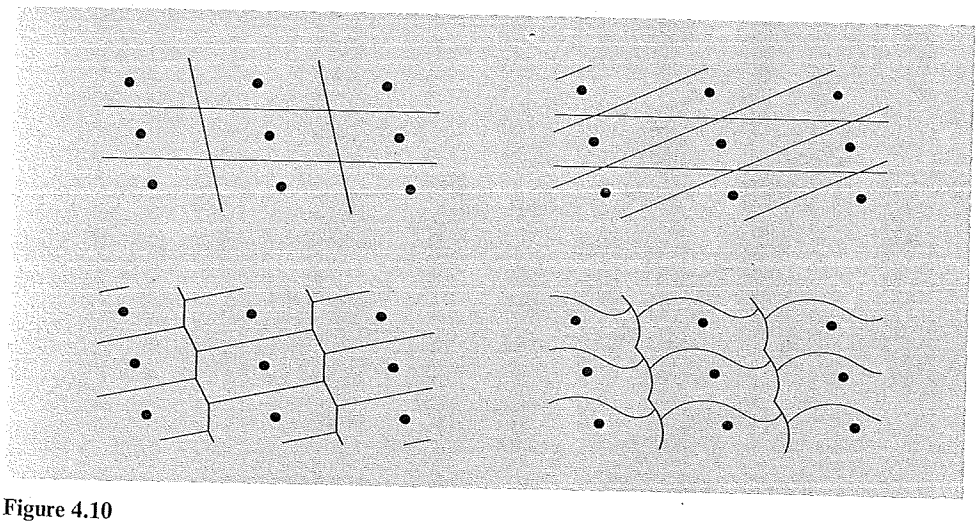

Figure 4.10
Several possible choices of primitive cell for a single two-dimensional Bravais lattice.

A primitive cell must contain precisely one lattice point (unless it is so positioned that there are points on its surface). It follows that if n is the density of points in the lattice[9] and v is the volume of the primitive cell, then $nv = 1$. Thus $v = 1/n$. Since

[8] Translations of the primitive cell may possess common surface points; the nonoverlapping proviso is only intended to prohibit overlapping regions of nonzero volume.

[9] The density n of Bravais lattice points need not, of course, be identical to the density of conduction electrons in a metal. When the possibility of confusion is present, we shall specify the two densities with different symbols.

this result holds for any primitive cell, the volume of a primitive cell is independent of the choice of cell.

It also follows from the definition of a primitive cell that, given any two primitive cells of arbitrary shape, it is possible to cut the first up into pieces, which, when translated through appropriate lattice vectors, can be reassembled to give the second. This is illustrated in Figure 4.11.

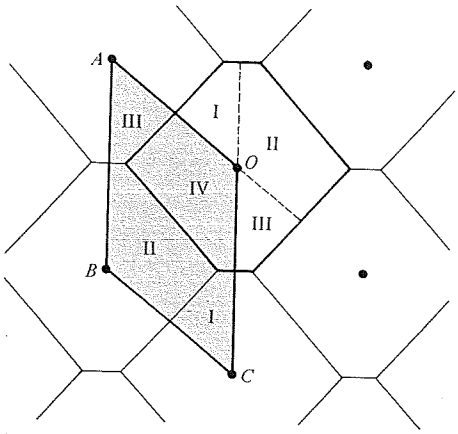

Figure 4.11
Two possible primitive cells for a two-dimensional Bravais lattice. The parallelogram cell (shaded) is obviously primitive; additional hexagonal cells are indicated to demonstrate that the hexagonal cell is also primitive. The parallelogram can be cut into pieces, which, when translated through lattice vectors, reassemble to form the hexagon. The translations for the four regions of the parallelogram are: Region I—$\vec{CO}$; Region II—$\vec{BO}$; Region III—$\vec{AO}$; Region IV—no translation.

The obvious primitive cell to associate with a particular set of primitive vectors, $\mathbf{a}_1, \mathbf{a}_2, \mathbf{a}_3$, is the set of all points $\mathbf{r}$ of the form

$$\mathbf{r} = x_1\mathbf{a}_1 + x_2\mathbf{a}_2 + x_3\mathbf{a}_3 \tag{4.6}$$

for all x_i ranging continuously between 0 and 1; i.e., the parallelipiped spanned by the three vectors $\mathbf{a}_1$, $\mathbf{a}_2$, and $\mathbf{a}_3$. This choice has the disadvantage of not displaying the full symmetry of the Bravais lattice. For example (Figure 4.12), the unit cell (4.6) for the choice of primitive vectors (4.5) of the fcc Bravais lattice is an oblique parallelipiped, which does not have the full cubic symmetry of the lattice in which it is embedded. It is often important to work with cells that do have the full symmetry of their Bravais lattice. There are two widely used solutions to this problem:

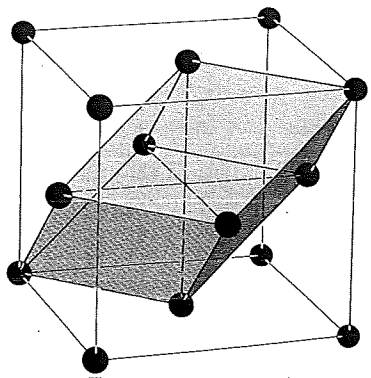

Figure 4.12
Primitive and conventional unit cells for the face-centered cubic Bravais lattice. The conventional cell is the large cube. The primitive cell is the figure with six parallelogram faces. It has one quarter the volume of the cube, and rather less symmetry.

UNIT CELL; CONVENTIONAL UNIT CELL

One can fill space up with nonprimitive unit cells (known simply as *unit cells* or *conventional unit cells*). A unit cell is a region that just fills space without any overlapping when translated through some *subset* of the vectors of a Bravais lattice. The conventional unit cell is generally chosen to be bigger than the primitive cell and to have the required symmetry. Thus one frequently describes the body-centered cubic lattice in terms of a cubic unit cell (Figure 4.13) that is twice as large as a primitive bcc unit cell, and the face-centered cubic lattice in terms of a cubic unit cell (Figure 4.12) that has four times the volume of a primitive fcc unit cell. (That the conventional cells are two and four times bigger than the primitive cells is easily seen by asking how many lattice points the conventional cubic cell must contain when it is so placed that no points are on its surface.) Numbers specifying the size of a unit cell (such as the single number a in cubic crystals) are called *lattice constants.*

Figure 4.13
Primitive and conventional unit cells for the body-centered cubic Bravais lattice. The primitive cell (shaded) has half the volume of the conventional cubic cell.

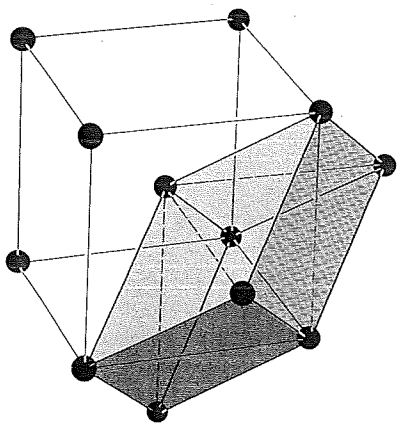

WIGNER-SEITZ PRIMITIVE CELL

One can always choose a *primitive* cell with the full symmetry of the Bravais lattice. By far the most common such choice is the *Wigner-Seitz cell.* The Wigner-Seitz cell about a lattice point is the region of space that is closer to that point than to any other lattice point.[10] Because of the translational symmetry of the Bravais lattice, the Wigner-Seitz cell about any one lattice point must be taken into the Wigner-Seitz cell about any other, when translated through the lattice vector that joins the two points. Since any point in space has a unique lattice point, as its nearest neighbor[11] it will belong to the Wigner-Seitz cell of precisely one lattice point. It follows that a

[10] Such a cell can be defined for any set of discrete points that do not necessarily form a Bravais lattice. In this broader context the cell is known as a Voronoy polyhedron. In contrast to the Wigner-Seitz cell, the structure and orientation of a general Voronoy polyhedron will depend on which point of the array it encloses.

[11] Except for points on the common surface of two or more Wigner-Seitz cells.

DIR

Wigner-Seitz cell, when translated through all lattice vectors, will just fill space without overlapping; i.e., the Wigner-Seitz cell is a primitive cell.

Since there is nothing in the definition of the Wigner-Seitz cell that refers to any particular choice of primitive vectors, the Wigner-Seitz cell will be as symmetrical as the Bravais lattice.[12]

The Wigner-Seitz unit cell is illustrated for a two-dimensional Bravais lattice in Figure 4.14 and for the three-dimensional body-centered cubic and face-centered cubic Bravais lattices in Figures 4.15 and 4.16.

Note that the Wigner-Seitz unit cell about a lattice point can be constructed by drawing lines connecting the point to all others[13] in the lattice, bisecting each line

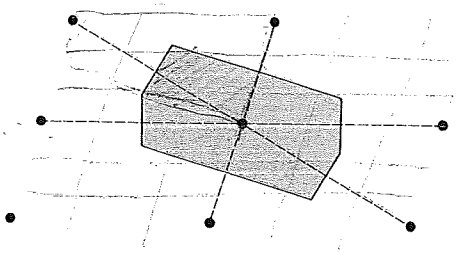

Figure 4.14
The Wigner-Seitz cell for a two-dimensional Bravais lattice. The six sides of the cell bisect the lines joining the central points to its six nearest neighboring points (shown as dashed lines). In two dimensions the Wigner-Seitz cell is always a hexagon unless the lattice is rectangular (see Problem 4a).

Figure 4.15
The Wigner-Seitz cell for the body-centered cubic Bravais lattice (a "truncated octahedron"). The surrounding cube is a conventional body-centered cubic cell with a lattice point at its center and on each vertex. The hexagonal faces bisect the lines joining the central point to the points on the vertices (drawn as solid lines). The square faces bisect the lines joining the central point to the central points in each of the six neighboring cubic cells (not drawn). The hexagons are regular (see Problem 4d).

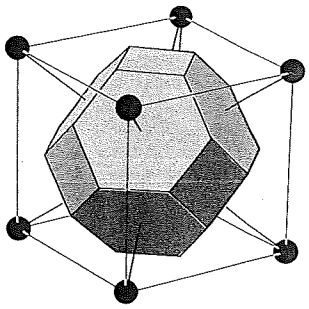

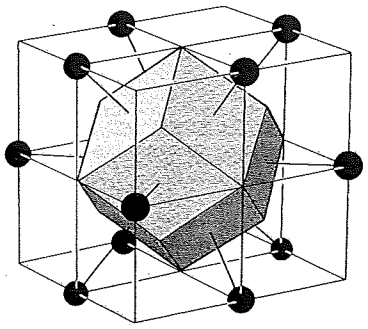

Figure 4.16
Wigner-Seitz cell for the face-centered cubic Bravais lattice (a "rhombic dodecahedron"). The surrounding cube is *not* the conventional cubic cell of Figure 4.12, but one in which lattice points are at the center of the cube and at the center of the 12 edges. Each of the 12 (congruent) faces is perpendicular to a line joining the central point to a point on the center of an edge.

[12] A precise definition of "as symmetrical as" is given in Chapter 7.
[13] In practice only a fairly small number of nearby points actually yield planes that bound the cell.

with a plane, and taking the smallest polyhedron containing the point bounded by these planes.

CRYSTAL STRUCTURE; LATTICE WITH A BASIS

A physical crystal can be described by giving its underlying Bravais lattice, together with a description of the arrangement of atoms, molecules, ions, etc., within a particular primitive cell. When emphasizing the difference between the abstract pattern of points composing the Bravais lattice and an actual physical crystal[14] embodying the lattice, the technical term "crystal structure" is used. A *crystal structure* consists of identical copies of the same physical unit, called the *basis*, located at all the points of a Bravais lattice (or, equivalently, translated through all the vectors of a Bravais lattice). Sometimes the term *lattice with a basis* is used instead. However, "lattice with a basis" is also used in a more general sense to refer to what results even when the basic unit is *not* a physical object or objects, but another set of points. For example, the vertices of a two-dimensional honeycomb, though not a Bravais lattice, can be represented as a two-dimensional triangular Bravais lattice[15] with a two-point basis (Figure 4.17). A crystal structure with a basis consisting of a single atom or ion is often called a monatomic Bravais lattice.

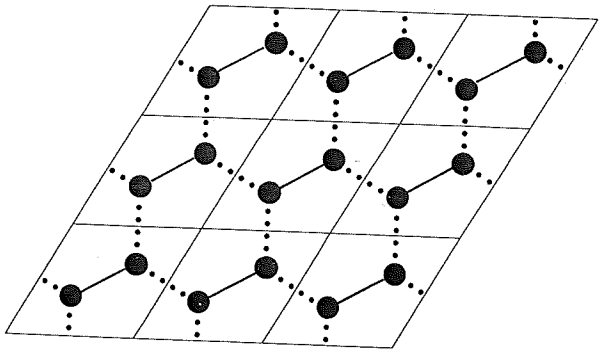

Figure 4.17
The honeycomb net, drawn so as to emphasize that it is a Bravais lattice with a two-point basis. The pairs of points joined by heavy solid lines are identically placed in the primitive cells (parallelograms) of the underlying Bravais lattice.

One also can describe a Bravais lattice as a lattice with a basis by choosing a non-primitive conventional unit cell. This is often done to emphasize the cubic symmetry of the bcc and fcc Bravais lattices, which are then described respectively, as simple cubic lattices spanned by $a\hat{\mathbf{x}}$, $a\hat{\mathbf{y}}$, and $a\hat{\mathbf{z}}$, with a two-point basis

$$\mathbf{0}, \quad \frac{a}{2}(\hat{\mathbf{x}} + \hat{\mathbf{y}} + \hat{\mathbf{z}}) \qquad \text{(bcc)} \tag{4.7}$$

or a four-point basis

$$\mathbf{0}, \quad \frac{a}{2}(\hat{\mathbf{x}} + \hat{\mathbf{y}}), \quad \frac{a}{2}(\hat{\mathbf{y}} + \hat{\mathbf{z}}), \quad \frac{a}{2}(\hat{\mathbf{z}} + \hat{\mathbf{x}}) \qquad \text{(fcc)}. \tag{4.8}$$

[14] But still idealized in being infinite in extent.
[15] Spanned by two primitive vectors of equal length, making an angle of 60°.

SOME IMPORTANT EXAMPLES OF CRYSTAL STRUCTURES AND LATTICES WITH BASES

Diamond Structure

The diamond lattice[16] (formed by the carbon atoms in a diamond crystal) consists of two interpenetrating face-centered cubic Bravais lattices, displaced along the body diagonal of the cubic cell by one quarter the length of the diagonal. It can be regarded as a face-centered cubic lattice with the two-point basis $\mathbf{0}$ and $(a/4)(\hat{\mathbf{x}} + \hat{\mathbf{y}} + \hat{\mathbf{z}})$. The coordination number is 4 (Figure 4.18). The diamond lattice is not a Bravais lattice,

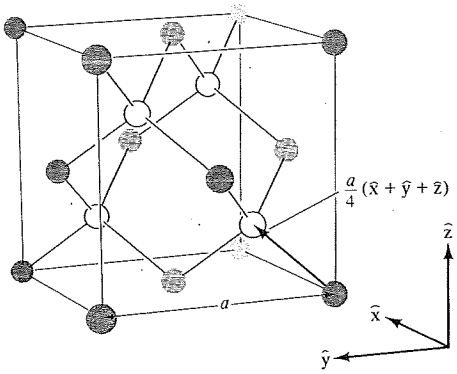

Figure 4.18
Conventional cubic cell of the diamond lattice. For clarity, sites corresponding to one of the two interpenetrating face-centered cubic lattices are unshaded. (In the zincblende structure the shaded sites are occupied by one kind of ion, and the unshaded by another.) Nearest-neighbor bonds have been drawn in. The four nearest neighbors of each point form the vertices of a regular tetrahedron.

because the environment of any point differs in orientation from the environments of its nearest neighbors. Elements crystallizing in the diamond structure are given in Table 4.3.

Table 4.3
ELEMENTS WITH THE DIAMOND CRYSTAL STRUCTURE

ELEMENT	CUBE SIDE a (Å)
C (diamond)	3.57
Si	5.43
Ge	5.66
α-Sn (grey)	6.49

Hexagonal Close-Packed Structure

Though not a Bravais lattice, the *hexagonal close-packed* (hcp) structure ranks in importance with the body-centered cubic and face-centered cubic Bravais lattices; about 30 elements crystallize in the hexagonal close-packed form (Table 4.4).

[16] We use the word "lattice," without qualifications, to refer either to a Bravais lattice or a lattice with a basis.

Table 4.4
ELEMENTS WITH THE HEXAGONAL CLOSE-PACKED CRYSTAL STRUCTURE

ELEMENT	a (Å)	c	c/a	ELEMENT	a (Å)	c	c/a
Be	2.29	3.58	1.56	Os	2.74	4.32	1.58
Cd	2.98	5.62	1.89	Pr	3.67	5.92	1.61
Ce	3.65	5.96	1.63	Re	2.76	4.46	1.62
α-Co	2.51	4.07	1.62	Ru	2.70	4.28	1.59
Dy	3.59	5.65	1.57	Sc	3.31	5.27	1.59
Er	3.56	5.59	1.57	Tb	3.60	5.69	1.58
Gd	3.64	5.78	1.59	Ti	2.95	4.69	1.59
He (2 K)	3.57	5.83	1.63	Tl	3.46	5.53	1.60
Hf	3.20	5.06	1.58	Tm	3.54	5.55	1.57
Ho	3.58	5.62	1.57	Y	3.65	5.73	1.57
La	3.75	6.07	1.62	Zn	2.66	4.95	1.86
Lu	3.50	5.55	1.59	Zr	3.23	5.15	1.59
Mg	3.21	5.21	1.62		—	—	
Nd	3.66	5.90	1.61	"Ideal"			1.63

Underlying the hcp structure is a *simple hexagonal* Bravais lattice, given by stacking two-dimensional triangular nets[15] directly above each other (Figure 4.19). The direction of stacking ($\mathbf{a}_3$, below) is known as the c-axis. Three primitive vectors are

$$\mathbf{a}_1 = a\hat{\mathbf{x}}, \quad \mathbf{a}_2 = \frac{a}{2}\hat{\mathbf{x}} + \frac{\sqrt{3}a}{2}\hat{\mathbf{y}}, \quad \mathbf{a}_3 = c\hat{\mathbf{z}}. \tag{4.9}$$

The first two generate a triangular lattice in the x-y plane, and the third stacks the planes a distance c above one another.

The hexagonal close-packed structure consists of two interpenetrating simple hexagonal Bravais lattices, displaced from one another by $\mathbf{a}_1/3 + \mathbf{a}_2/3 + \mathbf{a}_3/2$ (Figure 4.20). The name reflects the fact that close-packed hard spheres can be arranged in

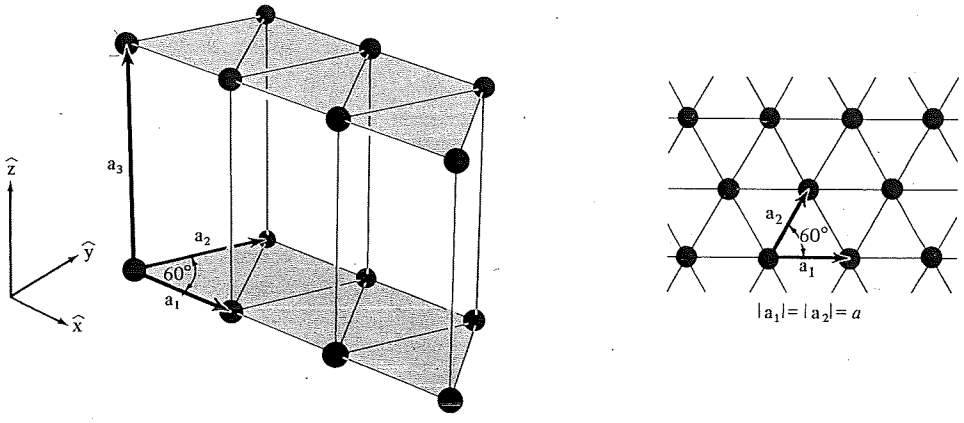

Figure 4.19
The simple hexagonal Bravais lattice. Two-dimensional triangular nets (shown in inset) are stacked directly above one another, a distance c apart.

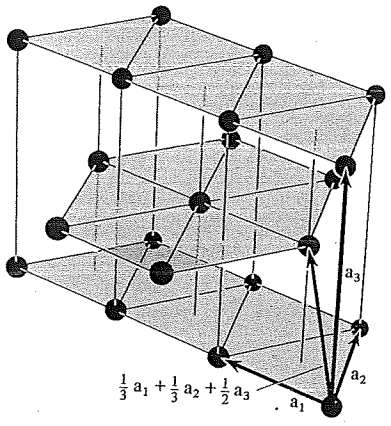

Figure 4.20
The hexagonal close-packed crystal structure. It can be viewed as two interpenetrating simple hexagonal Bravais lattices, displaced vertically by a distance $c/2$ along the common c-axis, and displaced horizontally so that the points of one lie directly above the centers of the triangles formed by the points of the other.

such a structure. Consider stacking cannonballs (Figure 4.21), starting with a close-packed triangular lattice as the first layer. The next layer is formed by placing a ball in the depressions left in the center of every other triangle in the first layer, thereby forming a second triangular layer, shifted with respect to the first. The third layer is formed by placing balls in alternate depressions in the second layer, so that they lie directly over the balls in the first layer. The fourth layer lies directly over the second, and so on. The resulting lattice is hexagonal close-packed with the particular value (see Problem 5):

$$c = \sqrt{\frac{8}{3}}\,a = 1.63299a. \tag{4.10}$$

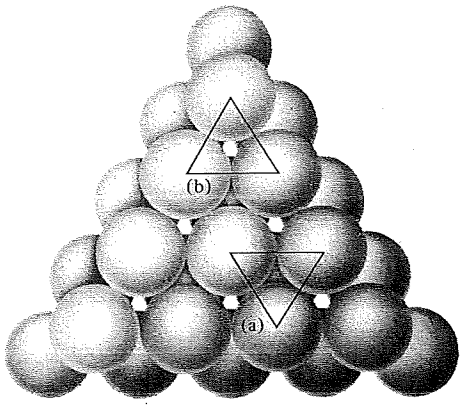

Figure 4.21
View from above of the first two layers in a stack of cannonballs. The first layer is arranged in a plane triangular lattice. Balls in the second layer are placed above alternate interstices in the first. If balls in the third layer are placed directly above those in the first, at sites of the type shown in inset (a), balls in the fourth directly above those in the second, etc., the resulting structure will be close-packed hexagonal. If, however, balls in the third layer are placed directly above those interstices in the first that were *not* covered by balls in the second, at sites of the type shown in inset (b), balls in the fourth layer placed directly above those in the first, balls in the fifth directly above those in the second, etc., the resulting structure will be face-centered cubic (with the body diagonal of the cube oriented vertically.)

Because, however, the symmetry of the hexagonal close-packed lattice is independent of the c/a ratio, the name is not restricted to this case. The value $c/a = \sqrt{8/3}$ is sometimes called "ideal," and the truly close-packed structure, with the ideal value of c/a, is known as an ideal hcp structure. Unless, however, the physical units in the hcp structure are actually close-packed spheres, there is no reason why c/a should be ideal (see Table 4.4).

Note, as in the case of the diamond structure, that the hcp lattice is not a Bravais lattice, because the orientation of the environment of a point varies from layer to layer along the c-axis. Not also that, when viewed along the c-axis, the two types of planes merge to form the two-dimensional honeycomb array of Figure 4.3, which is not a Bravais lattice.

Other Close-Packing Possibilities

Note that the hcp structure is not the only way to close-pack spheres. If the first two layers are laid down as described above, but the third is placed in the *other* set of depressions in the second—i.e., those lying above unused depressions in *both* the first and second layers (see Figure 4.21)—and then the fourth layer is placed in depressions in the third directly above the balls in the first, the fifth above the second, and so on, one generates a Bravais lattice. This Bravais lattice turns out to be nothing but the face-centered cubic lattice, with the cube diagonal perpendicular to the triangular planes (Figures 4.22 and 4.23).

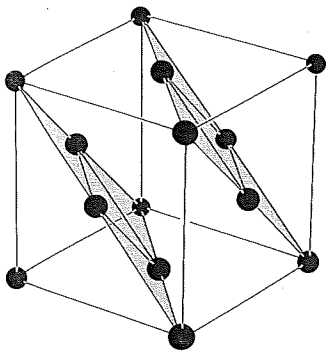

Figure 4.22
How to section the face-centered cubic Bravais lattice to get the layers pictured in Figure 4.21.

Figure 4.23
A cubic section of some face-centered cubic close-packed spheres.

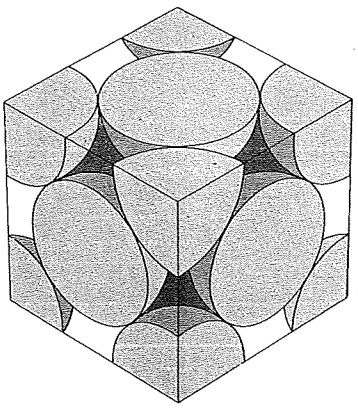

There are infinitely many other close-packing arrangements, since each successive layer can be placed in either of two positions. Only fcc close-packing gives a Bravais lattice, and the fcc (...*ABCABCABC*...) and hcp (...*ABABAB*...) structures are by far the most commonly encountered. Other close-packed structures are observed, however. Certain rare earth metals, for example, take on a structure of the form (...*ABACABACABAC*...).

DIR

The Sodium Chloride Structure

We are forced to describe the hexagonal close-packed and diamond lattices as lattices with bases by the intrinsic geometrical arrangement of the lattice points. A lattice with a basis is also necessary, however, in describing crystal structures in which the atoms or ions are located only at the points of a Bravais lattice, but in which the crystal structure nevertheless lacks the full translational symmetry of the Bravais lattice because more than one kind of atom or ion is present. For example, sodium chloride (Figure 4.24) consists of equal numbers of sodium and chlorine ions placed at alternate points of a simple cubic lattice, in such a way that each ion has six of the other kind of ions as its nearest neighbors.[17] This structure can be described as a face-centered cubic Bravais lattice with a basis consisting of a sodium ion at $\mathbf{0}$ and a chlorine ion at the center of the conventional cubic cell, $(a/2)(\hat{\mathbf{x}} + \hat{\mathbf{y}} + \hat{\mathbf{z}})$.

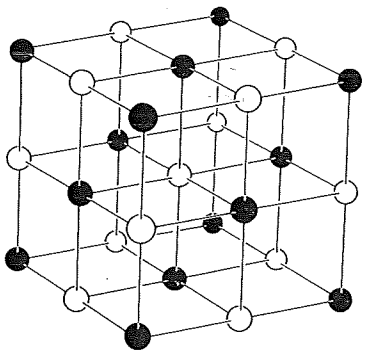

Figure 4.24
The sodium chloride structure. One type of ion is represented by black balls, the other type by white. The black and white balls form interpenetrating fcc lattices.

NaCl
interpenetrating FCC

FCC + BASIS $\frac{a}{2}(\hat{x}+\hat{y}+\hat{z})$ Na
0 Cl

Table 4.5
SOME COMPOUNDS WITH THE SODIUM CHLORIDE STRUCTURE

CRYSTAL	a (Å)	CRYSTAL	a (Å)	CRYSTAL	a (Å)
LiF	4.02	RbF	5.64	CaS	5.69
LiCl	5.13	RbCl	6.58	CaSe	5.91
LiBr	5.50	RbBr	6.85	CaTe	6.34
LiI	6.00	RbI	7.34	SrO	5.16
NaF	4.62	CsF	6.01	SrS	6.02
NaCl	5.64	AgF	4.92	SrSe	6.23
NaBr	5.97	AgCl	5.55	SrTe	6.47
NaI	6.47	AgBr	5.77	BaO	5.52
KF	5.35	MgO	4.21	BaS	6.39
KCl	6.29	MgS	5.20	BaSe	6.60
KBr	6.60	MgSe	5.45	BaTe	6.99
KI	7.07	CaO	4.81		

The Cesium Chloride Structure

Similarly, cesium chloride (Figure 4.25) consists of equal numbers of cesium and chlorine ions, placed at the points of a body-centered cubic lattice so that each ion

[17] For examples see Table 4.5.

has eight of the other kind as its nearest neighbors.[18] The translational symmetry of this structure is that of the simple cubic Bravais lattice, and it is described as a simple cubic lattice with a basis consisting of a cesium ion at the origin **0** and a chlorine ion at the cube center $(a/2)(\hat{\mathbf{x}} + \hat{\mathbf{y}} + \hat{\mathbf{z}})$.

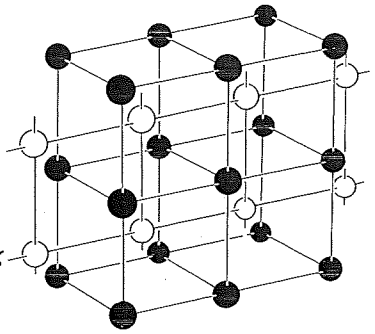

Figure 4.25
The cesium chloride structure. One type of ion is represented by black balls, the other type by white. The black and white balls form interpenetrating simple cubic lattices.

Table 4.6
SOME COMPOUNDS WITH THE CESIUM CHLORIDE STRUCTURE

CRYSTAL	a (Å)	CRYSTAL	a (Å)
CsCl	4.12	TlCl	3.83
CsBr	4.29	TlBr	3.97
CsI	4.57	TlI	4.20

The Zincblende Structure

Zincblende has equal numbers of zinc and sulfur ions distributed on a diamond lattice so that each has four of the opposite kind as nearest neighbors (Figure 4.18). This structure[19] is an example of a lattice with a basis, which must be so described both because of the geometrical position of the ions and because two types of ions occur.

Table 4.7
SOME COMPOUNDS WITH THE ZINCBLENDE STRUCTURE

CRYSTAL	a (Å)	CRYSTAL	a (Å)	CRYSTAL	a (Å)
CuF	4.26	ZnS	5.41	AlSb	6.13
CuCl	5.41	ZnSe	5.67	GaP	5.45
CuBr	5.69	ZnTe	6.09	GaAs	5.65
CuI	6.04	CdS	5.82	GaSb	6.12
AgI	6.47	CdTe	6.48	InP	5.87
BeS	4.85	HgS	5.85	InAs	6.04
BeSe	5.07	HgSe	6.08	InSb	6.48
BeTe	5.54	HgTe	6.43	SiC	4.35
MnS (red)	5.60	AlP	5.45		
MnSe	5.82	AlAs	5.62		

[18] For examples see Table 4.6.
[19] For examples see Table 4.7.

3.1 INTRODUCTION

In the previous chapter we saw that macroscopic properties of materials are influenced strongly by atomic scale structure. In previous discussions we focused our attention on an individual atom or ion and looked first at its spatial relationship to a single neighboring atom, specifically, at its equilibrium separation distance; and then at its spatial relationship to a small group of atoms known as its nearest neighbors, as manifested in its coordination number and bond angles. As mentioned in Section 2.6, the local arrangement of nearest-neighbor atoms about a central atom is known as short-range order (SRO).

In this chapter we expand our view of materials to incorporate larger numbers of atoms. Materials that exhibit order over distances much greater than the bond length are said to have long-range order (LRO). In fact, materials can be classified on the basis of the extent of LRO they exhibit: *amorphous* solids show SRO in three dimensions, but no LRO; *crystalline* solids exhibit both SRO and LRO in three dimensions. As a general rule, most metals are crystalline, while ceramics and polymers may be either crystalline, amorphous, or a combination of the two.

Since an understanding of SRO and LRO is central to this chapter, it is appropriate to pause and present a few examples. In the case of a noble gas, under most conditions the interaction between atoms is minimal. Consequently, there is no significant positional relationship between one gas atom and another. The material shows neither SRO nor LRO. This is not true in most condensed phases. In a liquid, for example, nearest neighbors are positioned at well-defined distances and SRO is established. The order within most liquids, however, does not persist beyond nearest-neighbor distances. The same type of order, SRO but no LRO, can occur in solids. As you might expect, the structure of amorphous solids, or glasses, is similar to that of a "frozen" liquid. A detailed discussion of amorphous solids is the subject of Chapter 6.

Many solids are crystalline. The establishment of LRO requires that atoms be arranged on a three-dimensional array that repeats in space. The 3-D framework is known as a **crystal lattice.** The details of the lattice pattern strongly influence the macroscopic properties of crystalline engineering materials.

The organization of this chapter is as follows. First we describe the concept of a crystal lattice and then present a few simple crystal structures. We will see that even for simple structures, a language is needed to describe specific points, directions, and planes in crystals. After introducing the appropriate nomenclature, we describe several methods to quantify various characteristics of crystal lattices. We then turn our attention to a description of more complex crystal structures, those structures typically associated with ionic, covalent, or molecular crystals. Next, we describe the fundamental relationship between crystal structure and macroscopic properties, a relationship that is emphasized throughout the textbook. Finally, we conclude the chapter with an introduction to X-ray diffraction, the technique most commonly used to characterize crystal structure.

3.2 BRAVAIS LATTICES AND UNIT CELLS

A **lattice** can be defined as an indefinitely extended arrangement of points each of which is surrounded by an identical grouping of neighboring points. Before proceeding to a discussion of three-dimensional (3-D) crystal lattices, we will introduce some of the important characteristics of a lattice using a 2-D analogy.

Wallpaper is a common example of a 2-D lattice. The smallest region that completely describes the pattern is known as the **unit cell.** Once the unit cell is established, the entire

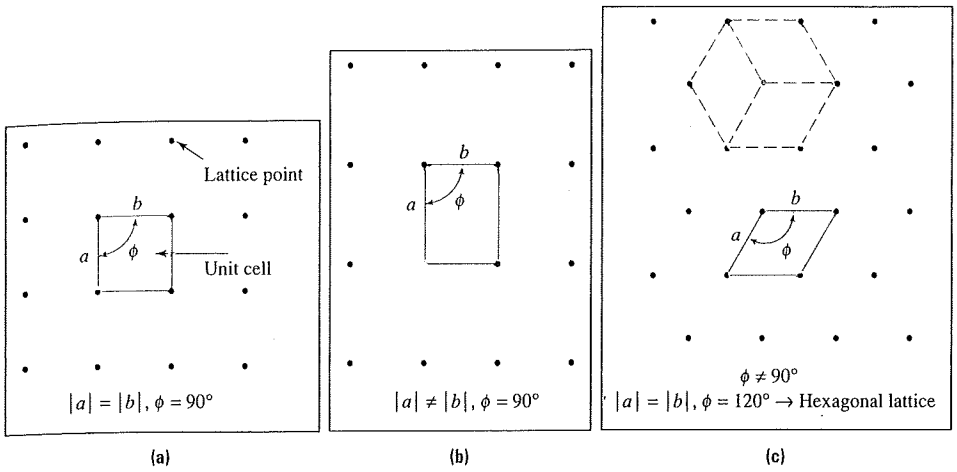

FIGURE 3.2–1 The possible unit cells of wallpaper, or any other 2-D pattern, include: **(a)** a square, **(b)** a rectangle, or **(c)** a parallelogram. The restrictions on the lattice parameters, *a* and *b*, and the angle between the edges of the unit cell, ϕ, are listed for each type of cell.

extended pattern can be generated by translating the unit cell in 2-D. As shown in Figure 3.2–1, the only permissible shapes for 2-D unit cells are a square, a rectangle, or a parallelogram. The reason for this is that the unit cell must have a shape that permits it to be arranged in a way that completely fills space. The vertices of the unit cell are known as **lattice points.** The lengths of the unit-cell edges are known as the **lattice parameters.** The angles and lengths within the repeat unit determine the class to which the lattice cell belongs.

Note that all three patterns in Figure 3.2–2 have exactly the same rectangular lattice, yet the patterns are distinguishable. Thus, the specification of a lattice alone is not sufficient to uniquely define a pattern. In addition, one must describe exactly what is located at each lattice point. The name given to the "group of things" located on a lattice point is the **basis.** For wallpaper the basis is one or more illustrations, while for a 3-D crystal the basis is one or more atoms. This idea can be formalized by the relationship

$$\text{Lattice} + \text{Basis} = \text{Crystal structure} \qquad \textbf{(3.2–1)}$$

Having introduced the important properties of a lattice in 2-D, we can focus on our main objective—the description of 3-D crystal lattices.

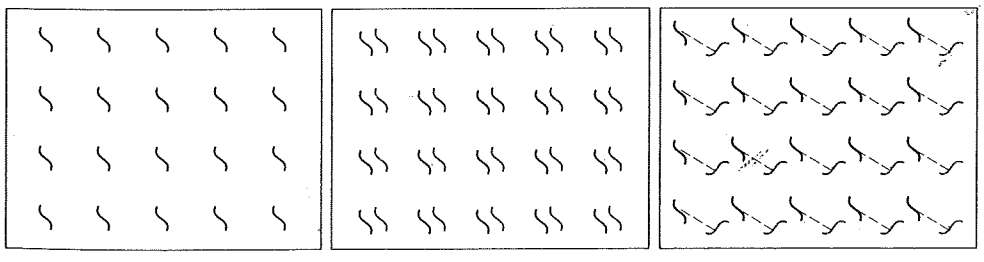

FIGURE 3.2–2 Three examples of 2-D patterns all created using the same rectangular lattice but each having a different basis: **(a)** the basis is a single character; **(b)** the basis contains a repeated character, and **(c)** the basis contains two characters with different orientations.

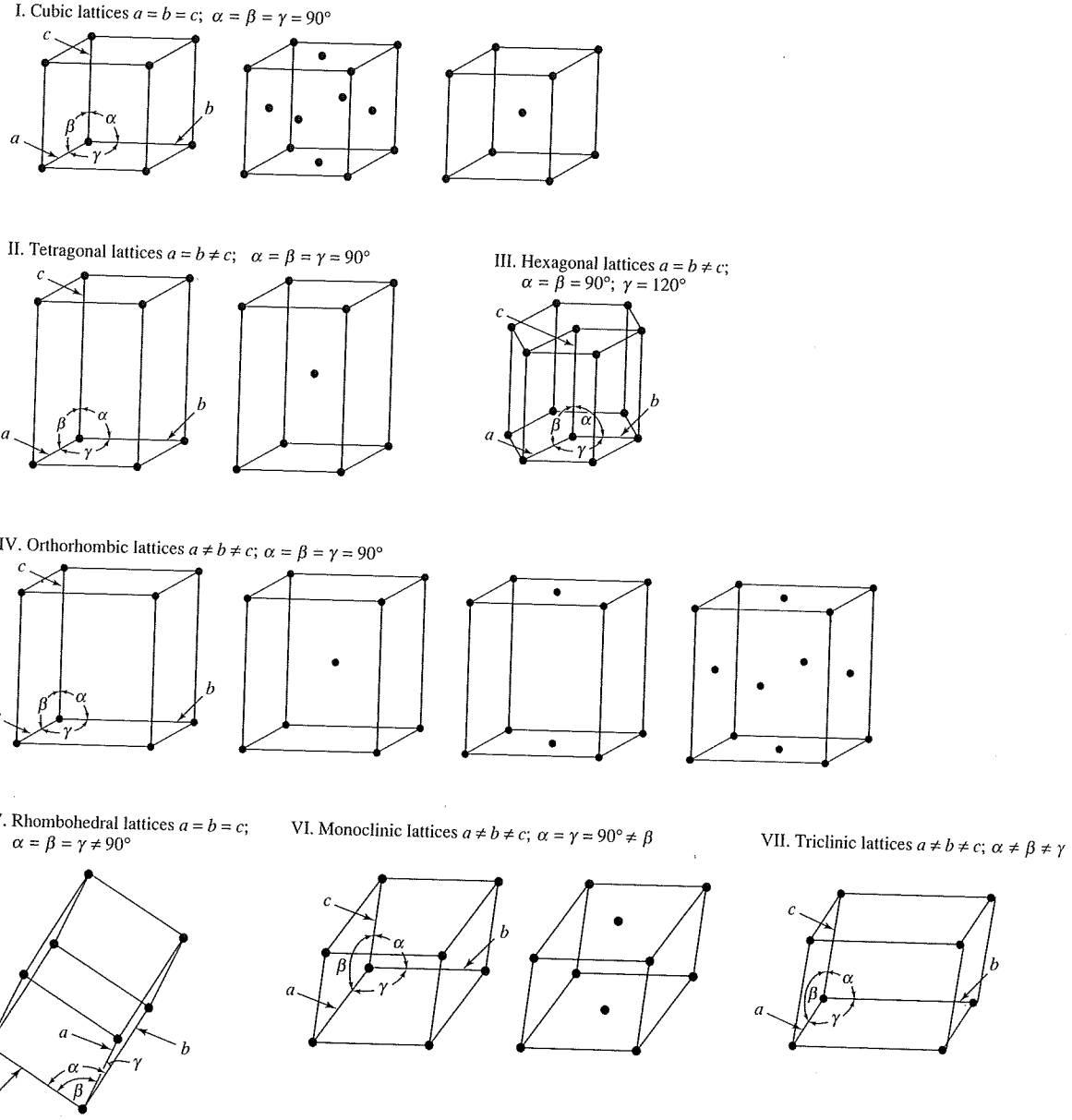

FIGURE 3.2–3 The 14 Bravais lattices grouped into the 7 lattice types. The restrictions on the lattice parameters *a*, *b*, and *c* and the angles between the edges of the unit cell α, β, and γ are listed for each unit cell.

There are 14 valid 3-D lattices, on which the basis—atoms or groups of atoms—can be placed. They are called Bravais lattices and are shown in Figure 3.2–3. Each of the lattice points is equivalent; that is, the lattice points are indistinguishable. The equivalence of lattice points is demonstrated in Figure 3.2–4 for the body-centered cubic crystal, in which the axis system is redrawn so that the "new" origin corresponds to the center of the "original" cube.

The unit cell is the smallest volume that shows all the characteristics of the system. Each of the cells repeats indefinitely in all directions, to the physical limits of the crystal. The properties of a unit cell are the same as those of the crystal. Hence, a unit cell is a convenient representative structure that can be used to calculate theoretical properties of a crystal, such as density.

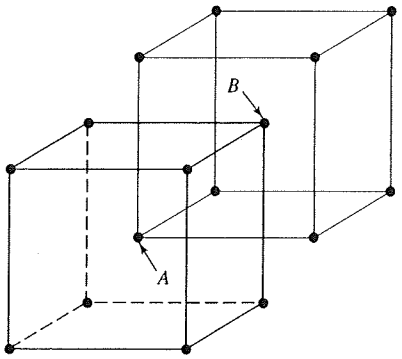

FIGURE 3.2–4 The equivalence of the lattice points is demonstrated for the body-centered cubic crystal by redrawing the axis system so that the "new" origin corresponds to the center of the "original" cube. Note that atom *A* is at the center of the black cube and the front left bottom corner of the colored cube. Atom *B* is at the back right top corner of the black cube and the center of the colored cube.

As in the previous 2-D example, 3-D unit cells are described in terms of the cell parameters—the lengths of the cell edges and the angles between axes. Consider, for example, the cell with the highest symmetry, the cubic cell. The axes in the cubic system are orthogonal (all angles 90°) and the lengths of the sides of the cube are equal. Hence, a cubic crystal is completely characterized by a single lattice parameter a_0. The lattice parameter a_0 is not equivalent to the equilibrium separation distance x_0. The former quantity represents the length of a cubic unit-cell edge and the latter represents the distance between the centers of adjacent nearest-neighbor atoms. At the other extreme, description of a triclinic crystal requires the specification of three lengths (a, b, and c) and three angles (α, β, and γ).

We will see in the next section that many metals have cubic structures and some have hexagonal structures. Materials with ionic bonds typically have larger, more complex crystal structures than metals. Since there is more than one type of atom present in ionic solids, the complexity of the basis increases. Polymers also have complex bases and crystal structures with large unit cells.

3.3 CRYSTALS WITH ONE ATOM PER LATTICE SITE AND HEXAGONAL CRYSTALS

In this section we examine and develop important concepts regarding unit cells for metals. The simplest unit cell, called the **simple cubic (SC)** structure, has atoms located in each of the cell corners. We will not dwell on the SC structure here, since no important metals have this structure. Instead, we will investigate the more common metal structures.

3.3.1 Body-Centered Cubic Crystals

The simplest cells are those with cubic symmetry and one atom per lattice position (i.e., the basis is a single atom). Consider the structure of tungsten, shown in Figure 3.3–1. An atom lies at each corner of the cube and one in the center. This is the **body-centered cubic (BCC)** structure. Each corner atom touches the central atom, but the corner atoms do not touch each other. Other metals with the BCC structure at room temperature include chromium, iron, molybdenum, and vanadium.

Three important characteristics of a cubic unit cell are the length of its lattice parameter a_0, the number of atoms in the unit cell, and the coordination number of each atom. Although values of a_0 for many materials are available in the technical literature, it is important to recognize that estimates for a_0 can be obtained from a knowledge of the

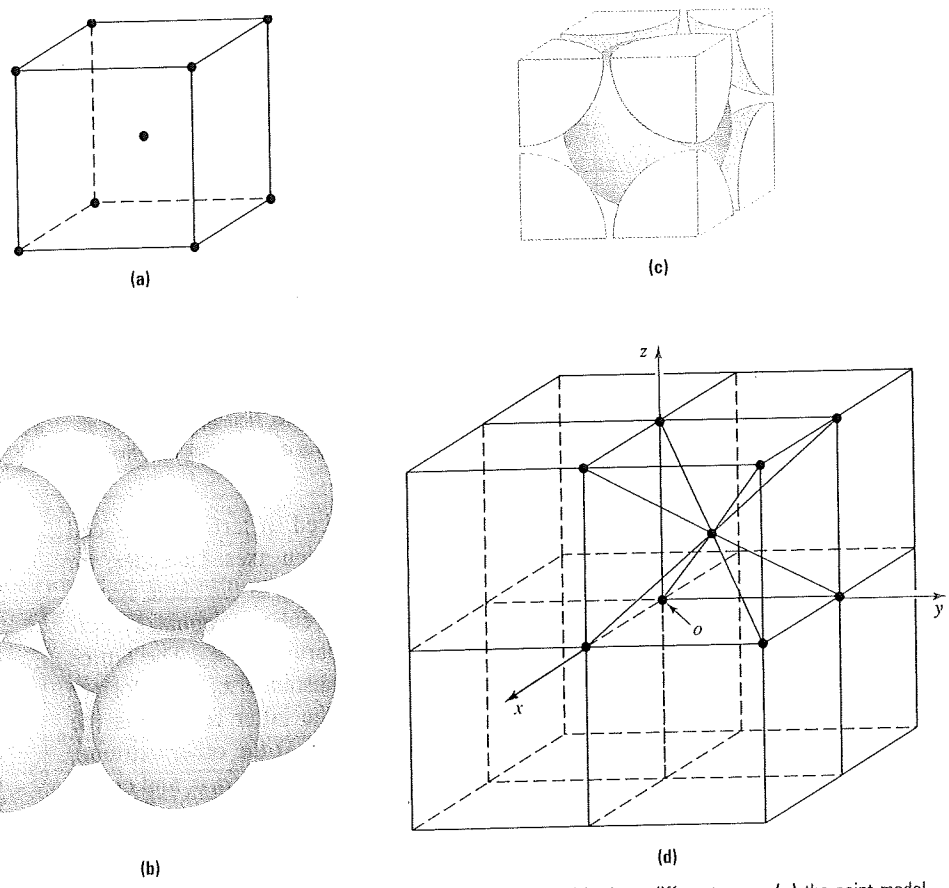

FIGURE 3.3–1 The structure of tungsten, a body-centered cubic metal, is illustrated in three different ways: **(a)** the point model shows only the locations of the atom centers, **(b)** the full solid sphere model shows all five atoms associated with the unit cell, and **(c)** the partial solid sphere model shows just the fractions of each atom contained within the unit cell. **(d)** An illustration of eight adjacent unit cells showing that some of the atoms in the BCC unit cell are shared among several adjacent unit cells.

radius of the atoms involved, r, and the geometry of the unit cell. To obtain the relationship between the lattice parameter and the atomic radius (the a_0-r relationship), find a direction in which atoms are touching, and equate the expression for atom center-to-center distance in terms of a_0 to the equivalent distance in terms of r.

Figure 3.3–2a shows that for a cube with edge length a_0, the length of any face diagonal is $a_0\sqrt{2}$ and the length of any body diagonal is $a_0\sqrt{3}$. Therefore, the distance between adjacent atoms in the BCC structure is $a_0\sqrt{3}/2$ (see Figure 3.3–2b). The repeat distance in terms of r is $2r$, so that the a_0-r relationship is

$$\frac{a_0\sqrt{3}}{2} = 2r \quad \text{or} \quad a_0(\text{BCC}) = \frac{4r}{\sqrt{3}} \tag{3.3–1}$$

Next, we determine the number of atoms per cell. Examination of Figure 3.3–1d shows that nine atoms are associated with each cell but some atoms are shared among several cells. Notice that each corner atom is shared by eight cells. Therefore, only 1/8 of any corner atom is associated with each cell. In contrast, a center atom is totally contained within its cell. Thus, the total number of atoms per unit cell is two $[(8 \times 1/8) + (1 \times 1)]$. Examination of Figure 3.3–1 shows that each atom in the BCC structure has eight nearest neighbors [CN(BCC) = 8].

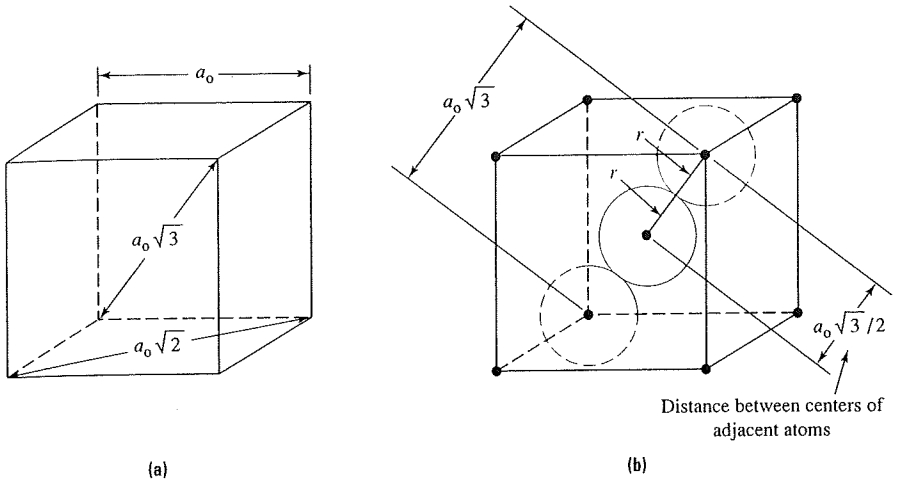

FIGURE 3.3–2 **(a)** For a cube with edge length a_0, the length of any face diagonal is $a_0\sqrt{2}$ and the length of any body diagonal is $a_0\sqrt{3}$. **(b)** The distance between adjacent atoms in the BCC structure may be expressed as either $a_0\sqrt{3}/2$ or, equivalently, $2r$.

EXAMPLE 3.3–1

Using data on atomic weight and atomic radius (in Appendices B and C), calculate the density of BCC Fe.

Solution

Density is defined to be mass divided by volume. Since the unit cell completely describes the crystal structure, we can calculate the density of iron based on the mass and volume of its unit cell. The mass of the unit cell, M_{uc}, can be determined by noting:

$$M_{uc} = \frac{\text{Number of atoms}}{\text{Unit cell}} \times \frac{\text{Mass}}{\text{Atom}}$$

The volume of the unit cell, V_{uc}, is just a_0^3. For iron,

$$M_{uc} = \left(\frac{2 \text{ atoms}}{\text{BCC unit cell}}\right)\left[(55.85 \text{ g/mol Fe})\left(\frac{1 \text{ mol Fe}}{6.023 \times 10^{23} \text{ atoms Fe}}\right)\right]$$
$$= 1.85 \times 10^{-22} \text{ g/(unit cell)}$$

and

$$V_{uc} = a_0^3 = \left(\frac{4r}{\sqrt{3}}\right)^3 = \left[\frac{4 \times (1.24 \times 10^{-8} \text{ cm})}{\sqrt{3}}\right]^3$$
$$= 2.35 \times 10^{-23} \text{ cm}^3\text{/(unit cell)}$$

Therefore, the density of iron is calculated as

$$\rho = \frac{1.85 \times 10^{-22} \text{ g/(unit cell)}}{2.35 \times 10^{-23} \text{ cm}^3\text{/(unit cell)}}$$
$$= 7.87 \text{ g/cm}^3$$

The measured density of Fe is also 7.87 g/cm^3. In general, however, we should not expect perfect agreement between the density estimate obtained using this method and the measured density of a solid, since our model assumes that the crystal is "perfect" while real crystals contain defects. These defects will be discussed in the next two chapters.

3.3.2 Face-Centered Cubic Crystals

Another common unit cell with cubic symmetry and one atom per position is the **face-centered cubic (FCC)** structure. Metals that have the FCC structure at room temperature include aluminum, calcium, copper, gold, lead, nickel, platinum, and silver. As shown in Figure 3.3–3, this structure has an atom at each corner plus an additional atom at the center of each face. Each corner atom touches the atoms in the centers of the three adjacent faces, but corner atoms do not touch other corner atoms.

Since atoms touch along a face diagonal, the repeat distance is $a_0\sqrt{2}/2$, or, equivalently, $2r$. The a_0-r relationship is:

$$a_0(\text{FCC}) = \frac{4r}{\sqrt{2}} \tag{3.3–2}$$

Since each face is shared by two unit cells, there are four atoms per FCC cell $[(8 \times 1/8) + (6 \times 1/2)]$. Examination of Figure 3.3–3 shows that each atom in the FCC structure has 12 nearest neighbors, or CN(FCC) = 12. Consider, for example, the

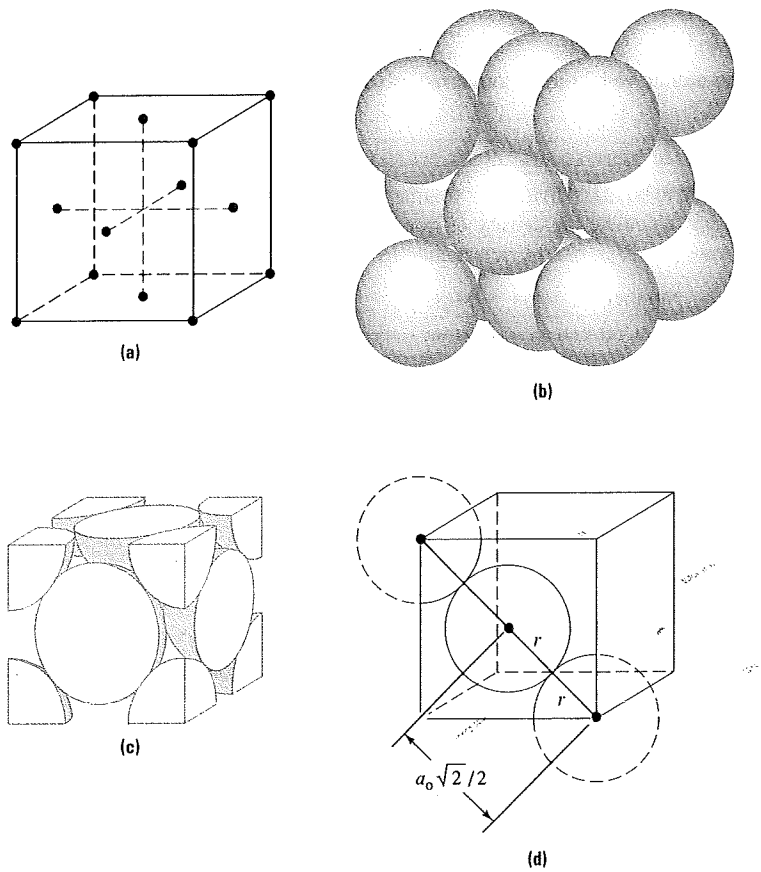

FIGURE 3.3–3 The structure of a face-centered cubic unit cell: **(a)** the point model shows only the locations of the atom centers, **(b)** the full solid sphere model shows all 14 atoms associated with this unit cell, and **(c)** the partial solid sphere model shows just the fractions of each atom contained within this unit cell; **(d)** The distance between adjacent atom centers in FCC can be expressed as either $a_0\sqrt{2}/2$ or, equivalently, $2r$.

atom in the center of the top surface of the cube. Its nearest neighbors are the four atoms in the centers of the vertical faces of the unit cell, the four corner atoms on the top surface of the cell, and the four atoms on the vertical faces of the unit cell that is positioned just above this unit cell.

EXAMPLE 3.3–2

Calculate the density of aluminum. Then discuss why the aerospace industry prefers aluminum-based alloys to iron-based alloys and why iron-based alloys are preferred over aluminum alloys in structural members of bridges and buildings.

Solution

Using the procedure in Example 3.3–1, we find

$$\text{Density} = \frac{M_{uc}}{V_{uc}}$$

with

$$M_{uc} = \left(\frac{\text{Number of atoms}}{\text{Unit cell}}\right) \times \left(\frac{\text{Mass}}{\text{Atom}}\right)$$

and

$$V_{uc} = a_0^3$$

For FCC aluminum,

$$M_{uc} = \left(\frac{4 \text{ atoms}}{\text{FCC unit cell}}\right)\left[(26.98 \text{ g/mol Al})\left(\frac{1 \text{ mol Al}}{6.023 \times 10^{23} \text{ atoms Al}}\right)\right]$$

$$= 1.79 \times 10^{-22} \text{ g/(unit cell)}$$

and

$$V_{uc} = a_0^3 = \left(\frac{4r}{\sqrt{2}}\right)^3 = \left[\frac{4 \times (1.43 \times 10^{-8} \text{ cm})}{\sqrt{2}}\right]^3$$

$$= 6.62 \times 10^{-23} \text{ cm}^3\text{/(unit cell)}$$

Therefore, the density of aluminum is calculated as

$$\rho = \frac{1.79 \times 10^{-22} \text{ g/(unit cell)}}{6.62 \times 10^{-23} \text{ cm}^3\text{/(unit cell)}}$$

$$= 2.70 \text{ g/cm}^3$$

The measured density of aluminum is also 2.70 g/cm^3. A comparison of the density of aluminum with that of iron ($\rho = 7.87$ g/cm^3) partially explains why aluminum alloys are preferred to iron alloys in the aerospace and other industries where minimizing the weight of structures is a critical design parameter. For the same cross-sectional area, steels (iron-based alloys) can sustain higher load levels and can also provide more stiffness against bending compared with aluminum alloys. Thus, if weight is not a consideration but volume of material is important, steel members have a higher load-bearing capacity than aluminum alloys. Other advantages of steel include cost and its weldability compared with aluminum.

3.3.3 Hexagonal Close-Packed Structures

The structure of a hexagonal system is most easily visualized by considering three unit cells arranged to form one larger cell, as shown in Figure 3.3–4a. The larger cell is not a unit cell, since the structure can be completely characterized by an even smaller volume

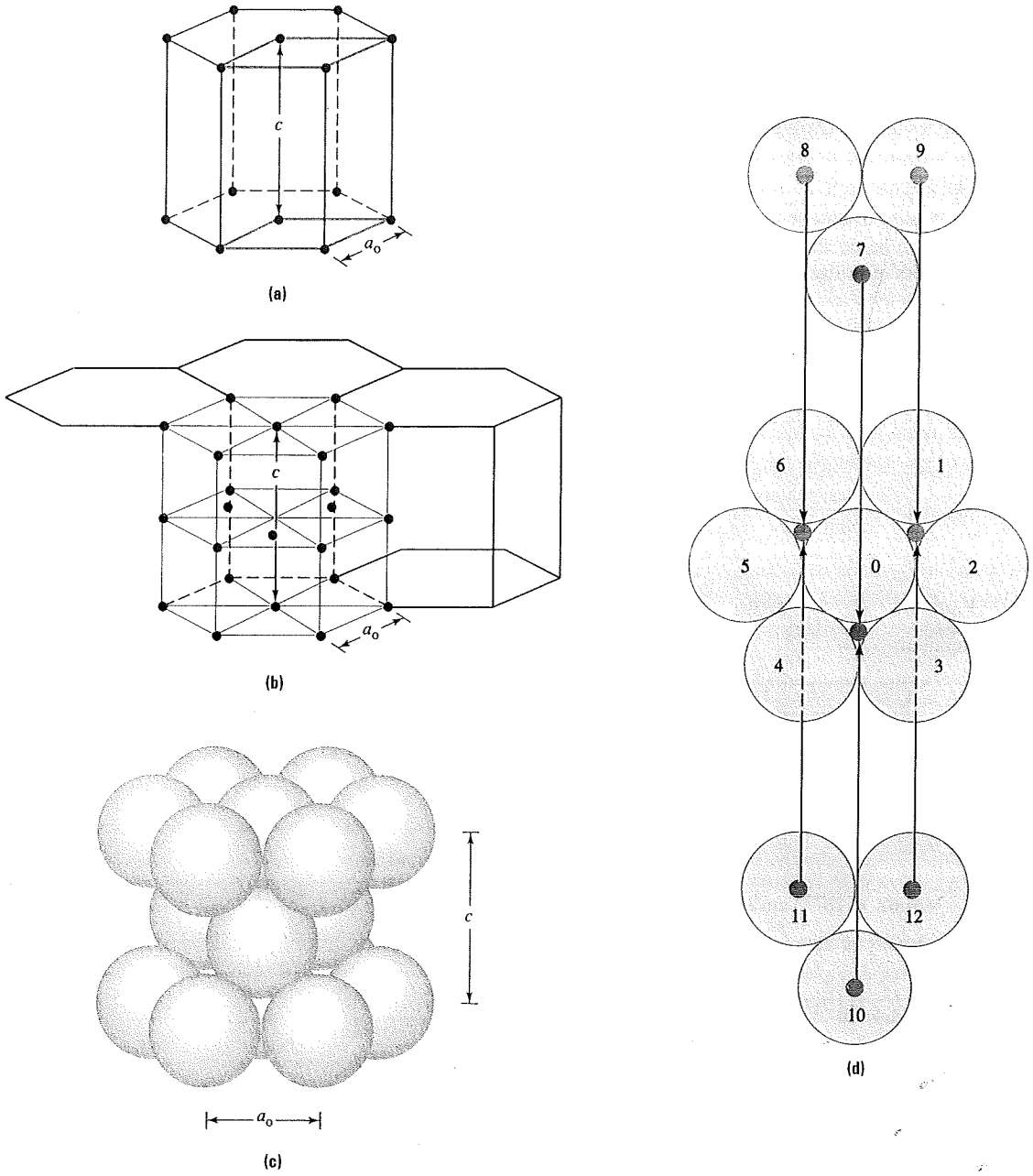

FIGURE 3.3–4 The structure of simple hexagonal (SH) and hexagonal close-packed (HCP) unit cells: **(a)** a point model of an SH unit cell showing the geometric relationship between the smaller primitive unit cell and the more convenient "large" unit cell; **(b)** a point model of the "large" unit cell for the HCP structure showing several neighboring unit cells; **(c)** the full solid sphere model for the HCP structure; and **(d)** an illustration of the 12 nearest neighbors for an atom in an HCP unit cell.

of material. Nevertheless, it is often more convenient to visualize and solve problems using this "big" cell. The upper and lower surfaces of the large cell are hexagons, and the six side faces are rectangles. In the simple hexagonal (SH) structure, atoms are positioned at each corner and in the center of the hexagonal faces. Although the SH structure is not a common crystal structure, one of its variations, the **hexagonal close-packed (HCP)**

structure, is characteristic of many metals, including cadmium, cobalt, magnesium, titanium, yttrium, and zinc at room temperature. The HCP crystal structure is shown in Figure 3.3–4b. Note that there are six atoms at the corners of the top and bottom planes, each shared by six unit cells; one atom in the center of the upper and lower basal planes, each shared by two cells; and three atoms in the midplane. Thus, the total number of atoms in the large HCP cell is six $[(12 \times 1/6) + (2 \times 1/2) + (3 \times 1)]$. Since each large cell consists of three unit cells, each unit cell contains two atoms.

As shown in Figure 3.3–4c, each of the six corner atoms in the top and bottom hexagonal planes, known as the **basal planes,** touches the central atom. If a_0 is defined to be the length of the unit-cell edge, then the a_0-r relationship is simply $a_0 = 2r$. A complete description of the dimensions of the cell, however, requires an expression for its height, or the perpendicular distance between the basal planes. In the ideal HCP unit cell, the height, c, is related to a_0, and hence r, through the expression

$$c = \left(\frac{4}{\sqrt{6}}\right)a_0 = 1.633a_0 = 3.266r \tag{3.3–3}$$

This relationship assumes that the atoms are perfect rigid spheres. Since this assumption is not always satisfied, many real HCP metals display a c/a_0 ratio significantly different from 1.633 (see Table 3.3–1). The volume of a "large" HCP cell is

$$V_{uc}(\text{large HCP}) = \left(\frac{\sqrt{3}}{2}\right)a_0^2 c \tag{3.3–4}$$

The number of nearest neighbors in the HCP system is 12, or CN(HCP) = 12. This can be seen by considering the central atom in the lower basal plane. As shown in Figure 3.3–4a, this atom has six nearest neighbors in its own plane and three nearest neighbors in the parallel planes above and below.

TABLE 3.3–1 The c/a ratios for selected HCP metals at room temperature.

Metal	c/a ratio
Cd	1.886
Zn	1.856
"Ideal" HCP	1.633
Mg	1.624
Co	1.621
Zr	1.593
Ti	1.587
Be	1.568

3.4 MILLER INDICES

In this section we introduce the notation known as **Miller indices,** which is the most common convention used to describe specific points, directions, and planes in the crystal-lattice systems. Before proceeding with the details of the convention, however, we show the need for indexing using an example. Consider the geometry shown in Figure 3.4–1. In the next chapter we will need to know the angle between the direction from left to right along the bottom back edge of the cube and the direction from the bottom back left corner through the center of the cube. The Miller index notation not only simplifies the

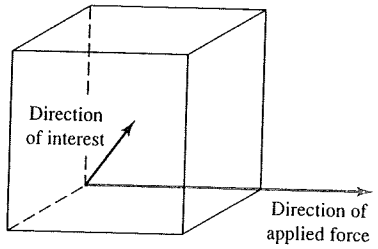

FIGURE 3.4–1 Examples of two directions, in a cubic unit cell. The direction of the applied force can be described as a projection from the bottom back left corner of the cube through the bottom back right cube corner. The cumbersome nature of this description provides some of the motivation for the development of a more concise nomenclature for naming points, directions, and planes in crystals.

description of directions, but also permits simple vector operations like the dot and cross products.

3.4.1 Coordinates of Points

The first step in the description of crystal structures is to select a coordinate system. We have elected, as is customary, to use a right-hand Cartesian coordinate system throughout the text. The next step is to orient the coordinate system in the unit cell. As shown in Figure 3.4–2 for a cubic unit cell, the most common orientation is to align the three coordinate axes with the edges of the unit cell, with the origin at a corner of the cell. It is important to note, however, that the choice of an origin is arbitrary, and the selection of an origin is a matter of convenience for each problem under consideration.

Having defined a coordinate system, points within the lattice are written in the form h, k, l, where the three indices correspond to fractions of the lattice parameters a, b, and c. Recall that the lattice parameters a, b, and c correspond to the length of the unit-cell edge in the x, y, and z directions. Hence, with reference to Figure 3.4–2, the three corners along the axes, marked A, B, and C, are 1, 0, 0; 0, 1, 0; and 0, 0, 1. Across the body diagonal at point D, the position is 1, 1, 1. Across the face diagonal the coordinates at E, F, and G are 1, 1, 0; 0, 1, 1; and 1, 0, 1.

FIGURE 3.4–2
Miller indices—h, k, l—for naming points in a crystal lattice. The origin has been arbitrarily selected as the bottom left back corner of the unit cell.

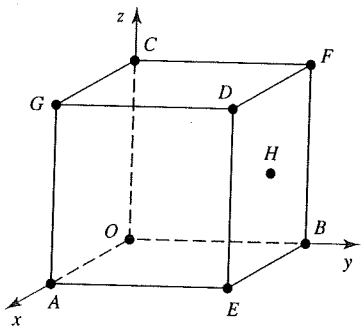

Position	Coordinate
O	0, 0, 0 (Origin)
A	1, 0, 0
B	0, 1, 0
C	0, 0, 1
D	1, 1, 1
E	1, 1, 0
F	0, 1, 1
G	1, 0, 1
H	1/2, 1, 1/2

EXAMPLE 3.4–1

Sketch a cubic unit cell and answer these questions:

a. What are the coordinates of the points located at the centers of the six faces?
b. What are the coordinates of the point at the center of the cube?
c. Locate the point 1/4, 3/4, 1/4.

Solution

A cubic unit cell is sketched in Figure 3.4–3. The first step is to select an origin and orient the coordinate axes. We have elected to use the bottom back left corner of the cube as our origin.

a. As shown in the figure, the six face centers have coordinates 0, 1/2, 1/2; 1/2, 0, 1/2; 1/2, 1/2, 0; 1, 1/2, 1/2; 1/2, 1, 1/2; and 1/2, 1/2, 1.

b. The cube center has coordinates 1/2, 1/2, 1/2.

c. The point 1/4, 3/4, 1/4 can be located by starting at the origin and moving out a distance of 1/4 of a lattice parameter in the x direction, then 3/4 in the y direction, and finally 1/4 in the z direction. This procedure is shown in Figure 3.4–3b.

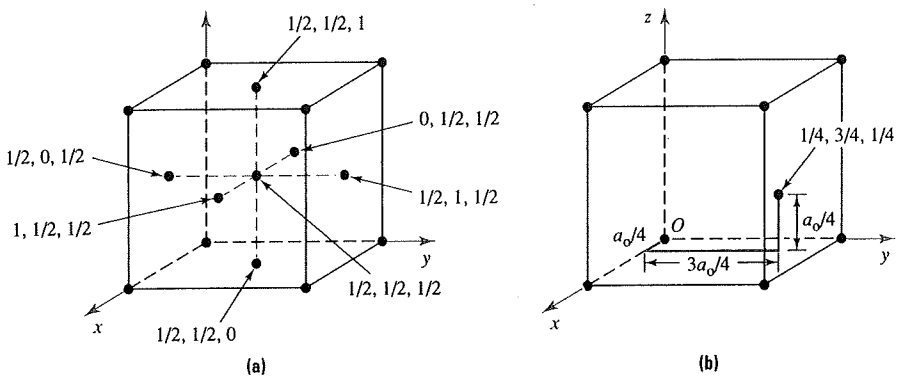

FIGURE 3.4–3 A cubic unit cell with the origin, point *O*, located at the bottom back left corner showing **(a)** the coordinates of the six face centers and the center of the cube, and **(b)** the location of the point 1/4, 3/4, 1/4, which is found by starting at the origin and moving a distance $a_0/4$ in the x direction, then $3a_0/4$ in the y direction, and finally $a_0/4$ in the z direction.

3.4.2 Indices of Directions

Miller indices for directions are obtained using the following procedure:

1. Determine the coordinates of two points that lie in the direction of interest—h_1, k_1, l_1 and h_2, k_2, l_2. The calculation is simplified if the second point corresponds with the origin of the coordinate system.
2. Subtract the coordinates of the second point from those of the first point: $h' = h_1 - h_2$; $k' = k_1 - k_2$; and $l' = l_1 - l_2$.
3. Clear fractions from the differences—h', k', and l'—to give indices in lowest integer values, h, k, and l.
4. Write the indices in square brackets without commas: [h k l].
5. Negative integer values are indicated by placing a bar over the integer. For example, if $h < 0$, we write [$\bar{h}$ k l].

Several examples are shown in Figure 3.4–4. Again we have used a cubic unit cell with the origin at a cube corner, although the technique is not restricted to this simple geometry. The nearest cube corners are in the directions [1 0 0], [0 1 0], and [0 0 1] as well as [$\bar{1}$ 0 0], [0 $\bar{1}$ 0], and [0 0 $\bar{1}$]. The body diagonal is [1 1 1]. The face diagonals are [0 1 1], [1 0 1], and [1 1 0].

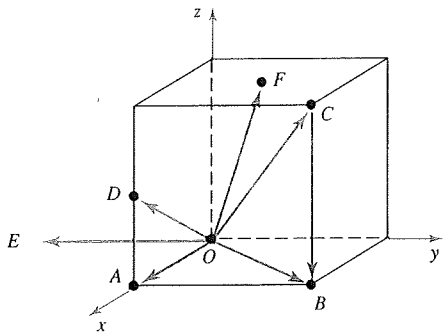

Direction	Indices [h k l]
$\overrightarrow{OA}$	[1 0 0]
$\overrightarrow{OB}$	[1 1 0]
$\overrightarrow{OC}$	[1 1 1]
$\overrightarrow{OD}$	[2 0 1]
$\overrightarrow{OE}$	[0 $\bar{1}$ 0]
$\overrightarrow{OF}$	[1 1 2]
$\overrightarrow{CB}$	[0 0 $\bar{1}$]

FIGURE 3.4–4 Miller indices—[*h k l*]—for naming directions in a crystal lattice. The origin has been arbitrarily selected as the bottom left back corner of the unit cell.

EXAMPLE 3.4–2

Determine the Miller indices of the directions shown in Figure 3.4–1.

Solution

The problem can be simplified by selecting the bottom left back corner of the cube as the origin and defining the *x*, *y*, and *z* axes as shown in Figure 3.4–4. Since the coordinates of the bottom right back corner of the cube are 0, 1, 0, we find:

$$h_1, k_1, l_1 = 0, 1, 0 \qquad \text{and} \qquad h_2, k_2, l_2 = 0, 0, 0 \text{ (the origin)}$$

and $h' = 0$, $k' = 1$, and $l' = 0$. Since there are no fractions to clear, the indices for the direction along the bottom back edge are [0 1 0]. The second direction can be named in a similar way with reference to the point at the center of the cube (i.e., $h_1, k_1, l_1 = 1/2, 1/2, 1/2$). In this case we find $h' = k' = l' = 1/2$. Is the direction then [1/2 1/2 1/2]? No, this notation is invalid, since we have agreed that the indices for directions will always take on integer values. We must clear the fractions in [1/2 1/2 1/2] by multiplying each term by 2 in order to obtain the correct notation, [1 1 1].

If the properties of a crystal are measured in two different directions and found to be identical, then those directions are termed equivalent. For example, the properties of a cubic crystal measured along [1 0 0] are the same as those along [0 $\bar{1}$ 0] or [0 0 1]. Similarly, all the face diagonals are equivalent, and all the body diagonals are equivalent. We refer to these **families of directions** using angle brackets: ⟨*h k l*⟩. Thus, the edges of a cube comprise the family of directions ⟨1 0 0⟩, the face diagonals comprise ⟨1 1 0⟩, and the body diagonals comprise ⟨1 1 1⟩. Note that for cubic unit cells the individual members of a family can be generated by taking all of the permutations of the symbols *h*, *k*, and *l*, using both positive and negative integers.

EXAMPLE 3.4–3

List the individual members of the family of directions ⟨1 1 0⟩ for a cubic unit cell.

Solution

We must find all of the permutations, both positive and negative, of the values 1, 1, and 0: [1 1 0], [1 0 1], [0 1 1], [$\bar{1}$ 1 0], [$\bar{1}$ 0 1], [0 $\bar{1}$ 1], [1 $\bar{1}$ 0], [1 0 $\bar{1}$], [0 1 $\bar{1}$], [$\bar{1}$ $\bar{1}$ 0], [$\bar{1}$ 0 $\bar{1}$], and [0 $\bar{1}$ $\bar{1}$]. It may be useful for you to sketch these 12 directions and convince yourself that they are in fact equivalent.

It is frequently necessary to determine the angle between directions. After you have drawn the directions of interest in a unit cell, it is sometimes possible to determine the angle by inspection. Alternatively, in cubic crystals only, the angle between directions can be determined by taking the vector dot product. If

$$\mathbf{A} = u\mathbf{i} + v\mathbf{j} + w\mathbf{k} \qquad \text{and} \qquad \mathbf{B} = u'\mathbf{i} + v'\mathbf{j} + w'\mathbf{k}$$

then

$$\mathbf{A} \cdot \mathbf{B} = |\mathbf{A}||\mathbf{B}| \cos \theta \tag{3.4–1}$$

where θ is the angle between the two vectors. Solving for θ yields:

$$\theta = \cos^{-1}\left[\frac{uu' + vv' + ww'}{(u^2 + v^2 + w^2)^{1/2}(u'^2 + v'^2 + w'^2)^{1/2}}\right] \tag{3.4–2}$$

Note that because of step 3 in the algorithm used to define directions, in which fractions were cleared to result in indices with integer values, directions do not contain information about length. Consequently, directions are not true vectors. Fortunately, it is still possible to perform vector algebra operations on crystallographic directions, as long as only directional information is utilized. Information related to magnitude has no physical meaning for crystallographic directions.

EXAMPLE 3.4–4

Determine the angle between the directions [0 1 $\bar{1}$] and [0 0 $\bar{1}$].

Solution

By inspection of the sketch shown in Figure 3.4–5 we can see that the angle between the cube edge and the face diagonal is 45°. The solution can also be obtained using Equation 3.4–2:

$$\theta = \cos^{-1}\left[\frac{0 \times 0 + 1 \times 0 + (-1) \times (-1)}{\sqrt{(0 + 1 + 1)}\sqrt{(0 + 0 + 1)}}\right]$$

$$= \cos^{-1}\left(\frac{1}{\sqrt{2}}\right) = 45°$$

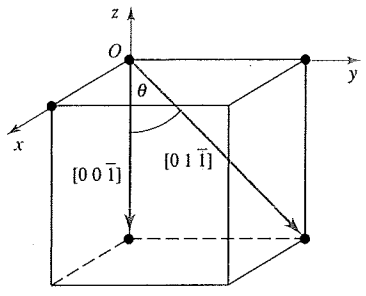

FIGURE 3.4–5 A sketch of a cubic unit cell showing the directions [0 1 $\bar{1}$] and [0 0 $\bar{1}$] and the angle θ between them. The origin was selected as the top left back corner of the cube so that both directions could be drawn within the boundaries of the unit cell.

3.4.3 Indices of Planes

Miller indices for planes are obtained using the following procedure:

1. Identify the coordinate intercepts of the plane, that is, the coordinates at which the plane intersects the x, y, and z axes. If the plane is parallel to one of the axes, the intercept is taken as infinity (∞). If the plane passes through the origin, consider an equivalent plane in an adjacent unit cell or change the location of the origin used to name the plane.
2. Take the reciprocal of the intercepts.
3. Clear fractions, but do not reduce to lowest integers.
4. Cite planes in parentheses—$(h\ k\ l)$—again placing bars over negative indices.

Several examples of planes are shown in Figure 3.4–6. The (1 0 0), (0 1 0), and (0 0 1) planes—the cube faces—are mutually orthogonal. Similarly, (1 1 0) and ($\bar{1}$ 1 0)—the planes that connect opposite edges through face diagonals—are orthogonal. **Families of planes** are expressed in braces: $\{h\ k\ l\}$. All planes in a family are equivalent in that they contain exactly the same arrangement of atoms. In cubic systems the members of a family of planes can be listed by taking all possible permutations of the indices. For example, the members of {1 0 0} are (1 0 0), (0 1 0), and (0 0 1) and their negatives ($\bar{1}$ 0 0), (0 $\bar{1}$ 0), and (0 0 $\bar{1}$).

Working with the indices for directions and planes will familiarize you with several important features and relationships:

1. Planes and their negatives are equivalent. The negatives of directions are not equivalent but rather point in opposite directions.
2. Planes are not necessarily equivalent to their multiples. Directions are invariant to a multiplier.
3. In cubic crystals, a plane and a direction with the same indices are orthogonal.

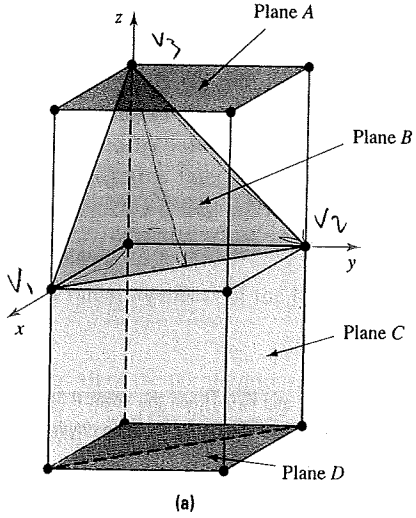

(a)

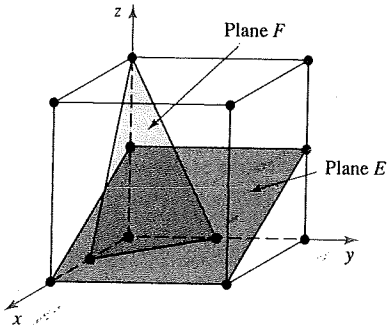

Plane	Intercepts	Indices
A	$\infty, \infty, 1$	(0 0 1)
B	1, 1, 1	(1 1 1)
C	1, 1, ∞	(1 1 0)
D	$\infty, \infty, -1$	(0 0 $\bar{1}$)
E	1, ∞, 1/2	(1 0 2)
F	1/2, 1/2, 1	(2 2 1)

(b)

FIGURE 3.4–6
Miller indices—$(h\ k\ l)$—for naming planes in a crystal lattice. The origin has been arbitrarily selected as the bottom left back corner of the upper unit cell in part **(a)** and the bottom left back corner of the unit cell in part **(b)**.

EXAMPLE 3.4–5

Determine the indices of the planes labeled A and B in Figure 3.4–7a. Then sketch plane (1 $\bar{3}$ 0).

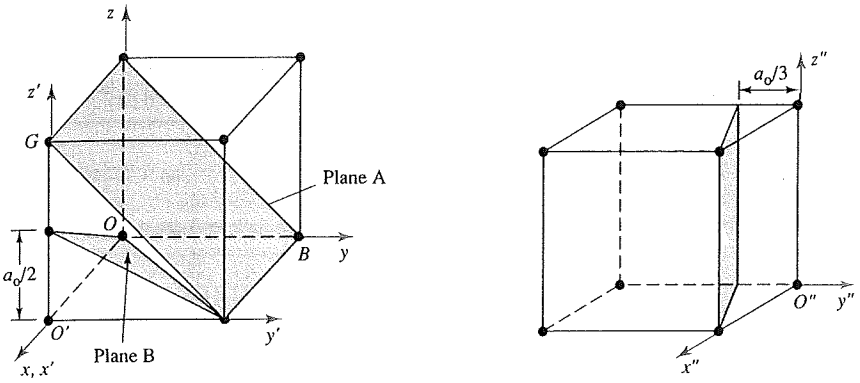

FIGURE 3.4–7 The cubic unit cells, coordinate systems, and planes referred to in Example 3.4–5.

Solution

Plane A can be named by choosing the bottom back left corner of the cube as the origin. Plane A is parallel to the x axis (intercept $= \infty$) and intersects both the y and z axes at 1. Taking reciprocals of the intercepts, plane A is the (0 1 1) plane with respect to origin O. Since plane B passes through O, it cannot be named using the same coordinate axes. What point should we use for the new origin? Although there is no unique answer to this question, a good choice is the front left bottom corner. The intercepts for this origin (O' in the figure) are $x' = -1$, $y' = 1$, and $z' = 1/2$. Taking reciprocals of the intercepts, plane B is the ($\bar{1}$ 1 2) plane with respect to O'. To sketch the plane (1 $\bar{3}$ 0), we note that the reciprocals of the indices are the intercepts: $x = 1, y = -1/3$, and $z = \infty$. The infinite intercept in the z direction means that the plane is parallel to the z axis. Since the x intercept is positive and the y intercept is negative, a good choice for the origin is the bottom back right corner (O'' in the figure). After plotting the x and y intercepts, draw lines through each intercept parallel to the z axis. The two lines define the plane (1 $\bar{3}$ 0).

3.4.4 Indices in the Hexagonal System

The notation used to describe points, directions, and planes in hexagonal lattices is similar to that used in cubic systems. As shown in Figure 3.4–8, there are four crystallographic axes in the hexagonal solid, which are most often referenced with respect to an origin located in the center of the basal plane. The three a axes are contained within the basal plane and the c axis is perpendicular to the basal plane. Since the hexagonal lattice has four coordinate axes rather than the three axes characteristic of the cubic systems, the Miller index convention for hexagonal systems is a bit more complex. Since we will be able to describe most of the important characteristics of HCP crystals without the aid of the numerical naming convention, we have elected to simplify our presentation by omitting the development of such a convention. Instead, we will simply refer to the important directions and planes as the a and c directions and the basal planes.

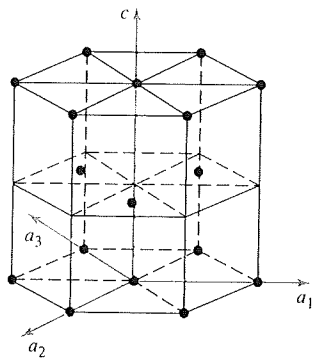

FIGURE 3.4–8
The important directions and planes in hexagonal unit cells.

3.5 DENSITIES AND PACKING FACTORS OF CRYSTALLINE STRUCTURES

The previous sections have introduced some of the terms and notations of crystallography. In the next few sections we use these tools to determine some important characteristics of crystals. In particular, this section deals with the calculation of linear, planar, and volumetric densities.

3.5.1 Linear Density

The **linear density** ρ_L is the number of equivalent lattice points per unit length along a direction. Thus, ρ_L is defined as:

$$\rho_L = \frac{\text{Number of atoms centered along direction within one unit cell}}{\text{Length of the line contained within one unit cell}} \qquad (3.5\text{–}1)$$

As an example, consider the [1 1 0] direction in an FCC crystal, as shown in Figure 3.5–1a. Atoms lie at the endpoints and the center of the face diagonal. Thus, there are three atoms associated with this direction. The two corner atoms, however, are shared with the continuation of the face diagonal in neighboring unit cells. Since some of the atoms are shared, we use weighting factors to determine the actual number of atoms along a face diagonal within a single unit cell. Since this is a linear calculation, the appropriate weighting factors can be envisioned using a linear sketch. Using Figure 3.5–1b, we see that we are interested in the fraction of the atomic diameter that lies within a single unit cell. In the case of ρ_L for [1 1 0] in FCC, therefore, the number of atoms is 2 [i.e., $(2 \times 1/2) + (1 \times 1)$], and the length of the line is $4r$. Thus, using Equation 3.5–1, ρ_L for [1 1 0] in FCC is $1/(2r)$.

The ⟨1 1 0⟩ family of directions has special significance in the FCC structure, since these are the directions in which atoms are in direct contact. As such, ⟨1 1 0⟩ directions have the highest ρ_L of any directions in the FCC system. In any crystal system, the directions with the highest ρ_L are termed the **close-packed directions.**

Note that the weighting factor for a corner atom or any other shared atom depends on the dimension of the calculation. In this linear calculation the corner atom contributed a factor of 1/2 (of a diameter). In contrast, its weighting factor was 1/8 (of a sphere) when we were counting the number of atoms in an FCC unit cell in Section 3.3.2 for a 3-D calculation.

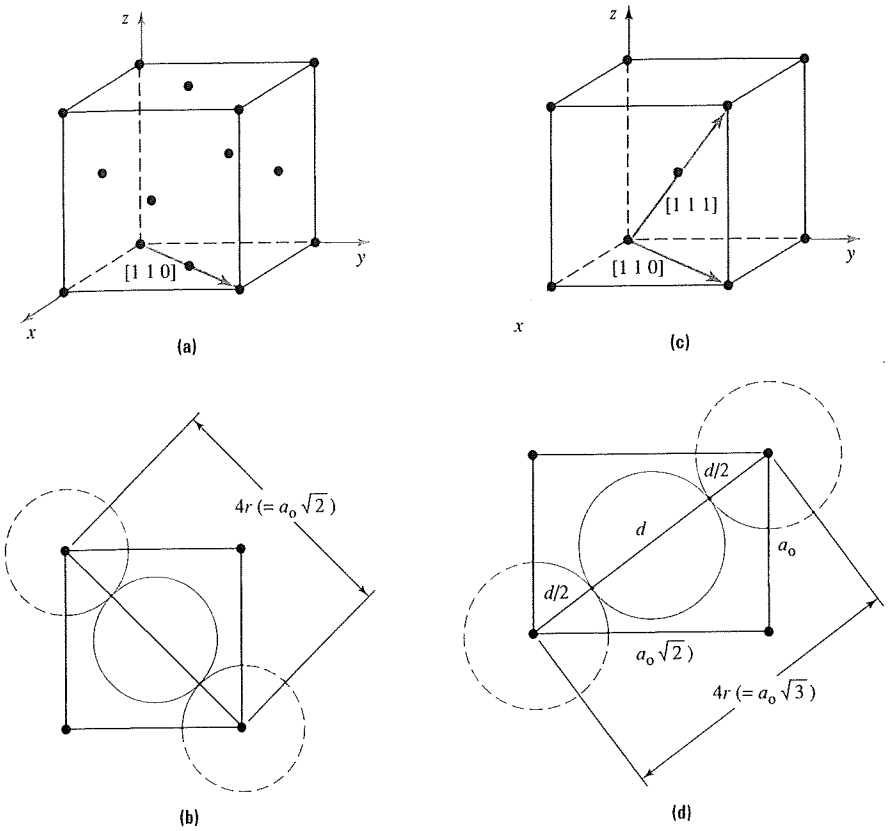

FIGURE 3.5–1 **(a)** The portion of the [1 1 0] direction contained within a single FCC unit cell is sketched in 3-D; **(b)** the same direction sketched in 1-D [shown within the (0 0 $\bar{1}$) plane]; **(c)** the portion of the [1 1 1] direction contained within a single BCC unit cell is sketched in 3-D; **(d)** the same direction sketched in 1-D [shown within the (1 $\bar{1}$ 0) plane].

EXAMPLE 3.5–1

Calculate the linear density along [1 1 1] in a BCC material. Repeat the calculation for the [1 1 0] direction in BCC.

Solution

The appropriate sketches are shown in Figure 3.5–1c and d. Using Equation 3.5–1, we find:

$$\rho_L = \frac{(2 \text{ corner atoms} \times 1/2) + (1 \text{ body-centered atom} \times 1)}{4r}$$

Hence, the linear density along [1 1 1] in a BCC material is also $1/(2r)$. Since this is the direction in which atoms are in direct contact, the ⟨1 1 1⟩ directions are the close-packed directions in the BCC structure. For the [1 1 0] direction:

$$\rho_L = \frac{2 \text{ corner atoms} \times 1/2}{a_0\sqrt{2}} = \frac{\sqrt{3}}{4r\sqrt{2}}$$

where we have made use of the a_0-r relationship for BCC given in Equation 3.3–1. Thus, in BCC the linear density in the close-packed directions is about 63% higher than in the ⟨1 1 0⟩ directions.

3.5.2 Planar Density

Planar density ρ_P is the number of atoms per unit area on a plane of interest. Only atoms centered on the plane are considered, and the weighting factors for shared atoms are based on area fractions. In analogy with Equation 3.5–1, we define ρ_P as:

$$\rho_P = \frac{\text{Number of atoms centered on a plane within one unit cell}}{\text{Area of the plane contained within one unit cell}} \tag{3.5–2}$$

Consider the planer density of the (1 1 1) plane in an FCC crystal. As shown in Figure 3.5–2a and b, the portion of this plane contained within a unit cell is composed of an equilateral triangle. The length of the side of each triangle is $4r$, since atoms are in direct contact along each edge of the triangle (note that each edge is a member of the ⟨1 1 0⟩ family of directions). The area of this triangular plane can be calculated as $4r^2\sqrt{3}$. Next we determine the number of atoms in the plane. Each of the three atoms at the corners of the triangular plane contributes an area fraction of 1/6 (i.e., 60°/360°), and the three atoms along the edges of the triangular plane each contribute an area fraction of 1/2. Thus, the total number of atoms on the plane is two. Using Equation 3.5–2, we find that the planar density on the (1 1 1) plane of an FCC crystal is $1/(2\sqrt{3}r^2)$.

This value of ρ_P represents the highest possible planar density for spherical atoms. Therefore, any plane in any crystal system that has a value of $\rho_P = 1/(2\sqrt{3}r^2)$ will be referred to as a **close-packed plane.** While all crystal systems have close-packed directions, not all systems contain close-packed planes. For any specific crystal system, however, there will be a family of planes with a maximum ρ_P value for that system. We will

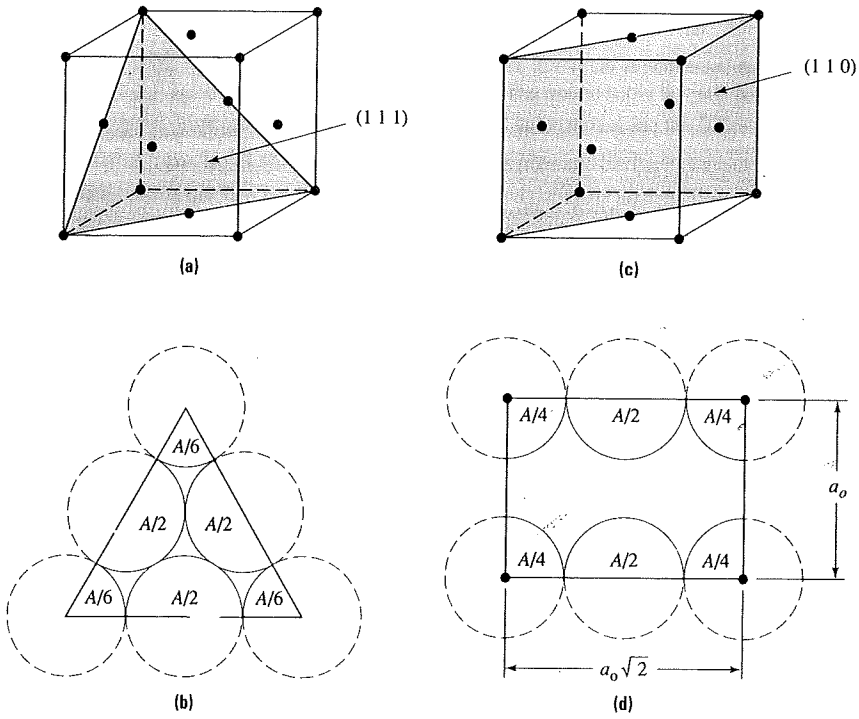

FIGURE 3.5–2 **(a)** The portion of the (1 1 1) plane contained within a single FCC unit cell is sketched in 3-D; **(b)** the same plane sketched in 2-D; **(c)** the portion of the (1 1 0) plane contained within a single FCC unit cell is sketched in 3-D; **(d)** the same plane sketched in 2-D.

TABLE 3.5–1 The close-packed directions and highest-density planes in the BCC, FCC, and HCP crystal structures.

Crystal structure	Close-packed directions	Highest-density planes	Are the highest-density planes close-packed?
BCC	⟨1 1 1⟩	{1 1 0}	No
FCC	⟨1 1 0⟩	{1 1 1}	Yes
HCP	a	Basal	Yes

refer to these planes as the **highest-density planes.** By our definitions all close-packed planes are highest-density planes, but not all highest-density planes are close-packed planes. Table 3.5–1 lists the close-packed directions and the highest-density planes for the BCC, FCC, and HCP crystal structures.

EXAMPLE 3.5–2

Determine the planar density of (1 1 0) in an FCC crystal.

Solution

The appropriate sketches are shown in Figure 3.5–2c and d. Using Equation 3.5–2, we find:

$$\rho_P = \frac{(4 \text{ corners} \times 1/4) + (2 \text{ face centers} \times 1/2)}{a_0 \times a_0\sqrt{2}} = \frac{2}{a_0^2\sqrt{2}}$$

Using $a_0(\text{FCC}) = 4r/\sqrt{2}$, as given in Equation 3.3–2, we find:

$$\rho_P = \left(\frac{2}{\sqrt{2}}\right)\left(\frac{\sqrt{2}}{4r}\right)^2 = \frac{1}{4\sqrt{2}r^2}$$

The planar density of (1 1 0) in FCC is $1/(4\sqrt{2}r^2)$. It is interesting to compare this value with the corresponding ρ_P value for the (1 1 1) plane in FCC [$= 1/(2\sqrt{3}r^2)$]. ρ_P on the (1 1 0) planes is only about 61% of that on the close-packed planes.

EXAMPLE 3.5–3

The highest-density planes in the BCC structure are the (1 1 0) planes. Determine the planar density of (1 1 0) in a BCC crystal, then compare this value with the planar density of the close-packed planes in the FCC structure.

Solution

Using the same procedure as in the previous example, we find:

$$\rho_P = \frac{(4 \text{ corners} \times 1/4) + (1 \text{ body center} \times 1)}{a_0 \times a_0\sqrt{2}} = \frac{2}{a_0^2\sqrt{2}}$$

Using $a_0(\text{BCC}) = 4r/\sqrt{3}$, as given in Equation 3.3–1, we find:

$$\rho_P = \left(\frac{2}{\sqrt{2}}\right)\left(\frac{\sqrt{3}}{4r}\right)^2 = \frac{3}{8\sqrt{2}r^2}$$

Thus, ρ_P of (1 1 0) in BCC is $3/(8\sqrt{2}r^2)$. Comparing this with ρ_P of (1 1 1) in FCC [$= 1/(2\sqrt{3}r^2)$], we find that the value for the highest-density planes in BCC is about 92% of that for the close-packed planes in FCC. We will learn later that this result explains in part the difference in the mechanical properties of BCC and FCC metals.

3.5.3 Volumetric Density

Volumetric density (ρ_V) is the number of atoms per unit volume. The weighting factors for shared atoms are based on volume fractions.

Consider an FCC crystal. As shown previously, there are four atoms per unit cell. The cell volume is $V = a_0^3 = (4r/\sqrt{2})^3 = 16\sqrt{2}r^3$. Thus, ρ_V for FCC is $4/(16\sqrt{2}r^3) = 1/(4\sqrt{2}r^3)$. This is the highest volumetric density possible for spherical atoms. Crystal structures that display this value of ρ_V will be referred to as **close-packed structures.** As the name suggests, HCP crystals also have $\rho_V = 1/(4\sqrt{2}r^3)$.

EXAMPLE 3.5–4

Verify that $\rho_V = 1/(4\sqrt{2}r^3)$ for HCP.

Solution

The volume of the "big" HCP unit cell is equal to the area of the basal plane multiplied by the height of the cell. As shown in Figure 3.3–4b, the basal plane is composed of six equilateral triangles. The side of each triangle is $2r$, since atoms are centered at each apex and touch at the midpoint of each side. The area of each triangle can be calculated as:

$$\text{Area} = \left(\frac{1}{2}\right)b \times h = \left(\frac{1}{2}\right)(2r)(r\sqrt{3}) = r^2\sqrt{3}$$

The area of the basal plane is then $6r^2\sqrt{3}$. Combining this result with the $c:r$ relationship, $c = (8/\sqrt{6}r)$, yields:

$$V(\text{HCP}) = (6\sqrt{3}r^2)\left(\frac{8}{\sqrt{6}}\right)r = 24\sqrt{2}r^3$$

The number of atoms in the "big" HCP unit cell has been shown previously to be six. Therefore,

$$\rho_V(\text{HCP}) = \frac{6}{24\sqrt{2}r^3} = \frac{1}{4\sqrt{2}r^3}$$

3.5.4 Atomic Packing Factors and Coordination Numbers

The ratio of the volume occupied by the atoms to the total available volume is defined to be the **atomic packing factor (APF)** for the crystal structure. Thus, APF is calculated using any of the following equivalent expressions:

$$\text{APF} = \frac{\text{Volume of atoms in the unit cell}}{\text{Volume of the unit cell}} \tag{3.5–3a}$$

or

$$\text{APF} = \frac{(\text{Number of atoms in cell}) \times (\text{Volume of an atom})}{\text{Volume of the unit cell}} \tag{3.5–3b}$$

or

$$\text{APF} = \rho_V\left[\left(\frac{4}{3}\right)\pi r^3\right] \tag{3.5–3c}$$

For the crystal structures discussed previously: APF(SC) = 0.52, APF(BCC) = 0.68, and APF(FCC) = APF(HCP) = 0.74. It should not be surprising to find that the highest APFs occur for the two close-packed structures.

Why is it that most metals have either the FCC or the HCP structure whereas no important metals have the SC structure? It has been shown previously that it is energetically favorable for atoms to arrange themselves in a way that leads to the tightest packing and highest coordination numbers possible within the constraints of atom size (and valence in the case of covalent bonds). Combining the above information about APFs with a listing of the CNs for the various metal structures [CN(SC) = 6, CN(BCC) = 8, and CN(FCC) = CN(HCP) = 12] provides the answer to this question. In most cases one of the two close-packed structures represents the energetically favored arrangement of atoms. The SC structure is the least favorable atomic arrangement, and BCC is intermediate. In the next section we will investigate the differences between FCC and HCP structures.

EXAMPLE 3.5–5

Use a calculation to verify that the APF for the BCC structure is 0.68.

Solution

As discussed in Section 3.3.1, there are two atoms per cell in the BCC structure, and the $a_0 : r$ relationship is $a_0(\text{BCC}) = 4r/\sqrt{3}$. Substituting these values into the definition of APF given in Equation 3.5–3b yields:

$$\text{APF(BCC)} = \frac{2[(4/3)\pi r^3]}{(4r/\sqrt{3})^3} = \frac{\pi\sqrt{3}}{8} = 0.68$$

3.5.5 Close-Packed Structures

Although the FCC and HCP structures are similar, they have important fundamental differences. Both structures are characterized by an APF of 74% and a CN of 12. Both have sets of planes with the highest possible planar density, the close-packed planes; and both have directions with the highest possible linear density, the close-packed directions. The difference between the structures is in the arrangement of their close-packed planes.

Stacking sequence can be visualized by looking along the c direction in the HCP structure and along $[1\ \bar{1}\ 1]$ in the FCC structure, as shown in Figure 3.5–3a and b. Consider the arrangement of atoms on one of the close-packed planes. Each atom is surrounded by six nearest neighbors in that plane. When a second layer of close-packed atoms is placed on top of the first layer, the atoms in the second layer do not lie directly on top of the atoms in the first layer. Rather, they lie in wells directly above the centers of the "holes" in the first layer (see Figure 3.5–3c).

There are two viable options for the placement of the third layer. One is to position each atom in the third layer directly above an atom in the first layer. This arrangement is shown in Figure 3.5–4b and corresponds to the HCP structure. The other option is to place the atoms in the third layer above the "holes" in the first layer that were not covered by atoms in the second layer. This arrangement, shown in Figure 3.5–4a, corresponds to the FCC structure. Thus, the distinction between HCP and FCC is in the placement of the third layer of close-packed atoms.

If we refer to any close-packed layer with its atoms in the positions associated with the first layer as an "A" layer, those layers with atoms positioned as in the second layer as "B" layers, and those with atoms positioned above the holes in both the A and B layers as "C" layers, then the stacking sequence in HCP is ABABAB . . . and the sequence in FCC is ABCABC . . . (see Figure 3.5–4).

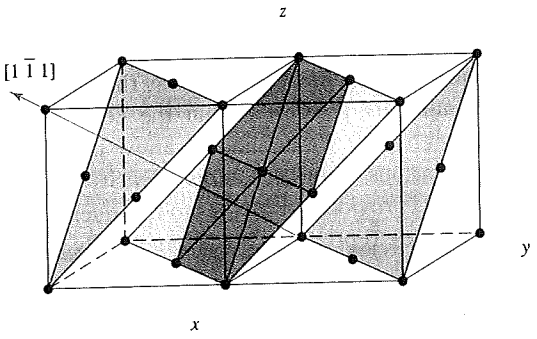

(a)

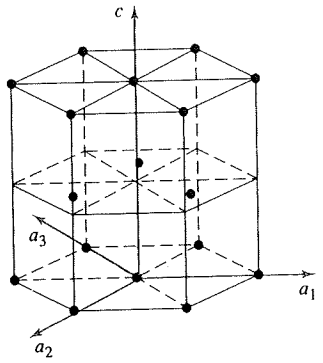

(b)

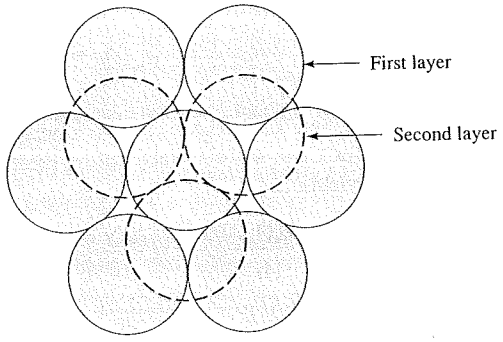

(c)

FIGURE 3.5–3 The stacking sequence of close-packed planes as viewed along **(a)** the [1 1̄ 1] direction in an FCC unit cell and **(b)** the *c* direction in an HCP unit cell. **(c)** The atoms in the second layer lie in wells directly above the centers of the "holes" in the first layer.

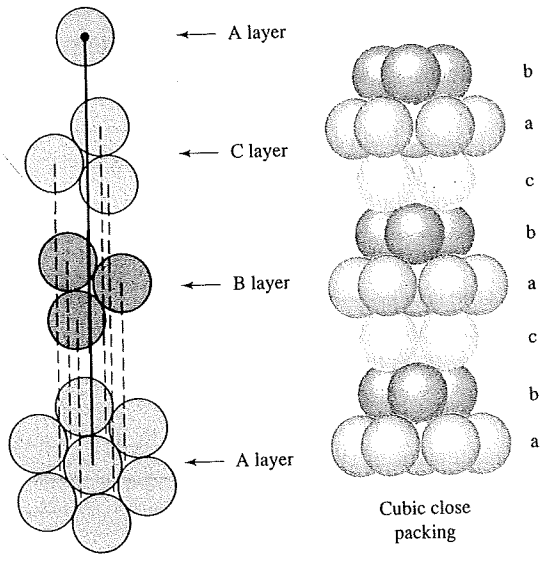

(a)

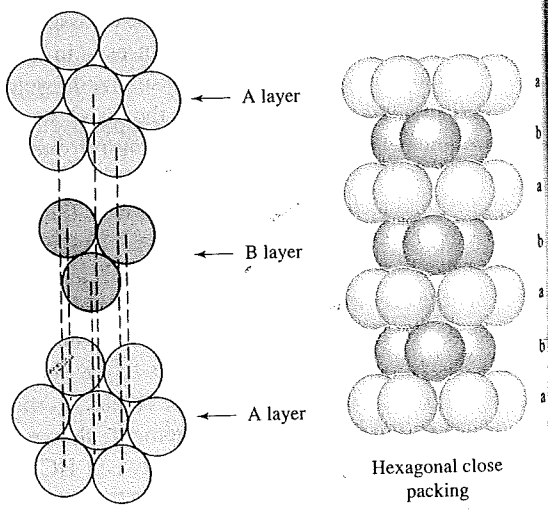

(b)

Illustrations of the stacking sequence of close-packed planes in **(a)** the FCC structure and **(b)** the HCP structure. Note that the stacking sequence is ABCABC . . . in FCC and ABABAB . . . in HCP.

3.6 INTERSTITIAL POSITIONS AND SIZES

The 3-D lattices that we have described are not completely filled with atoms (APF < 1.0 for all crystals). There are spaces around all and between some of the atoms. In this section we will investigate the size and position of the largest holes, or **interstices,** in the FCC, BCC, and HCP systems. We will then discuss crystals that contain more than one type of atom. As a rule, small atoms are positioned in the larger interstices. In ionic structures, positioning of the smaller ions depends on the stoichiometry of the compound, the charge on the ions, and the radius ratio.

3.6.1 Interstices in the FCC Structure

The largest hole in an FCC structure is at the center of the unit cell, as shown in Figure 3.6–1a. It is at this position that the largest sphere can be fitted into the cubic close-packed structure. The CN of an atom placed in this position is 6, since the atoms in the center of each face are equidistant. The polyhedron that connects the equidistant atoms can be used to describe the geometry of the interstitial site. In this case it has eight sides. Hence, this type of interstice is called an **octahedral site.** Equivalent sites are located at the center of each edge. These edge sites are shared among four unit cells. Hence there are four [i.e., $(12 \times 1/4) + (1 \times 1)$] octahedral sites per FCC unit cell.

The size of the octahedral holes is defined as the radius of the largest sphere that can be placed within it. It can be calculated from the geometry of the structure. As shown in Figure 3.6–1, the distance from the center of the top face to the center of the bottom face is equal to the lattice parameter a_0 for the unit cell. If κ is the radius of the hole, then $a_0 = 2r + 2\kappa$. Using the a_0-r relationship in FCC [$a_0(\text{FCC}) = 4r/\sqrt{2}$] and solving for the radius ratio yields $\kappa/r = 0.414$. Thus, an atom roughly 40% of the size of the host atoms can "fit" into an octahedral interstitial position in the FCC structure.

The FCC structure also contains **tetrahedral sites,** as shown in Figure 3.6–1b. These sites are bounded by four atoms and lie completely within the cell in the $l/4$, $m/4$, $n/4$ positions, where l, m, and n are 1 or 3. Each cell contains eight of these 1/4, 1/4, 1/4–type tetrahedral sites. Using arguments similar to those employed above, it can be shown that the κ/r ratio for tetrahedral sites is 0.225. This means that atoms up to ~20% of the size of the host atoms can "fit" in the tetrahedral interstitial positions in FCC structures. Note the similarities between the κ/r ratios for sizing interstitial holes in the FCC structure and the critical r/R ratios for determining CNs in ionic compounds (see Table 2.6–1). This should not be surprising, since the relevant geometries are identical. In summary, while there are twice as many tetrahedral sites as there are octahedral sites, each tetrahedral site is only about half the diameter of an octahedral site in the FCC structure.

EXAMPLE 3.6–1

Determine whether it is possible for a hydrogen atom to fit into either a tetrahedral or an octahedral site in FCC aluminum.

Solution

Using Appendix C, we find that $r(\text{H}) = 0.046$ nm and $r(\text{Al}) = 0.143$ nm. The important radius ratio is $r(\text{H})/r(\text{Al}) = 0.046/0.143 = 0.32$. Comparing this value with the critical κ/r ratios in the text (i.e., $\kappa/r \leq 0.414$ for octahedral sites and $\kappa/r \leq 0.225$ for tetrahedral sites) shows that H can fit only into the octahedral interstitial positions in Al.

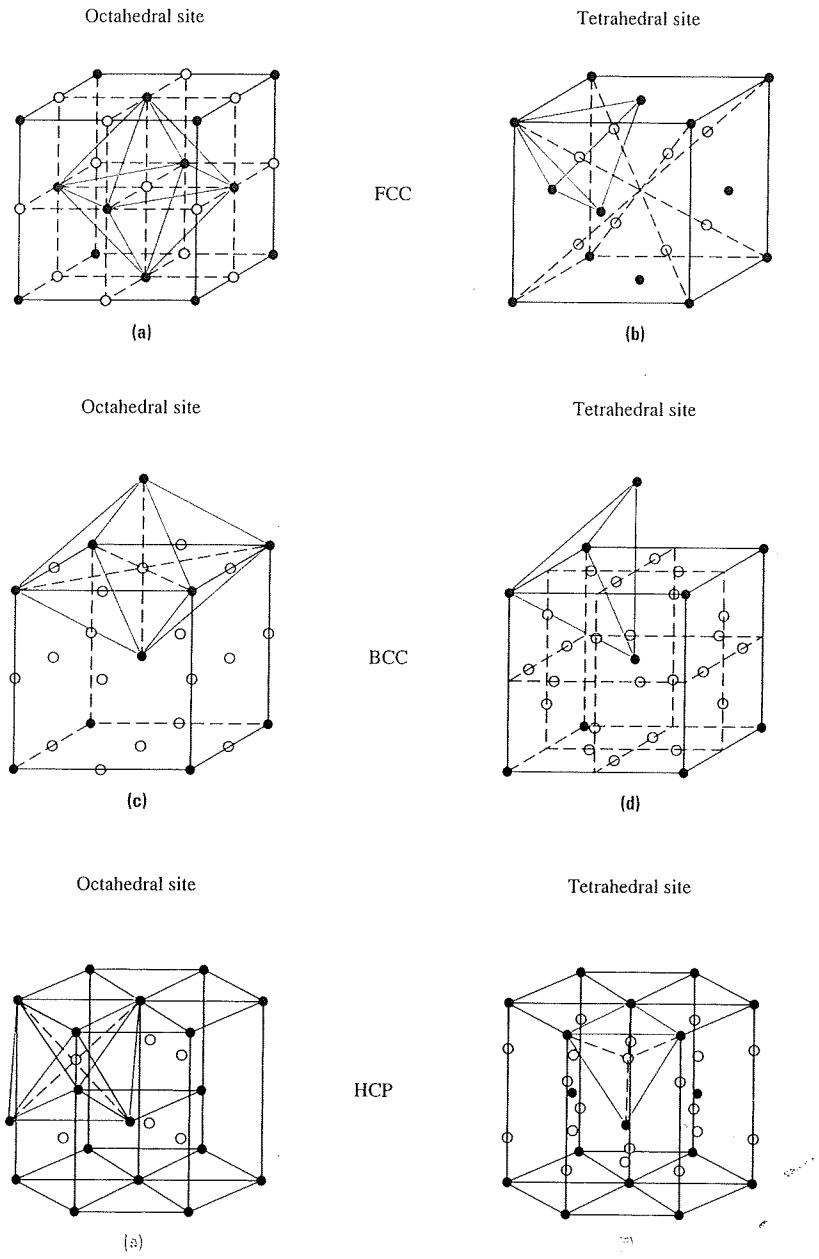

FIGURE 3.6–1
The locations of the interstitial sites in the common crystal structures: **(a)** octahedral sites in FCC, **(b)** tetrahedral sites in FCC, **(c)** octahedral sites in BCC, **(d)** tetrahedral sites in BCC, **(e)** octahedral sites in HCP, and **(f)** tetrahedral sites in HCP.

3.6.2 Interstices in the BCC Structure

Like the FCC structure, the BCC structure also contains both octahedral and tetrahedral sites. As shown in Figure 3.6–1c, the octahedral sites are located in the center of each face and the center of each edge, giving a total of six sites per unit cell. The diameter of the octahedral site cannot be determined by examination of the face diagonal. The BCC structure is not a close-packed structure, and the atoms that surround the interstitial site are not all equidistant neighbors. When the largest possible atom occupies the octahedral position, the atoms touch only along ⟨1 0 0⟩ as measured from one central atom to

another. Hence, $a_0 = 2r + 2\kappa$. Using the a_0-r relationship in BCC [a_0(BCC) = $4r/\sqrt{3}$] and solving for the radius ratio yields $\kappa/r = 0.155$.

The tetrahedral sites in BCC structures are located in the 1/4, 1/2, 0–type positions, which are on the {1 0 0} faces, as shown in Figure 3.6–1d. There are 24 such sites, each shared with another cell, for a total of 12 tetrahedral sites per unit cell. The diameter of the largest atom that just fits into the tetrahedral site can be calculated by considering atomic packing along ⟨2 1 0⟩ and is found to be $\kappa/r = 0.291$. Note that the tetrahedral sites in the BCC structure are more numerous and larger than the octahedral sites.

EXAMPLE 3.6–2

Determine whether it is possible for a carbon atom to dissolve in BCC iron.

Solution

Using Appendix C, we find: r(C) = 0.077 nm and r(Fe) = 0.124 nm. Hence, r(C)/r(Fe) = 0.077/0.124 = 0.62. Comparing this with the critical κ/r ratios given in the previous section ($\kappa/r \leq 0.155$ for octahedral sites and $\kappa/r \leq 0.291$ for tetrahedral sites), we find that C does not fit easily into either type of interstitial position in BCC Fe. We will learn later that this is one of the key reasons for the high strength of steel alloys, which are composed of a mixture of small amounts of C in Fe. In addition, this "misfit" limits the solubility of C in the Fe crystal structure.

3.6.3 Interstices in the HCP Structure

As anticipated, the HCP structure also contains both octahedral and tetrahedral interstices. The positions of the interstices are shown in Figure 3.6–1e and f. There are 6 octahedral sites per "big" cell or 2 sites per unit cell and 12 tetrahedral sites per big cell or 4 per unit cell. Since both FCC and HCP are close-packed crystal structures, the relative sizes of the interstitial sites are the same in these two types of crystals. Table 3.6–1 summarizes the number and size of the tetrahedral and octahedral interstitial sites in the BCC, FCC, and HCP structures.

TABLE 3.6–1 The size and number of tetrahedral and octahedral interstitial sites in the BCC, FCC, and HCP crystal structures. The sizes of the interstitial sites are given in terms of the radius ratio (κ/r) where κ is the radius of the largest atom that can "fit" into the interstitial position and r is the radius of the host atoms. The number of interstitial sites is given in terms of both the number of sites per cell and, in parentheses, the number of sites per host atom.

Crystal structure	Size of tetrahedral sites	Size of octahedral sites	Number of tetrahedral sites per unit cell (per host atom)	Number of octahedral sites per unit cell (per host atom)
BCC	$\kappa/r = 0.291$	$\kappa/r = 0.155$	12 (6)	6 (3)
FCC	$\kappa/r = 0.225$	$\kappa/r = 0.414$	8 (2)	4 (1)
HCP	$\kappa/r = 0.225$	$\kappa/r = 0.414$	12 (2)	6 (1)

3.7 CRYSTALS WITH MULTIPLE ATOMS PER LATTICE SITE

In this section we expand our list of crystal structures to include systems with a basis of two or more atoms, that is, with multiple atoms per lattice point. In some cases the atoms are the same; in other cases the atoms are different. Examples of a 2-D lattice with a basis containing multiple characters can be found in the prints by the artist M. C. Escher shown in Figure 3.7–1.

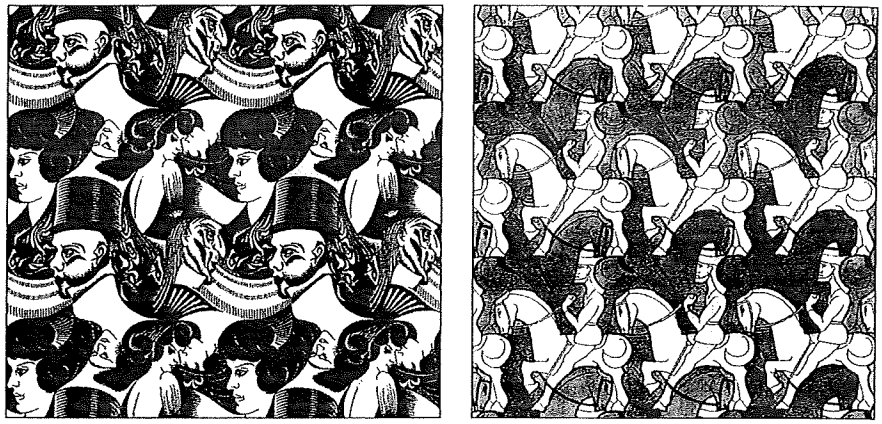

FIGURE 3.7–1
Examples of the work of artist M. C. Escher showing a two-dimensional pattern with a complex basis involving more than one character. *(Source: © 1994 M. C. Escher/Cordon Art, Baarn, Holland. All rights reserved.)*

3.7.1 Crystals with Two Atoms per Lattice Site

The Cesium Chloride Structure

Cesium chloride is an ionic solid. Its crystal structure, shown in Figure 3.7–2a, is composed of a simple cubic lattice with two ions, one of each type, per lattice position. One of the ions is centered on each lattice point, and the other is positioned at a distance of $a_0\sqrt{3}/2$ in the $[1\ 1\ \bar{1}]$ direction with respect to each lattice position. This structure is not a BCC structure, because there are two different atoms present. In this case the center position is not equivalent to a corner position. As shown in Figure 3.7–2b, the CsCl structure can be envisioned as a pair of interwoven SC lattices. This model clearly demonstrates the symmetry of the CsCl structure. Either atom can reside in cube corners with the other atom at the cube center.

The coordination number for each ion in the CsCl structure is 8, and there is one ion of each type per unit cell. The lattice constant can be readily determined by noting that ions touch along the body diagonal. Thus,

$$\frac{a_0\sqrt{3}}{2} = r + R \qquad \text{or} \qquad a_0(\text{CsCl}) = \frac{2(r+R)}{\sqrt{3}} \tag{3.7–1}$$

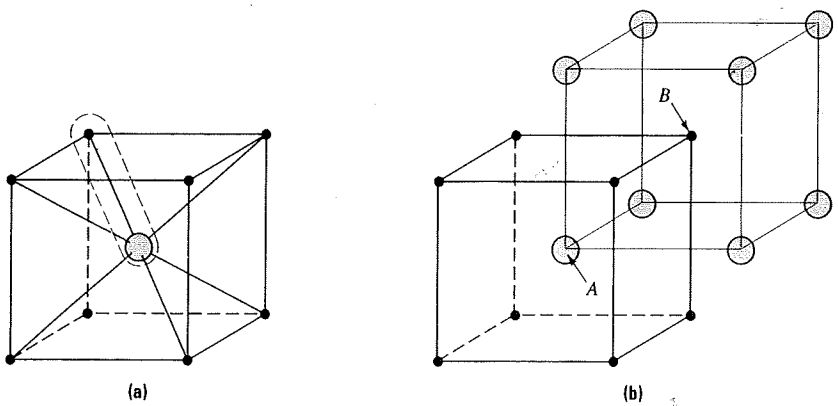

FIGURE 3.7–2 The CsCl crystal structure: **(a)** A simple cubic lattice with two different atoms per lattice point; **(b)** Alternatively, the structure can be viewed as a pair of interwoven simple cubic lattices.

Although there are other ionic solids with the CsCl structure, such as CsBr and CsI, the structure also occurs in other types of materials. For example, when equal numbers of copper and zinc atoms are mixed, they can crystallize under certain conditions into the CsCl structure.

EXAMPLE 3.7–1

Calculate the theoretical density of CsCl.

Solution

From Appendix B we find that the atomic weights of Cs and Cl are 132.9 g/mol and 35.45 g/mol. From Appendix C, $r(Cs^+) = 0.167$ nm and $R(Cl^-) = 0.181$ nm. Using the same procedure as in Example 3.3–1, we find:

$$\text{Density} = \frac{M_{uc}}{V_{uc}}$$

with

$$M_{uc} = \left(\frac{\text{Number of ions}}{\text{Unit cell}}\right) \times \left(\frac{\text{Mass}}{\text{Ion}}\right)$$

For CsCl,

$$M_{uc} = \left(\frac{1\ Cs^+}{\text{Cell}}\right)\left(\frac{\text{At. wt. Cs}}{\text{Avogadro's number}}\right) + \left(\frac{1\ Cl^-}{\text{Cell}}\right)\left(\frac{\text{At. wt. Cl}}{\text{Avogadro's number}}\right)$$

$$= (132.9\ \text{g/mol Cs})\left(\frac{1\ \text{mol}}{6.023 \times 10^{23}\ \text{atoms}}\right) + (35.45\ \text{g/mol Cl})\left(\frac{1\ \text{mol}}{6.023 \times 10^{23}\ \text{atoms}}\right)$$

$$= 2.80 \times 10^{-22}\ \text{g/(unit cell)}$$

Using Equation 3.7–1:

$$V_{uc} = a_0^3 = \left\{\frac{2[r(Cs^+) + R(Cl^-)]}{\sqrt{3}}\right\}^3 = \left[\frac{2(1.67 + 1.81) \times 10^{-8}\ \text{cm}}{\sqrt{3}}\right]^3$$

$$= 6.49 \times 10^{-23}\ \text{cm}^3\text{/(unit cell)}$$

Therefore,

$$\rho(\text{CsCl}) = \frac{2.80 \times 10^{-22}\ \text{g/cell}}{6.49 \times 10^{-23}\ \text{cm}^3\text{/cell}} = 4.31\ \text{g/cm}^3$$

The experimental density of CsCl is 3.99 g/cm^3.

The Sodium Chloride Structure

As shown in Figure 3.7–3a, the NaCl structure is composed of an FCC arrangement of anions complemented with cations located in all of the octahedral positions. A more precise definition of the NaCl structure is an FCC lattice with a basis of two different atoms—one ion type is located on the FCC positions and the other ion type is positioned at a distance of $a_0/2$ in the [1 0 0] direction with respect to each lattice position. Figure 3.7–3b shows that the NaCl structure can be envisioned as a pair of interwoven FCC lattices.

There are four ions of each type in the NaCl structure, and the a_0-r relationship is $a_0(\text{NaCl}) = 2(r + R)$. Ions touch along the cube edge. Other compounds with this

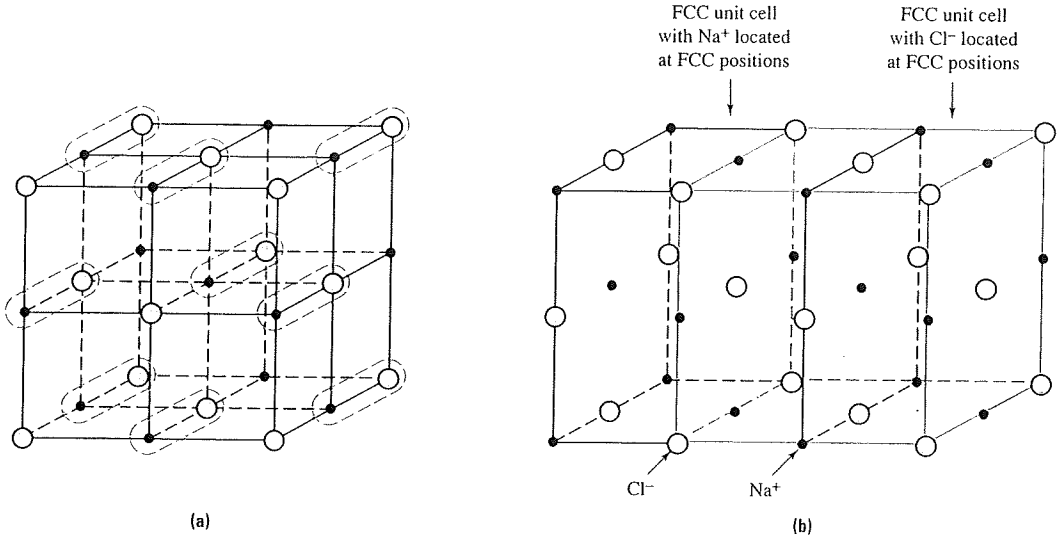

FIGURE 3.7–3 The NaCl crystal structure: **(a)** An FCC lattice with two different atoms per lattice point; **(b)** Alternatively, the structure can be viewed as a pair of interwoven FCC lattices.

structure are all ceramics and include a number of metal oxides (MgO, CaO, SrO, FeO, BaO, MnO, NiO) and alkali halides (KCl).

The Diamond Cubic Structure

One of the crystalline forms of pure carbon is diamond. In the diamond cubic crystal structure, shown in Figure 3.7–4a, the atoms are arranged on an FCC lattice with additional atoms in half of the tetrahedral or 1/4, 1/4, 1/4–type positions. Alternatively, this structure can be described as having two atoms per site—one centered on each FCC position and the other located at a distance of $a_0\sqrt{3}/4$ in the $[1\ 1\ \bar{1}]$ direction with respect to each lattice position. Note that there are eight atoms per unit cell.

Why would carbon atoms assume this structure rather than any of those previously mentioned? The answer is that it must represent a lower-energy arrangement than any of the other structures. But why is this so? As discussed in Chapter 2, the covalent bonding in diamond requires that CN = 4 and that the C-C-C bond angle be 109.5°. While none

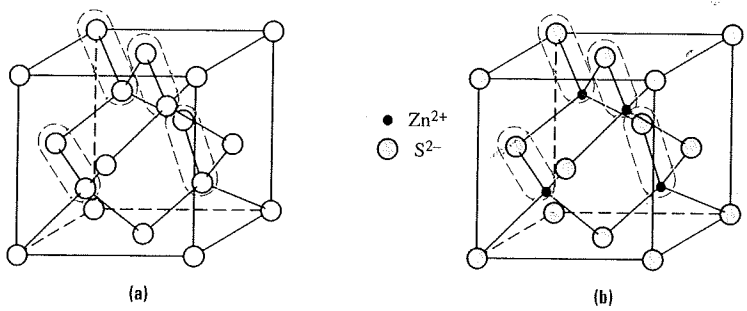

FIGURE 3.7–4 **(a)** The diamond cubic crystal structure is composed of an FCC lattice with two atoms per lattice point. One atom from each pair is centered on each lattice point, and the second atom is positioned at $(a_0\sqrt{3}/4)$ $[1\ 1\ \bar{1}]$. **(b)** The zinc blende crystal structure is similar to the diamond cubic structure, except that the basis is composed of two different atoms.

of the previous structures satisfy these requirements, a examination of Figure 3.7–4a shows that the diamond cubic crystal structure fulfills the bonding criteria. The a_0-r relationship is a_0 (diamond cubic) $= 8r/\sqrt{3}$. Atoms touch along 1/4 of the body diagonal. Carbon is not the only material to have this structure. Silicon and germanium, both covalent semiconductors, crystallize in the diamond cubic structure.

The Zinc Blende Structure

As shown in Figure 3.7–4b, the zinc blende structure is similar to the diamond cubic structure. Atoms are located in the same positions, but here the two atoms per lattice site are different. The structure is named after an ionic compound ZnS, although a number of covalently bonded semiconductors such as GaAs and CdTe have this structure.

Why are only half of the tetrahedral sites filled? Why not fill all eight of the sites? The answers to these questions are related to the stoichiometry of the compound. The chemical formula implies that there is an equal number of each atom type in the compound. Since there are four FCC sites per cell and eight tetrahedral sites per cell, the one-to-one atom ratio demands that half the tetrahedral sites be empty. The zinc blende structure has a coordination number of 4, there are four atoms of each type per cell, and the a_0-r relationship is a_0(zinc blende) $= 4(r + R)/\sqrt{3}$. Atoms are in contact along 1/4 of a body diagonal.

We have examined three crystal structures that an ionic material with equal numbers of anions and metal cations, that is, compounds with MX stoichiometry, might assume. How does the material "choose" its crystal structure? The key concepts are the r/R ratio and stoichiometry. For example, consider MgO. It might crystallize into the NaCl structure, the CsCl structure, or the zinc blende structure. The ratio $r(Mg^{2+})/R(O^{2-})$ is 0.59. Using the stability criteria summarized in Table 2.6–1, one can determine that the most stable coordination number is 6. Consequently, MgO forms crystals of the NaCl type.

EXAMPLE 3.7–2

Predict the most likely crystal for (*a*) CsI and (*b*) GaAs.

Solution

We must first predict the CNs for each compound and then use these values to predict the crystal structure, noting that CN(zinc blende) = 4, CN(NaCl) = 6, and CN(CsCl) = 8. We begin by determining the primary bond type in each compound. Using electronegativity values in Appendix B, CsI is ionic and GaAs is covalent.

a. Since CsI is ionic, the ratio $r(Cs^+)/R(I^-)$ = (0.167 nm)/(0.220 nm) $\approx$ 0.76, with Table 2.6–1, shows that $CN(Cs^+) = CN(I^-) = 8$. Thus, we predict CsI has the CsCl structure.

b. Since GaAs is covalent, the CNs are determined by the $8 - N_{ve}$ rule. In this compound, and many similar compounds, it is the average number of valence electrons that determines the structure. Ga has three valence electrons and As has five valence electrons, so the average number of valence electrons is four. GaAs has the zinc blende crystal structure.

For these two compounds the observed crystal structures are in agreement with predictions.[1]

[1] The simplified approach presented here, however, does not always yield the correct result. Recall that our model assumes the atoms to be rigid spheres. This assumption is not always valid. The interested reader should compare the predicted and observed crystal structures for the compound CaO.

3.7.2 Crystals with Three Atoms per Lattice Site

Compounds with a two-to-one ratio of atoms, such as CaF_2, SiO_2, and Li_2O, generally have crystal structures with a basis of three atoms. We will see in the following discussion that the complexity of the crystal structure tends to increase with the complexity of the basis.

The Fluorite Structure

Calcium fluoride (CaF_2) and a number of other materials with the MX_2 formula crystallize into a structure in which the M ions are located in the FCC positions and the X ions fill all the tetrahedral sites. The structure is shown in Figure 3.7–5. The stoichiometry dictates that there be double the number of X atoms as M atoms per unit cell. The M ions have CN(M) = 8 and the X ions have CN(X) = 4. Other compounds with this structure include UO_2, ThO_2, and ZrO_2.

Several compounds with the formula M_2X, including Li_2O, Na_2O, and K_2O, crystallize in the antifluorite structure. This structure is simply the inverse of the fluorite structure with the X ions at the FCC positions and the M ions filling all of the tetrahedral positions.

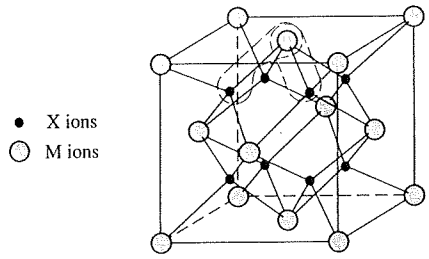

FIGURE 3.7–5
The fluorite crystal structure. The structure is composed of an FCC lattice with three atoms per lattice point. The M ions are located at the FCC positions and the X ions occupy all of the tetrahedral interstitial positions.

The Crystobalite Structure

While SiO_2 (silica) has three atoms per lattice site, it is much easier to visualize the structure of crystobalite, an important crystalline form of silica, in a different fashion. The short-range order of any compound of Si and O requires that each Si atom form single covalent bonds with its four nearest neighbor O atoms. In turn, each O atom is covalently bonded to two Si atoms. Hence, as shown in Figure 3.7–6a, the basic building block for all Si-O compounds is the negatively charged $(SiO_4)^{4-}$tetrahedron. The crystobalite crystal structure, shown in Figure 3.7–6b, can be envisioned as the diamond cubic structure with an $(SiO_4)^{4-}$ tetrahedron positioned on each lattice site. Since each O atom

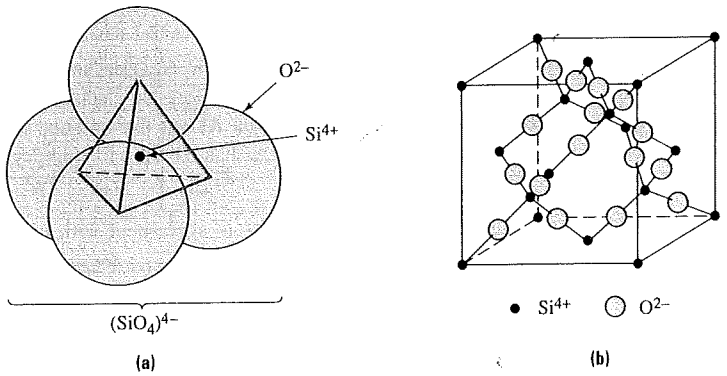

FIGURE 3.7–6
The crystal structure of crystobalite is an FCC lattice with six atoms per lattice site. It can be envisioned as being composed of an $(SiO_4)^{4-}$ tetrahedron of atoms centered on each of the diamond cubic positions.

is shared by two tetrahedra, each tetrahedron contains one Si and two O atoms, or one SiO_2 group. Thus, crystobalite has an FCC lattice with six atoms, or two tetrahedra, per lattice site.

3.7.3 Other Crystal Structures

The structures presented to this point are some of the simplest crystal structures found. They serve to illustrate the essential salient concepts associated with crystallography, yet they represent the structures of a number of important materials. You will note that most metals are either cubic or hexagonal. Most nonmetals are neither cubic nor hexagonal. In the following discussion we will add to our list of important crystal structures. The basic concepts remain unchanged with these structures; however, the structures are more complex.

The Perovskite Structure

Calcium titanate ($CaTiO_3$) crystallizes with the perovskite structure, as shown in Figure 3.7–7a. The Ca^{2+} ions are located at the cube corners, the O^{2-} ions are at the center of each face, and a Ti^{4+} ion resides at the center of the cube. Thus, there are a total of five ions in the unit cell. As mentioned previously, the choice of an origin for the coordinate axis is arbitrary. It is equally valid to draw the perovskite unit cell with a Ti^{4+} ion located at the origin. (See Figure 3.7–7b.) Note that when the origin coincides with one of the Ti^{4+} ions, the O^{2-} ions are at the edge centers rather than the face centers.

Similar materials, such as $BaTiO_3$, have similar structures. In the case of barium titanate, however, the structure is simple tetragonal rather than cubic. What this means is that the lengths of the edges of the unit cell are not equal. As shown in Figure 3.7–8, in the case of $BaTiO_3$ the difference is small: $a = b = 0.398$ nm, $c = 0.403$ nm. Careful inspection of this figure shows that the central Ti^{4+} ion does not lie in the same plane as the four oxygen atoms in the side faces of the tetragonal unit cell. This charge displacement gives $BaTiO_3$ some important electrical properties. The shift in the relative positions of the central Ti cation and the surrounding O anions results in the formation of a local electric dipole. The strength of the dipole, which is related to the magnitude of the atomic displacement, can be altered by either an applied force or an electric field. The result, which will be discussed in more detail in Chapter 11, is that a barium titanate crystal can be used as a transducer, to convert electrical voltages into mechanical energy and vice versa. This leads to applications in telephone receivers and phonograph cartridges.

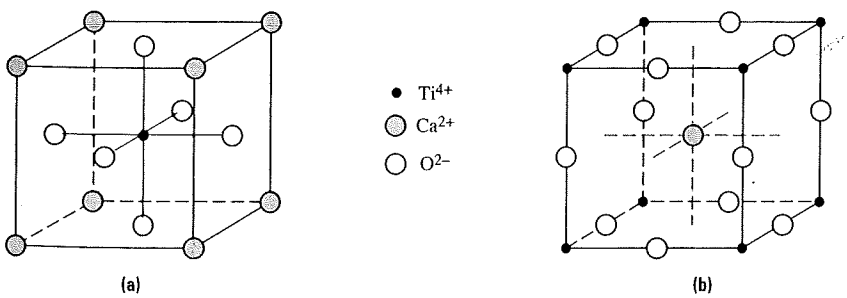

FIGURE 3.7–7 The perovskite unit cell for $CaTiO_3$ drawn **(a)** with the origin coinciding with a Ca^{2+} ion, and **(b)** with the origin coinciding with a Ti^{4+} ion.

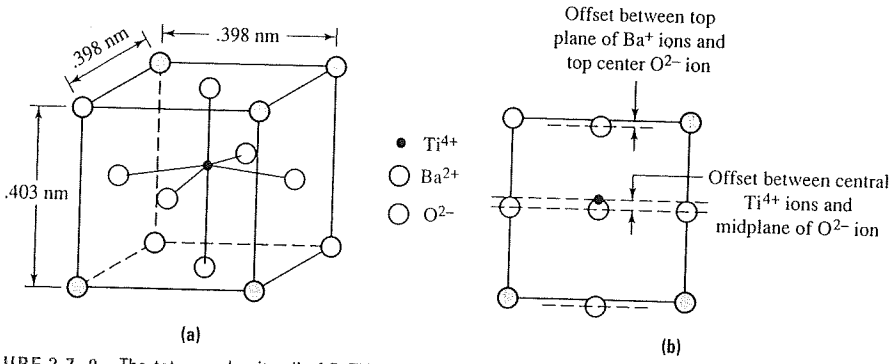

FIGURE 3.7–8 The tetragonal unit cell of $BaTiO_3$ shown **(a)** in 3-D, and **(b)** in 2-D.

The Structure of Methane

Methane (CH_4) is a gas at room temperature. Hence, it is not a material that is often used in solid form. The chief purpose of including it here is to show that the structures of low–molecular-weight organic crystals are similar in all respects to those of inorganic crystals. Below −183°C, methane crystallizes into an FCC structure. On each lattice site are placed five atoms. Similar to the case of crystobalite, it is perhaps easiest to envision the structure as having a carbon atom tetrahedrally coordinated by hydrogen atoms at each lattice site.

The Structure of Polyethylene

The unit cells of macromolecules (polymers) are more complex than those of metals, ionic compounds, or small-molecule organic crystals. In general, polymers crystallize only partially or not at all, and it is the linear ones that may be semicrystalline. The discussion below focuses on only those parts of the polymer that have been laid down to form crystals. We will revisit the subject of polymer crystallization in Chapter 6.

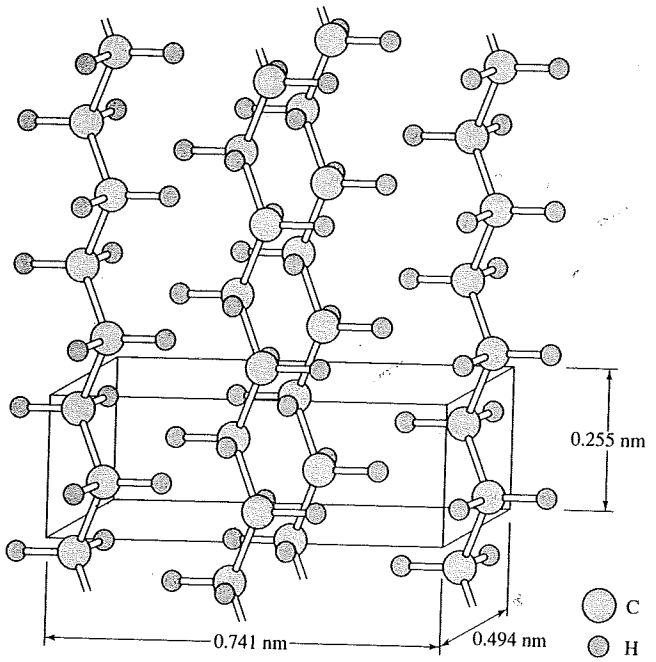

FIGURE 3.7–9
Crystalline polyethylene is composed of polyethylene chains arranged in an orthorhombic unit cell. *(Adapted from C. W. Bunn, Chemical Crystallography, 1945, by permission of Oxford University Press.)*

As mentioned in the previous chapter, polyethylene is a chain of CH_2 groups linked together with covalent bonds. Because of its simple symmetrical structure, polyethylene, in the scheme of polymers, crystallizes readily. In crystals, segments of the polymer chains line up parallel with one another in order to maximize intermolecular interactions, that is, secondary bond formation. The structure of a polyethylene crystal is shown in Figure 3.7–9. The unit cell is orthorhombic, meaning that no two edges have the same length but all angles are 90°. It is customary to use the c direction as the chain direction. Unit-cell dimensions for polymers are typically larger than those for metals; however, complex ionic crystals also have large cell parameters.

3.8 LIQUID CRYSTALS

As discussed in the introduction to this chapter, the order in most liquids is short range only. The term **liquid crystal** is given to fluids that show some degree of long-range order. The extent of the long-range order in these materials is intermediate between that of a crystalline solid and a liquid with SRO only. The order in one type of liquid crystals consists essentially of an association of molecules, giving regions of near parallel alignment of molecules as shown in Figure 3.8–1. In another type of liquid crystal the molecules twist cooperatively. This latter class of liquid crystals has found household applications as liquid crystal displays (i.e., the illuminated numbers in digital clocks and other electronic devices).

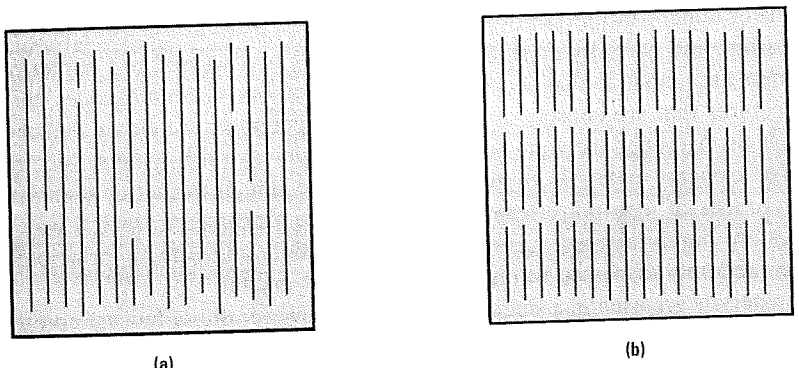

FIGURE 3.8–1 Schematic illustrations of the structure of some liquid crystals: **(a)** chain ends are unaligned; **(b)** chain ends are aligned.

3.9 SINGLE CRYSTALS AND POLYCRYSTALLINE MATERIALS

We have been concerned exclusively with the order of crystalline materials in this chapter. Indeed, many materials are crystalline but not quite as perfect as you may have been led to believe thus far. Virtually all metals form crystalline structures under normal conditions of cooling from the molten liquid; however, an entire part cast from the melt is rarely a single crystal. Rather, the casting is made up of a number of crystals with identical structures but different orientations. Most metals form **polycrystalline** structures, as shown in Figure 3.9–1. The grains are small crystals that are typically on the order of 0.5–50 μm across, but they may be up to a centimeter in diameter. The grain boundaries are internal surfaces of finite thickness where crystals of different orientations meet. It is possible that you have seen grains and grain boundaries on old brass doorknobs that have been polished and etched with perspiration through years of use.

In summary, we have identified two possible types of point defects in crystals: vacancies and interstitials. It has been demonstrated that not only are such defects possible but their existence is thermodynamically necessary. Point defects play a major role in determining several properties of crystals, and their effects will be discussed throughout this and subsequent chapters.

4.2.2 Vacancies and Interstitials in Ionic Crystals

Just as vacancies and interstitials occur in nonionic crystals, similar point defects are also found in ionic solids. However, an extremely important difference between ionic and nonionic crystals arises with respect to the generation of vacancies. In ionic crystals, isolated single vacancies do not occur, since the removal of a single ion would result in an electrical charge imbalance in the crystal. Instead, vacancies can occur only in small groups with the cation : anion vacancy ratio such that the crystal as a whole remains electrically neutral. These electrically neutral cation-anion vacancy clusters are called **Schottky defects.** Examples of Schottky defects in NaCl and $MgCl_2$ are shown in Figure 4.2–2. In NaCl, in which there are equal numbers of cations and anions, electrical neutrality requires equal numbers of cation and anion vacancies, and the Schottky defect is composed of a single anion/cation vacancy pair. In contrast, in $MgCl_2$, for every Mg^{2+} vacancy there are two Cl^- vacancies to maintain electroneutrality.

The Schottky defect is not the only point-defect cluster that can maintain charge neutrality. Another possibility involves the formation of a vacancy/interstitial pair. These small point-defect clusters are known as **Frenkel defects** and are shown schematically in Figure 4.2–3 for the compound AgCl. Generally speaking, Frenkel defects involving cation interstitials are far more common than those involving anion interstitials, since most interstices are too small to accommodate the larger ions, usually anions.

The relative concentrations of the various point defects are determined by the energies of defect formation and the requirement of electroneutrality. Using thermodynamic

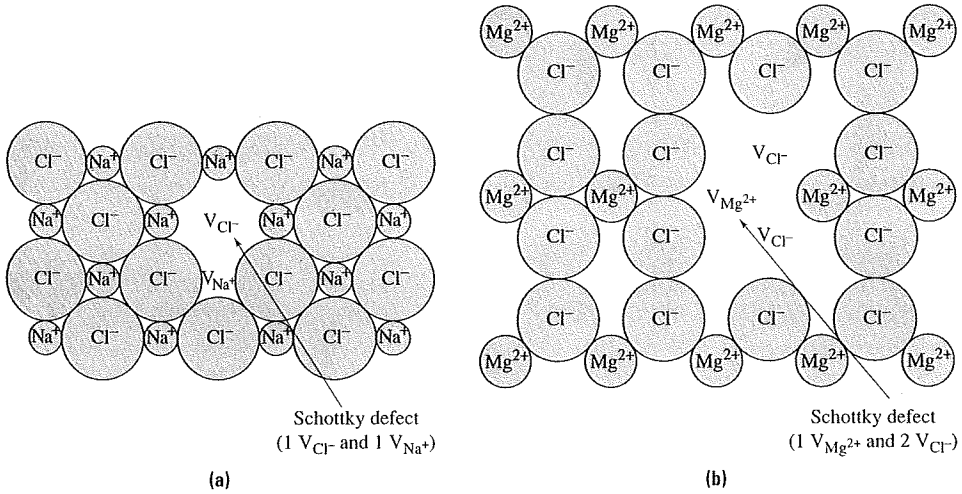

FIGURE 4.2–2 Schottky defects in **(a)** NaCl and **(b)** $MgCl_2$. The vacancies are created so that overall charge neutrality is maintained. The figure shows the vacancies associated (close together); however, the cation and anion vacancies need not be located spatially close to one another.

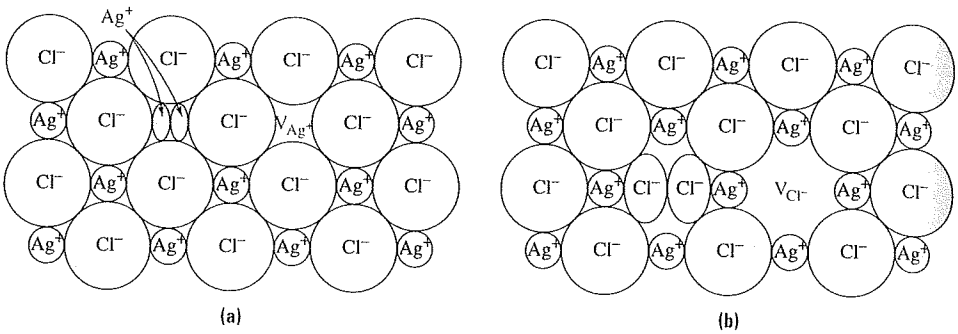

FIGURE 4.2–3 Frenkel defects in AgCl. The defect consists of vacancy/interstitial pairs. Frenkel defects involving cations **(a)** are more common than those involving anions **(b)**, since cations are usually smaller.

reasoning similar to that used to develop the expression for the vacancy concentration in nonionic solids, the concentrations of vacancies and interstitials in ionic solids can be estimated.

For Frenkel defects:

$$C_v = \frac{N_v}{N_T} = \exp\left(-\frac{Q_{fri}}{2RT}\right) = \frac{N_i}{N_T} = C_i \tag{4.2–3}$$

where C_v and C_i are respectively the concentrations of vacancies and interstitials and Q_{fvi} is the energy required to form a vacancy and an interstitial. The factor of 2 in the denominator of the exponential occurs because two defects are created in the process.

For Schottky defects in an MX compound:

$$C_{v,\text{cat}} = \frac{N_{v,\text{cat}}}{N_T} = \exp\left(-\frac{Q_{fvp}}{2RT}\right) = \frac{N_{v,\text{an}}}{N_T} = C_{v,\text{an}} \tag{4.2–4a}$$

where $C_{v,\text{cat}}$ and $C_{v,\text{an}}$ are respectively the concentrations of cation and anion vacancies and Q_{fvp} is the energy required to form a cation/anion vacancy pair. For Schottky defects in M_nX_p compounds:

$$pC_{v,\text{cat}} = (np)\exp\left[-\frac{Q_{fvc}}{(n^2 + p^2)RT}\right] = nC_{\text{an}} \tag{4.2–4b}$$

where Q_{fvc} is the energy required to form a cluster of n cation vacancies and p anion vacancies.

4.3 IMPURITIES

Impurities exist at some level in practically all materials. Often they enter the host material during processing and confer undesirable properties. On the other hand, they may be intentionally added either to enhance properties or to produce new desirable effects. In the latter case they are referred to as alloying elements in metals, as additives in polymers and ceramics, or as dopants in semiconductors. Examples of undesirable impurities include sulfur in steels and moisture in nylon fibers. In both cases the impurities degrade the mechanical properties of the host material. In contrast, the addition of phosphorus to silicon to confer desirable electrical (semiconducting) characteristics, carbon to iron to increase strength, methyl acrylate to polyacrylonitrile to give a dyeable polymer, and metallic ions to window glass to produce desirable colors are examples of

beneficial impurity additions. In this section we describe the different types of impurities, demonstrate the basis for their existence, and discuss their practical effects.

4.3.1 Impurities in Crystals

Just as vacancies and interstitials in pure materials lower the free energy, in many cases impurities dissolved in a material also lower the total free energy. While the internal energy is generally increased as a result of adding impurity atoms, the entropy is also increased, and at any temperature there will be a certain number of impurities for which the free energy is a minimum. The equilibrium concentration of impurity atoms at any temperature is determined by a trade-off between increases in the entropy and increases in the internal energy.

Atoms of the primary atomic species are called **solvent atoms,** while the impurities are usually referred to as **solute atoms.** In crystalline solids, impurity atoms can be either present in the spaces between the solvent atoms or substituted for the solvent atoms. When the impurities lie in the spaces between the solvent atoms, they are called interstitials, and the mixture formed by the two atomic species is called an **interstitial solid solution.** When impurities substitute for the solvent atoms, they are called **substitutional** atoms, and the mixture of the two species is called a **substitutional solid solution.** Examples of interstitial and substitutional solid solutions are shown in Figures 4.3–1 and 4.3–2, respectively.

There are certain requirements for the formation of either interstitial or substitutional solid solutions. For example, it is possible for atoms of the host species to exist in interstitial positions as a result of high-energy impacts, such as those received during irradiation. However, this is an unusual case: interstitial solid solutions normally form only when the interstitial atoms are significantly smaller than the solvent atoms and are

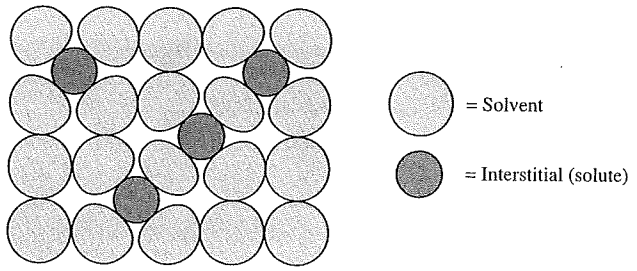

FIGURE 4.3–1 Interstitial solid solution. The solute atom is positioned in the void spaces between solvent atoms, causing strain in the lattice.

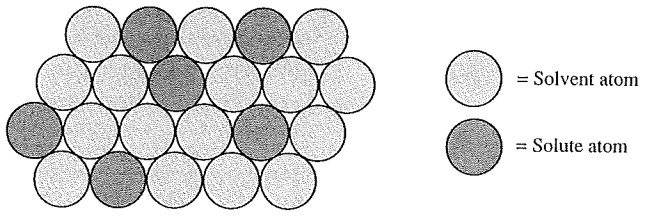

FIGURE 4.3–2 Substitutional solid solution. The solute and solvent atoms must have sizes (radii) within 15% and must have similar bond characteristics.

The reciprocal lattice plays a fundamental role in most analytic studies of periodic structures. One is led to it from such diverse avenues as the theory of crystal diffraction, the abstract study of functions with the periodicity of a Bravais lattice, or the question of what can be salvaged of the law of momentum conservation when the full translational symmetry of free space is reduced to that of a periodic potential. In this brief chapter we shall describe some important elementary features of the reciprocal lattice from a general point of view not tied to any particular application.

DEFINITION OF RECIPROCAL LATTICE

Consider a set of points $\mathbf{R}$ constituting a Bravais lattice, and a plane wave, $e^{i\mathbf{k}\cdot\mathbf{r}}$. For general $\mathbf{k}$, such a plane wave will not, of course, have the periodicity of the Bravais lattice, but for certain special choices of wave vector it will. *The set of all wave vectors* $\mathbf{K}$ *that yield plane waves with the periodicity of a given Bravais lattice is known as its reciprocal lattice.* Analytically, $\mathbf{K}$ belongs to the reciprocal lattice of a Bravais lattice of points $\mathbf{R}$, provided that the relation

$$e^{i\mathbf{K}\cdot(\mathbf{r}+\mathbf{R})} = e^{i\mathbf{K}\cdot\mathbf{r}} \tag{5.1}$$

holds for any $\mathbf{r}$, and for all $\mathbf{R}$ in the Bravais lattice. Factoring out $e^{i\mathbf{K}\cdot\mathbf{r}}$, we can characterize the reciprocal lattice as the set of wave vectors $\mathbf{K}$ satisfying

$$e^{i\mathbf{K}\cdot\mathbf{R}} = 1 \tag{5.2}$$

for all $\mathbf{R}$ in the Bravais lattice.

Note that a reciprocal lattice is defined with reference to a particular Bravais lattice. The Bravais lattice that determines a given reciprocal lattice is often referred to as the *direct lattice*, when viewed in relation to its reciprocal. Note also that although one could define a set of vectors $\mathbf{K}$ satisfying (5.2) for an arbitrary set of vectors $\mathbf{R}$, such a set of $\mathbf{K}$ is called a reciprocal lattice only if the set of vectors $\mathbf{R}$ is a Bravais lattice.[1]

THE RECIPROCAL LATTICE IS A BRAVAIS LATTICE

That the reciprocal lattice is itself a Bravais lattice follows most simply from the definition of a Bravais lattice given in footnote 7 of Chapter 4, along with the fact that if $\mathbf{K}_1$ and $\mathbf{K}_2$ satisfy (5.2), so, obviously, will their sum and difference.

It is worth considering a more clumsy proof of this fact, which provides an explicit algorithm for constructing the reciprocal lattice. Let $\mathbf{a}_1$, $\mathbf{a}_2$, and $\mathbf{a}_3$ be a set of primitive vectors for the direct lattice. Then the reciprocal lattice can be generated by the three primitive vectors

$$\begin{aligned}
\mathbf{b}_1 &= 2\pi \frac{\mathbf{a}_2 \times \mathbf{a}_3}{\mathbf{a}_1 \cdot (\mathbf{a}_2 \times \mathbf{a}_3)}, \\
\mathbf{b}_2 &= 2\pi \frac{\mathbf{a}_3 \times \mathbf{a}_1}{\mathbf{a}_1 \cdot (\mathbf{a}_2 \times \mathbf{a}_3)}, \\
\mathbf{b}_3 &= 2\pi \frac{\mathbf{a}_1 \times \mathbf{a}_2}{\mathbf{a}_1 \cdot (\mathbf{a}_2 \times \mathbf{a}_3)}.
\end{aligned} \tag{5.3}$$

[1] In particular, in working with a lattice with a basis one uses the reciprocal lattice determined by the underlying Bravais lattice, rather than a set of $\mathbf{K}$ satisfying (5.2) for vectors $\mathbf{R}$ describing both the Bravais lattice and the basis points.

To verify that (5.3) gives a set of primitive vectors for the reciprocal lattice, one first notes that the $\mathbf{b}_i$ satisfy[2]

$$\mathbf{b}_i \cdot \mathbf{a}_j = 2\pi\delta_{ij}, \tag{5.4}$$

where δ_{ij} is the Kronecker delta symbol:

$$\begin{aligned} \delta_{ij} &= 0, \quad i \neq j; \\ \delta_{ij} &= 1, \quad i = j. \end{aligned} \tag{5.5}$$

Now any vector $\mathbf{k}$ can be written as a linear combination[3] of the $\mathbf{b}_i$:

$$\mathbf{k} = k_1\mathbf{b}_1 + k_2\mathbf{b}_2 + k_3\mathbf{b}_3. \tag{5.6}$$

If $\mathbf{R}$ is any direct lattice vector, then

$$\mathbf{R} = n_1\mathbf{a}_1 + n_2\mathbf{a}_2 + n_3\mathbf{a}_3, \tag{5.7}$$

where the n_i are integers. It follows from (5.4) that

$$\mathbf{k} \cdot \mathbf{R} = 2\pi(k_1n_1 + k_2n_2 + k_3n_3). \tag{5.8}$$

For $e^{i\mathbf{k}\cdot\mathbf{R}}$ to be unity for all $\mathbf{R}$ (Eq. (5.2)) $\mathbf{k} \cdot \mathbf{R}$ must be 2π times an integer for any choices of the integers n_i. This requires the coefficients k_i to be integers. Thus the condition (5.2) that $\mathbf{K}$ be a reciprocal lattice vector is satisfied by just those vectors that are linear combinations (5.6) of the $\mathbf{b}_i$ with integral coefficients. Thus (compare Eq. (4.1)) the reciprocal lattice is a Bravais lattice and the $\mathbf{b}_i$ can be taken as primitive vectors.

THE RECIPROCAL OF THE RECIPROCAL LATTICE

Since the reciprocal lattice is itself a Bravais lattice, one can construct *its* reciprocal lattice. This turns out to be nothing but the original direct lattice.

One way to prove this is by constructing $\mathbf{c}_1$, $\mathbf{c}_2$, and $\mathbf{c}_3$ out of the $\mathbf{b}_i$ according to the same formula (5.3) by which the $\mathbf{b}_i$ were constructed from the $\mathbf{a}_i$. It then follows from simple vector identities (Problem 1) that $\mathbf{c}_i = \mathbf{a}_i$, $i = 1, 2, 3$.

A simpler proof follows from the observation that according to the basic definition (5.2), the reciprocal of the reciprocal lattice is the set of all vectors $\mathbf{G}$ satisfying

$$e^{i\mathbf{G}\cdot\mathbf{K}} = 1 \tag{5.9}$$

for all $\mathbf{K}$ in the reciprocal lattice. Since any direct lattice vector $\mathbf{R}$ has this property (again by (5.2)), all direct lattice vectors are in the lattice reciprocal to the reciprocal lattice. Furthermore, no other vectors can be, for a vector not in the direct lattice has the form $\mathbf{r} = x_1\mathbf{a}_1 + x_2\mathbf{a}_2 + x_3\mathbf{a}_3$ with at least one nonintegral x_i. For that value of i, $e^{i\mathbf{b}_i\cdot\mathbf{r}} = e^{2\pi i x_i} \neq 1$, and condition (5.9) is violated for the reciprocal lattice vector $\mathbf{K} = \mathbf{b}_i$.

---

[2] When $i \neq j$, Eq. (5.4) follows because the cross product of two vectors is normal to both. When $i = j$, it follows because of the vector identity

$$\mathbf{a}_1 \cdot (\mathbf{a}_2 \times \mathbf{a}_3) = \mathbf{a}_2 \cdot (\mathbf{a}_3 \times \mathbf{a}_1) = \mathbf{a}_3 \cdot (\mathbf{a}_1 \times \mathbf{a}_2).$$

[3] This is true for any three vectors not all in one plane. It is easy to verify that the $\mathbf{b}_i$ are not all in a plane as long as the $\mathbf{a}_i$ are not.

IMPORTANT EXAMPLES

The *simple cubic* Bravais lattice, with cubic primitive cell of side a, has as its reciprocal a simple cubic lattice with cubic primitive cell of side $2\pi/a$. This can be seen, for example, from the construction (5.3), for if

$$\mathbf{a}_1 = a\hat{\mathbf{x}}, \quad \mathbf{a}_2 = a\hat{\mathbf{y}}, \quad \mathbf{a}_3 = a\hat{\mathbf{z}}, \tag{5.10}$$

then

$$\mathbf{b}_1 = \frac{2\pi}{a}\hat{\mathbf{x}}, \quad \mathbf{b}_2 = \frac{2\pi}{a}\hat{\mathbf{y}}, \quad \mathbf{b}_3 = \frac{2\pi}{a}\hat{\mathbf{z}}. \tag{5.11}$$

The *face-centered cubic* Bravais lattice with conventional cubic cell of side a has as its reciprocal a body-centered cubic lattice with conventional cubic cell of side $4\pi/a$. This can be seen by applying the construction (5.3) to the fcc primitive vectors (4.5). The result is

$$\mathbf{b}_1 = \frac{4\pi}{a}\frac{1}{2}(\hat{\mathbf{y}} + \hat{\mathbf{z}} - \hat{\mathbf{x}}), \quad \mathbf{b}_2 = \frac{4\pi}{a}\frac{1}{2}(\hat{\mathbf{z}} + \hat{\mathbf{x}} - \hat{\mathbf{y}}), \quad \mathbf{b}_3 = \frac{4\pi}{a}\frac{1}{2}(\hat{\mathbf{x}} + \hat{\mathbf{y}} - \hat{\mathbf{z}}) \tag{5.12}$$

This has precisely the form of the bcc primitive vectors (4.4), provided that the side of the cubic cell is taken to be $4\pi/a$.

The *body-centered cubic* lattice with conventional cubic cell of side a has as its reciprocal a face-centered cubic lattice with conventional cubic cell of side $4\pi/a$. This can again be proved from the construction (5.3), but it also follows from the above result for the reciprocal of the fcc lattice, along with the theorem that the reciprocal of the reciprocal is the original lattice.

It is left as an exercise for the reader to verify (Problem 2) that the reciprocal to a *simple hexagonal* Bravais lattice with lattice constants c and a (Figure 5.1a) is another

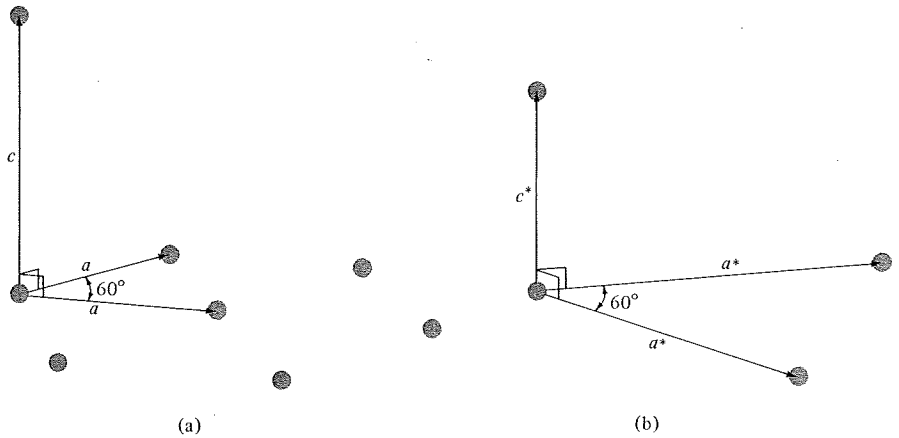

Figure 5.1
(a) Primitive vectors for the simple hexagonal Bravais lattice. (b) Primitive vectors for the lattice reciprocal to that generated by the primitive vectors in (a). The c and c^* axes are parallel. The a^* axes are rotated by 30° with respect to the a axes in the plane perpendicular to the c or c^* axes. The reciprocal lattice is also simple hexagonal.

simple hexagonal lattice with lattice constants $2\pi/c$ and $4\pi/\sqrt{3}a$ (Figure 5.1b), rotated through 30° about the c-axis with respect to the direct lattice.[4]

VOLUME OF THE RECIPROCAL LATTICE PRIMITIVE CELL

If v is the volume[5] of a primitive cell in the direct lattice, then the primitive cell of the reciprocal lattice has a volume $(2\pi)^3/v$. This is proved in Problem 1.

FIRST BRILLOUIN ZONE

The Wigner-Seitz primitive cell (page 73) of the reciprocal lattice is known as the *first Brillouin zone.* As the name suggests, one also defines higher Brillouin zones, which are primitive cells of a different type that arise in the theory of electronic levels in a periodic potential. They are described in Chapter 9.

Although the terms "Wigner-Seitz cell" and "first Brillouin zone" refer to identical geometrical constructions, in practice the latter term is applied only to the k-space cell. In particular, when reference is made to the first Brillouin zone of a particular r-space Bravais lattice (associated with a particular crystal structure), what is always meant is the Wigner-Seitz cell of the associated reciprocal lattice. Thus, because the reciprocal of the body-centered cubic lattice is face-centered cubic, the first Brillouin zone of the bcc lattice (Figure 5.2a) is just the fcc Wigner-Seitz cell (Figure 4.16). Conversely, the first Brillouin zone of the fcc lattice (Figure 5.2b) is just the bcc Wigner-Seitz cell (Figure 4.15).

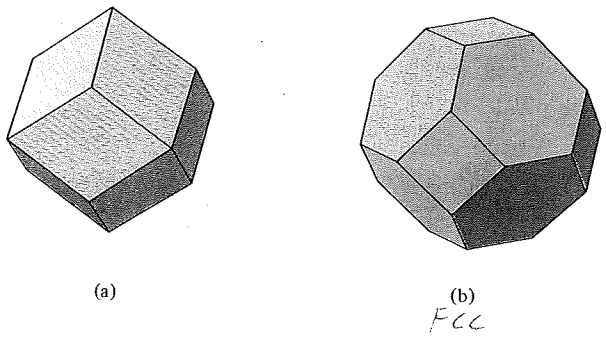

(a) (b)

Figure 5.2
(a) The first Brillouin zone for the body-centered cubic lattice. (b) The first Brillouin zone for the face-centered cubic lattice.

LATTICE PLANES

There is an intimate relation between vectors in the reciprocal lattice and planes of points in the direct lattice. This relation is of some importance in understanding the fundamental role the reciprocal lattice plays in the theory of diffraction, and will be applied to that problem in the next chapter. Here we shall describe the relation in general geometrical terms.

---

[4] The hexagonal close-packed *structure* is not a Bravais lattice, and therefore the reciprocal lattice used in the analysis of hcp solids is that of the simple hexagonal lattice (see footnote 1).

[5] The primitive cell volume is independent of the choice of cell, as proved in Chapter 4.

Given a particular Bravais lattice, a *lattice plane* is defined to be any plane containing at least three noncollinear Bravais lattice points. Because of the translational symmetry of the Bravais lattice, any such plane will actually contain infinitely many lattice points, which form a two-dimensional Bravais lattice within the plane. Some lattice planes in a simple cubic Bravais lattice are pictured in Figure 5.3.

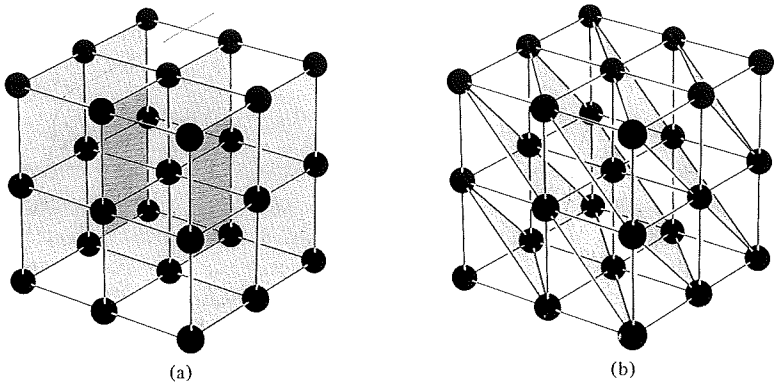

Figure 5.3
Some lattice planes (shaded) in a simple cubic Bravais lattice; (a) and (b) show two different ways of representing the lattice as a family of lattice planes.

By a *family of lattice planes* we mean a set of parallel, equally spaced lattice planes, which together contain all the points of the three-dimensional Bravais lattice. Any lattice plane is a member of such a family. Evidently the resolution of a Bravais lattice into a family of lattice planes is far from unique (Figure 5.3). The reciprocal lattice provides a very simple way to classify all possible families of lattice planes, which is embodied in the following theorem:

> For any family of lattice planes separated by a distance d, there are reciprocal lattice vectors perpendicular to the planes, the shortest of which have a length of $2\pi/d$. Conversely, for any reciprocal lattice vector $\mathbf{K}$, there is a family of lattice planes normal to $\mathbf{K}$ and separated by a distance d, where $2\pi/d$ is the length of the shortest reciprocal lattice vector parallel to $\mathbf{K}$.

The theorem is a straightforward consequence of (a) the definition (5.2) of reciprocal lattice vectors as the wave vectors of plane waves that are unity at all Bravais lattice sites and (b) the fact that a plane wave has the same value at all points lying in a family of planes that are perpendicular to its wave vector and separated by an integral number of wavelengths.

To prove the first part of the theorem, given a family of lattice planes, let $\hat{\mathbf{n}}$ be a unit vector normal to the planes. That $\mathbf{K} = 2\pi\hat{\mathbf{n}}/d$ is a reciprocal lattice vector follows from the fact that the plane wave $e^{i\mathbf{K}\cdot\mathbf{r}}$ is constant in planes perpendicular to $\mathbf{K}$ and has the same value in planes separated by $\lambda = 2\pi/K = d$. Since one of the lattice planes contains the Bravais lattice point $\mathbf{r} = \mathbf{0}$, $e^{i\mathbf{K}\cdot\mathbf{r}}$ must be unity for any point $\mathbf{r}$ in any of the planes. Since the planes contain all Bravais lattice points, $e^{i\mathbf{K}\cdot\mathbf{r}} = 1$ for all $\mathbf{R}$, so that $\mathbf{K}$ is indeed a reciprocal lattice vector. Furthermore, $\mathbf{K}$ is the shortest

reciprocal lattice vector normal to the planes, for any wave vector shorter than **K** will give a plane wave with wavelength greater than $2\pi/K = d$. Such a plane wave cannot have the same value on all planes in the family, and therefore cannot give a plane wave that is unity at all Bravais lattice points.

To prove the converse of the theorem, given a reciprocal lattice vector, let **K** be the shortest parallel reciprocal lattice vector. Consider the set of real space planes on which the plane wave $e^{i\mathbf{K}\cdot\mathbf{r}}$ has the value unity. These planes (one of which contains the point $\mathbf{r} = \mathbf{0}$) are perpendicular to **K** and separated by a distance $d = 2\pi/K$. Since the Bravais lattice vectors **R** all satisfy $e^{i\mathbf{K}\cdot\mathbf{R}} = 1$ for any reciprocal lattice vector **K**, they must all lie within these planes; i.e., the family of planes must contain within it a family of lattice planes. Furthermore the spacing between the lattice planes is also d (rather than some integral multiple of d), for if only every nth plane in the family contained Bravais lattice points, then according to the first part of the theorem, the vector normal to the planes of length $2\pi/nd$, i.e., the vector $\mathbf{K}/n$, would be a reciprocal lattice vector. This would contradict our original assumption that no reciprocal lattice vector parallel to **K** is shorter than **K**.

MILLER INDICES OF LATTICE PLANES

The correspondence between reciprocal lattice vectors and families of lattice planes provides a convenient way to specify the orientation of a lattice plane. Quite generally one describes the orientation of a plane by giving a vector normal to the plane. Since we know there are reciprocal lattice vectors normal to any family of lattice planes, it is natural to pick a reciprocal lattice vector to represent the normal. To make the choice unique, one uses the shortest such reciprocal lattice vector. In this way one arrives at the *Miller indices* of the plane:

The Miller indices of a lattice plane are the coordinates of the shortest reciprocal lattice vector normal to that plane, with respect to a specified set of primitive reciprocal lattice vectors. Thus a plane with Miller indices h, k, l, is normal to the reciprocal lattice vector $h\mathbf{b}_1 + k\mathbf{b}_2 + l\mathbf{b}_3$.

As so defined, the Miller indices are integers, since any reciprocal lattice vector is a linear combination of three primitive vectors with integral coefficients. Since the normal to the plane is specified by the shortest perpendicular reciprocal lattice vector, the integers h, k, l can have no common factor. Note also that the Miller indices depend on the particular choice of primitive vectors.

In simple cubic Bravais lattices the reciprocal lattice is also simple cubic and the Miller indices are the coordinates of a vector normal to the plane in the obvious cubic coordinate system. As a general rule, face-centered and body-centered cubic Bravais lattice are described in terms of a conventional cubic cell, i.e., as simple cubic lattices with bases. Since any lattice plane in a fcc or bcc lattice is also a lattice plane in the underlying simple cubic lattice, the same elementary cubic indexing can be used to specify lattice planes. In practice, it is only in the description of noncubic crystals that one must remember that the Miller indices are the coordinates of the normal in a system given by the reciprocal lattice, rather than the direct lattice.

The Miller indices of a plane have a geometrical interpretation in the direct lattice, which is sometimes offered as an alternative way of defining them. Because a lattice

REC

plane with Miller indices h, k, l is perpendicular to the reciprocal lattice vector $\mathbf{K} = h\mathbf{b}_1 + k\mathbf{b}_2 + l\mathbf{b}_3$, it will be contained in the continuous plane $\mathbf{K} \cdot \mathbf{r} = A$, for suitable choice of the constant A. This plane intersects the axes determined by the direct lattice primitive vectors $\mathbf{a}_i$ at the points $x_1\mathbf{a}_1$, $x_2\mathbf{a}_2$, and $x_3\mathbf{a}_3$ (Figure 5.4), where the x_i are determined by the condition that $x_i\mathbf{a}_i$ indeed satisfy the equation of the plane: $\mathbf{K} \cdot (x_i\mathbf{a}_i) = A$. Since $\mathbf{K} \cdot \mathbf{a}_1 = 2\pi h$, $\mathbf{K} \cdot \mathbf{a}_2 = 2\pi k$, and $\mathbf{K} \cdot \mathbf{a}_3 = 2\pi l$, it follows that

$$x_1 = \frac{A}{2\pi h}, \quad x_2 = \frac{A}{2\pi k}, \quad x_3 = \frac{A}{2\pi l}. \tag{5.13}$$

Thus the intercepts with the crystal axes of a lattice plane are inversely proportional to the Miller indices of the plane.

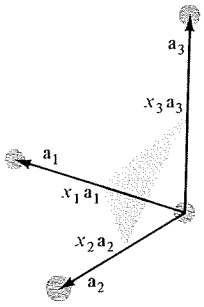

Figure 5.4
An illustration of the crystallographic definition of the Miller indices of a lattice plane. The shaded plane can be a portion of the continuous plane in which the points of the lattice plane lie, or any plane parallel to the lattice plane. The Miller indices are inversely proportional to the x_i.

Crystallographers put the cart before the horse, *defining* the Miller indices to be a set of integers with no common factors, inversely proportional to the intercepts of the crystal plane along the crystal axes:

$$h{:}k{:}l = \frac{1}{x_1}{:}\frac{1}{x_2}{:}\frac{1}{x_3}. \tag{5.14}$$

SOME CONVENTIONS FOR SPECIFYING DIRECTIONS

Lattice planes are usually specified by giving their Miller indices in parentheses: (h, k, l). Thus, in a cubic system, a plane with a normal $(4, -2, 1)$ (or, from the crystallographic viewpoint, a plane with intercepts $(1, -2, 4)$ along cubic axes) is called a $(4, -2, 1)$ plane. The commas are eliminated without confusion by writing $\bar{n}$ instead of $-n$, simplifying the description to $(4\bar{2}1)$. One must know what set of axes is being used to interpret these symbols unambiguously. Simple cubic axes are invariably used when the crystal has cubic symmetry. Some examples of planes in cubic crystals are shown in Figure 5.5.

A similar convention is used to specify directions in the direct lattice, but to avoid confusion with the Miller indices (directions in the reciprocal lattice) square brackets are used instead of parentheses. Thus the body diagonal of a simple cubic lattice lies in the [111] direction and, in general the lattice point $n_1\mathbf{a}_1 + n_2\mathbf{a}_2 + n_3\mathbf{a}_3$ lies in the direction $[n_1n_2n_3]$ from the origin.

There is also a notation specifying both a family of lattice planes and all those other families that are equivalent to it by virtue of the symmetry of the crystal. Thus

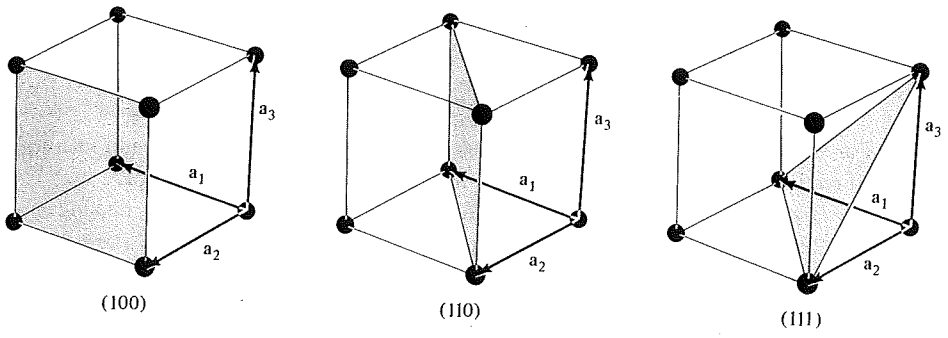

Figure 5.5
Three lattice planes and their Miller indices in a simple cubic Bravais lattice.

the (100), (010), and (001) planes are all equivalent in a cubic crystal. One refers to them collectively as the $\{100\}$ planes, and in general one uses $\{hkl\}$ to refer to the (hkl) planes and all those that are equivalent to them by virtue of the crystal symmetry. A similar convention is used with directions: the [100], [010], [001], $[\bar{1}00]$, $[0\bar{1}0]$, and $[00\bar{1}]$ directions in a cubic crystal are referred to, collectively, as the $\langle 100 \rangle$ directions.

This concludes our general geometrical discussion of the reciprocal lattice. In Chapter 6 we shall see an important example of the utility and the power of the concept in the theory of the diffraction of X rays by a crystal.

PROBLEMS

1. (a) Prove that the reciprocal lattice primitive vectors defined in (5.3) satisfy

$$\mathbf{b}_1 \cdot (\mathbf{b}_2 \times \mathbf{b}_3) = \frac{(2\pi)^3}{\mathbf{a}_1 \cdot (\mathbf{a}_2 \times \mathbf{a}_3)}. \tag{5.15}$$

(*Hint:* Write $\mathbf{b}_1$ (but not $\mathbf{b}_2$ or $\mathbf{b}_3$) in terms of the $\mathbf{a}_i$, and use the orthogonality relations (5.4).)

(b) Suppose primitive vectors are constructed from the $\mathbf{b}_i$ in the same manner (Eq. (5.3)) as the $\mathbf{b}_i$ are constructed from the $\mathbf{a}_i$. Prove that these vectors are just the $\mathbf{a}_i$ themselves; i.e., show that

$$2\pi \frac{\mathbf{b}_2 \times \mathbf{b}_3}{\mathbf{b}_1 \cdot (\mathbf{b}_2 \times \mathbf{b}_3)} = \mathbf{a}_1, \quad \text{etc.} \tag{5.16}$$

(*Hint:* Write $\mathbf{b}_3$ in the numerator (but not $\mathbf{b}_2$) in terms of the $\mathbf{a}_i$, use the vector identity $\mathbf{A} \times (\mathbf{B} \times \mathbf{C}) = \mathbf{B}(\mathbf{A} \cdot \mathbf{C}) - \mathbf{C}(\mathbf{A} \cdot \mathbf{B})$, and appeal to the orthogonality relations (5.4) and the result (5.15) above.)

(c) Prove that the volume of a Bravais lattice primitive cell is

$$v = |\mathbf{a}_1 \cdot (\mathbf{a}_2 \times \mathbf{a}_3)|, \tag{5.17}$$

where the $\mathbf{a}_i$ are three primitive vectors. (In conjunction with (5.15) this establishes that the volume of the reciprocal lattice primitive cell is $(2\pi)^3/v$.)

Typical interatomic distances in a solid are on the order of an angstrom (10^{-8} cm). An electromagnetic probe of the microscopic structure of a solid must therefore have a wavelength at least this short, corresponding to an energy of order

$$\hbar\omega = \frac{hc}{\lambda} = \frac{hc}{10^{-8}\text{ cm}} \approx 12.3 \times 10^3 \text{ eV}. \tag{6.1}$$

Energies like this, on the order of several thousands of electron volts (kilovolts or keV), are characteristic X-ray energies.

In this chapter we shall describe how the distribution of X rays scattered by a rigid,[1] periodic[2] array of ions reveals the locations of the ions within that structure. There are two equivalent ways to view the scattering of X rays by a perfect periodic structure, due to Bragg and to von Laue. Both viewpoints are still widely used. The von Laue approach, which exploits the reciprocal lattice, is closer to the spirit of modern solid state physics, but the Bragg approach is still in wide use by X-ray crystallographers. Both are described below, together with a proof of their equivalence.

BRAGG FORMULATION OF X-RAY DIFFRACTION BY A CRYSTAL

In 1913 W. H. and W. L. Bragg found that substances whose macroscopic forms were crystalline gave remarkably characteristic patterns of reflected X-radiation, quite unlike those produced by liquids. In crystalline materials, for certain sharply defined wavelengths and incident directions, intense peaks of scattered radiation (now known as Bragg peaks) were observed.

W. L. Bragg accounted for this by regarding a crystal as made out of parallel planes of ions, spaced a distance d apart (i.e., the lattice planes described in Chapter 5). The conditions for a sharp peak in the intensity of the scattered radiation were: (1) that the X rays should be specularly reflected[3] by the ions in any one plane and (2) that the reflected rays from successive planes should interfere constructively. Rays specularly reflected from adjoining planes are shown in Figure 6.1. The path difference between the two rays is just $2d \sin\theta$, where θ is the angle of incidence.[4] For the rays to interfere constructively, this path difference must be an integral number of wavelengths, leading to the celebrated Bragg condition:

$$n\lambda = 2d \sin\theta. \tag{6.2}$$

The integer n is known as the order of the corresponding reflection. For a beam of X rays containing a range of different wavelengths ("white radiation") many different reflections are observed. Not only can one have higher-order reflections from a given set of lattice planes, but in addition one must recognize that there are

[1] Actually the ions vibrate about their ideal equilibrium sites (Chapters 21–26). This does not affect the conclusions reached in this chapter (though in the early days of X-ray diffraction it was not clear why such vibrations did not obliterate the pattern characteristic of a periodic structure). It turns out that the vibrations have two main consequences (see Appendix N): (a) the intensity in the characteristic peaks that reveal the crystal structure is diminished, but not eliminated; and (b) a much weaker continuous background of radiation (the "diffuse background") is produced.

[2] Amorphous solids and liquids have about the same density as crystalline solids, and are therefore also susceptible to probing with X rays. However, the discrete, sharp peaks of scattered radiation characteristic of crystals are not found.

[3] In specular reflection the angle of incidence equals the angle of reflection.

[4] The angle of incidence in X-ray crystallography is conventionally measured from the plane of reflection rather than from the normal to that plane (as in classical optics). Note that θ is just half the angle of deflection of the incident beam (Figure 6.2).

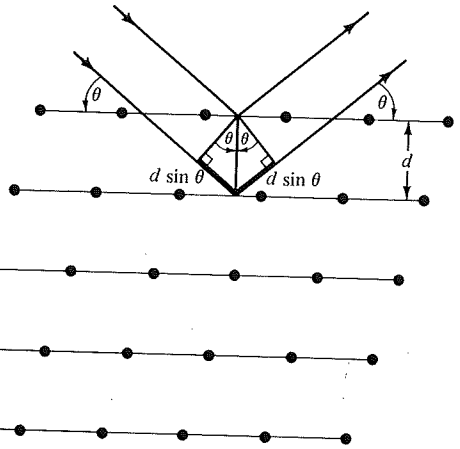

Figure 6.1
A Bragg reflection from a particular family of lattice planes, separated by a distance d. Incident and reflected rays are shown for the two neighboring planes. The path difference is $2d \sin \theta$.

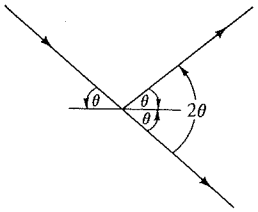

Figure 6.2
The Bragg angle θ is just half the total angle by which the incident beam is deflected.

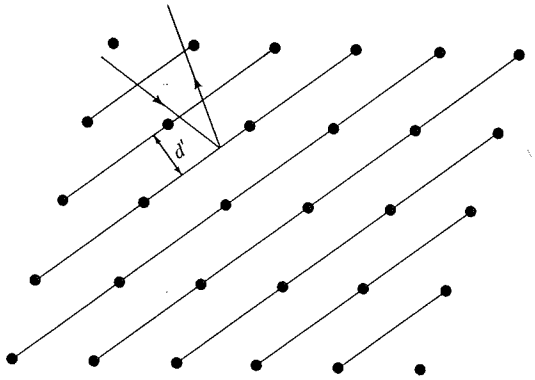

Figure 6.3
The same portion of Bravais lattice shown in Figure 6.1, with a different resolution into lattice planes indicated. The incident ray is the same as in Figure 6.1, but both the direction (shown in the figure) and wavelength (determined by the Bragg condition (6.2) with d replaced by d') of the reflected ray are different from the reflected ray in Figure 6.1. Reflections are possible, in general, for any of the infinitely many ways of resolving the lattice into planes.

many different ways of sectioning the crystal into planes, each of which will itself produce further reflections (see, for example, Figure 5.3 or Figure 6.3).

VON LAUE FORMULATION OF X-RAY DIFFRACTION BY A CRYSTAL

The von Laue approach differs from the Bragg approach in that no particular sectioning of the crystal into lattice planes is singled out, and no *ad hoc* assumption of specular reflection is imposed.[5] Instead one regards the crystal as composed of

[5] The Bragg assumption of specular reflection is, however, equivalent to the assumption that rays scattered from individual ions within each lattice plane interfere constructively. Thus both the Bragg and the von Laue approaches are based on the same physical assumptions, and their precise equivalence (see page 99) is to be expected.

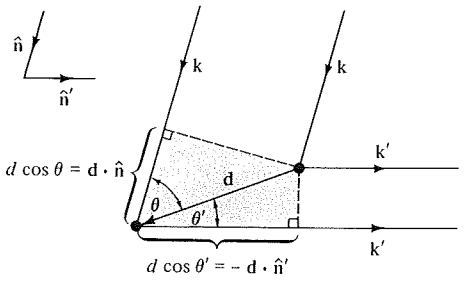

Figure 6.4
Illustrating that the path difference for rays scattered from two points separated by **d** is given by Eq. (6.3) or (6.4).

identical microscopic objects (sets of ions or atoms) placed at the sites **R** of a Bravais lattice, each of which can reradiate the incident radiation in all directions. Sharp peaks will be observed only in directions and at wavelengths for which the rays scattered from all lattice points interfere constructively.

To find the condition for constructive interference, consider first just two scatterers, separated by a displacement vector **d** (Figure 6.4). Let an X ray be incident from very far away, along a direction $\hat{\mathbf{n}}$, with wavelength λ, and wave vector $\mathbf{k} = 2\pi\hat{\mathbf{n}}/\lambda$. A scattered ray will be observed in a direction $\hat{\mathbf{n}}'$ with wavelength[6] λ and wave vector $\mathbf{k}' = 2\pi\hat{\mathbf{n}}'/\lambda$, provided that the path difference between the rays scattered by each of the two ions is an integral number of wavelengths. From Figure 6.4 it can be seen that this path difference is just

$$d\cos\theta + d\cos\theta' = \mathbf{d}\cdot(\hat{\mathbf{n}} - \hat{\mathbf{n}}'). \tag{6.3}$$

The condition for constructive interference is thus

$$\mathbf{d}\cdot(\hat{\mathbf{n}} - \hat{\mathbf{n}}') = m\lambda, \tag{6.4}$$

for integral m. Multiplying both sides of (6.4) by $2\pi/\lambda$ yields a condition on the incident and scattered wave vectors:

$$\mathbf{d}\cdot(\mathbf{k} - \mathbf{k}') = 2\pi m, \tag{6.5}$$

for integral m.

Next, we consider not just two scatterers, but an array of scatterers, at the sites of a Bravais lattice. Since the lattice sites are displaced from one another by the Bravais lattice vectors **R**, the condition that all scattered rays interfere constructively is that condition (6.5) hold simultaneously for all values of **d** that are Bravais lattice vectors:

$$\mathbf{R}\cdot(\mathbf{k} - \mathbf{k}') = 2\pi m, \quad \begin{array}{l}\text{for integral } m \text{ and}\\ \text{all Bravais lattice}\\ \text{vectors } \mathbf{R}.\end{array} \tag{6.6}$$

This can be written in the equivalent form

$$e^{i(\mathbf{k}'-\mathbf{k})\cdot\mathbf{R}} = 1, \quad \text{for all Bravais lattice vectors } \mathbf{R}. \tag{6.7}$$

---

[6] Here (and in the Bragg picture) we assume that the incident and scattered radiation has the same wavelength. In terms of photons this means that no energy has been lost in the scattering, i.e., that the scattering is elastic. To a good approximation the bulk of the scattered radiation *is* elastically scattered, though there is much to be learned from the study of that small component of the radiation that is inelastically scattered (Chapter 24 and Appendix N).

REC

Comparing this condition with the definition (5.2) of the reciprocal lattice, we arrive at the Laue condition that *constructive interference will occur provided that the change in wave vector,* $\mathbf{K} = \mathbf{k}' - \mathbf{k}$, *is a vector of the reciprocal lattice.*

It is sometimes convenient to have an alternative formulation of the Laue condition, stated entirely in terms of the incident wave vector $\mathbf{k}$. First note that because the reciprocal lattice is a Bravais lattice, if $\mathbf{k}' - \mathbf{k}$ is a reciprocal lattice vector, so is $\mathbf{k} - \mathbf{k}'$. Calling the latter vector $\mathbf{K}$, the condition that $\mathbf{k}$ and $\mathbf{k}'$ have the same magnitude is

$$k = |\mathbf{k} - \mathbf{K}|. \tag{6.8}$$

Squaring both sides of (6.8) yields the condition

$$\mathbf{k} \cdot \hat{\mathbf{K}} = \tfrac{1}{2}K; \tag{6.9}$$

i.e., the component of the incident wave vector $\mathbf{k}$ along the reciprocal lattice vector $\mathbf{K}$ must be half the length of $\mathbf{K}$.

Thus an incident wave vector $\mathbf{k}$ will satisfy the Laue condition if and only if the tip of the vector lies in a plane that is the perpendicular bisector of a line joining the origin of k-space to a reciprocal lattice point $\mathbf{K}$ (Figure 6.5). Such k-space planes are called *Bragg planes.*

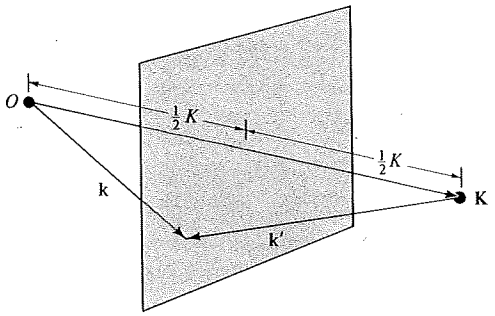

Figure 6.5
The Laue condition. If the sum of $\mathbf{k}$ and $-\mathbf{k}'$ is a vector $\mathbf{K}$, and if $\mathbf{k}$ and $\mathbf{k}'$ have the same length, then the tip of the vector $\mathbf{k}$ is equidistant from the origin O and the tip of the vector $\mathbf{K}$, and therefore it lies in the plane bisecting the line joining the origin to the tip of $\mathbf{K}$.

It is a consequence of the equivalence of the Bragg and von Laue points of view, demonstrated in the following section, that the k-space Bragg plane associated with a particular diffraction peak in the Laue formulation is parallel to the family of direct lattice planes responsible for the peak in the Bragg formulation.

EQUIVALENCE OF THE BRAGG AND VON LAUE FORMULATIONS

The equivalence of these two criteria for constructive interference of X rays by a crystal follows from the relation between vectors of the reciprocal lattice and families of direct lattice planes (see Chapter 5). Suppose the incident and scattered wave vectors, $\mathbf{k}$ and $\mathbf{k}'$, satisfy the Laue condition that $\mathbf{K} = \mathbf{k}' - \mathbf{k}$ be a reciprocal lattice vector. Because the incident and scattered waves have the same wavelength,[6] $\mathbf{k}'$ and $\mathbf{k}$ have the same magnitudes. It follows (see Figure 6.6) that $\mathbf{k}'$ and $\mathbf{k}$ make the same angle θ with the plane perpendicular to $\mathbf{K}$. Therefore the scattering can be viewed as a Bragg reflection, with Bragg angle θ, from the family of direct lattice planes perpendicular to the reciprocal lattice vector $\mathbf{K}$.

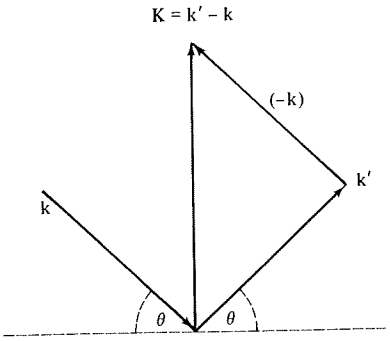

Figure 6.6
The plane of the paper contains the incident wave vector **k**, the reflected wave vector **k′**, and their difference **K** satisfying the Laue condition. Since the scattering is elastic ($k' = k$), the direction of **K** bisects the angle between **k** and **k′**. The dashed line is the intersection of the plane perpendicular to **K** with the plane of the paper.

To demonstrate that this reflection satisfies the Bragg condition (6.2), note that the vector **K** is an integral multiple[7] of the shortest reciprocal lattice vector $\mathbf{K}_0$ parallel to **K**. According to the theorem on page 90, the magnitude of $\mathbf{K}_0$ is just $2\pi/d$, where d is the distance between successive planes in the family perpendicular to $\mathbf{K}_0$ or to **K**. Thus

$$K = \frac{2\pi n}{d}. \tag{6.10}$$

On the other hand, it follows from Figure 6.6 that $K = 2k \sin\theta$, and thus

$$k \sin\theta = \frac{\pi n}{d}. \tag{6.11}$$

Since $k = 2\pi/\lambda$, Eq. (6.11) implies that the wavelength satisfies the Bragg condition (6.2).

Thus *a Laue diffraction peak corresponding to a change in wave vector given by the reciprocal lattice vector* **K** *corresponds to a Bragg reflection from the family of direct lattice planes perpendicular to* **K**. *The order, n, of the Bragg reflection is just the length of* **K** *divided by the length of the shortest reciprocal lattice vector parallel to* **K**.

Since the reciprocal lattice associated with a given Bravais lattice is far more easily visualized than the set of all possible planes into which the Bravais lattice can be resolved, the Laue condition for diffraction peaks is far more simple to work with than the Bragg condition. In the rest of this chapter we shall apply the Laue condition to a description of three of the most important ways in which X-ray crystallographic analyses of real samples are performed, and to a discussion of how one can extract information not only about the underlying Bravais lattice, but also about the arrangement of ions within the primitive cell.

EXPERIMENTAL GEOMETRIES SUGGESTED BY THE LAUE CONDITION

An incident wave vector **k** will lead to a diffraction peak (or "Bragg reflection") if and only if the tip of the wave vector lies on a k-space Bragg plane. Since the set of all

[7] This is an elementary consequence of the fact that the reciprocal lattice is a Bravais lattice. See Chapter 5, Problem 4.

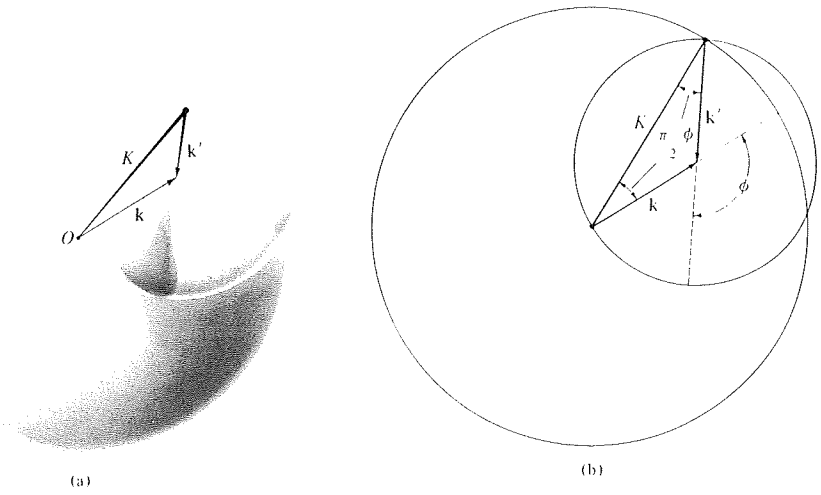

Figure 6.10
The Ewald construction for the powder method. (a) The Ewald sphere is the smaller sphere. It is centered on the tip of the incident wave vector $\mathbf{k}$ with radius k, so that the origin O is on its surface. The larger sphere is centered on the origin and has a radius K. The two spheres intersect in a circle (foreshortened to an ellipse). Bragg reflections will occur for any wave vector $\mathbf{k}'$ connecting any point on the circle of intersection to the tip of the vector $\mathbf{k}$. The scattered rays therefore lie on the cone that opens in the direction opposite to $\mathbf{k}$. (b) A plane section of (a), containing the incident wave vector. The triangle is isosceles, and thus $K = 2k \sin \frac{1}{2}\phi$.

By measuring the angles ϕ at which Bragg reflections are observed, one therefore learns the lengths of all reciprocal lattice vectors shorter than $2k$. Armed with this information, some facts about the macroscopic crystal symmetry, and the fact that the reciprocal lattice is a Bravais lattice, one can usually construct the reciprocal lattice itself (see, for example, Problem 1).

DIFFRACTION BY A MONATOMIC LATTICE WITH A BASIS; THE GEOMETRICAL STRUCTURE FACTOR

The preceding discussion was based on the condition (6.7) that rays scattered from each primitive cell should interfere constructively. If the crystal structure is that of a monatomic lattice with an n-atom basis (for example, carbon in the diamond structure or hexagonal close-packed beryllium, both of which have $n = 2$), then the contents of each primitive cell can be further analyzed into a set of identical scatterers at positions $\mathbf{d}_1, \ldots, \mathbf{d}_n$ within the cell. The intensity of radiation in a given Bragg peak will depend on the extent to which the rays scattered from these basis sites interfere with one another, being greatest when there is complete constructive interference and vanishing altogether should there happen to be complete destructive interference.

If the Bragg peak is associated with a change in wave vector $\mathbf{k}' - \mathbf{k} = \mathbf{K}$, then the path difference (Figure 6.4) between the rays scattered at $\mathbf{d}_i$ and $\mathbf{d}_j$ will be $\mathbf{K} \cdot (\mathbf{d}_i - \mathbf{d}_j)$ and the phases of the two rays will differ by a factor $e^{i\mathbf{K} \cdot (\mathbf{d}_i - \mathbf{d}_j)}$. Thus the phases of the rays scattered at $\mathbf{d}_1, \ldots, \mathbf{d}_n$ are in the ratios $e^{i\mathbf{K} \cdot \mathbf{d}_1}, \ldots, e^{i\mathbf{K} \cdot \mathbf{d}_n}$. The net ray scattered by

the entire primitive cell is the sum of the individual rays, and will therefore have an amplitude containing the factor

$$S_{\mathbf{K}} = \sum_{j=1}^{n} e^{i\mathbf{K}\cdot\mathbf{d}_j}. \tag{6.13}$$

The quantity $S_{\mathbf{K}}$, known as the *geometrical structure factor*, expresses the extent to which interference of the waves scattered from identical ions within the basis can diminish the intensity of the Bragg peak associated with the reciprocal lattice vector $\mathbf{K}$. The intensity in the Bragg peak, being proportional to the square of the absolute value of the amplitude, will contain a factor $|S_{\mathbf{K}}|^2$. It is important to note that this is not the only source of $\mathbf{K}$ dependence to the intensity. Further dependence on the change in wave vector comes both from the ordinary angular dependence of any electromagnetic scattering, together with the influence on the scattering of the detailed internal structure of each individual ion in the basis. Therefore the structure factor alone cannot be used to predict the absolute intensity in a Bragg peak.[8] It can, however, lead to a characteristic dependence on $\mathbf{K}$ that is easily discerned even though other less distinctive $\mathbf{K}$ dependences have been superimposed upon it. The one case, in which the structure factor can be used with assurance is when it vanishes. This occurs when the elements of the basis are so arranged that there is complete destructive interference for the $\mathbf{K}$ in question; in that case no features of the rays scattered by the individual basis elements can prevent the net ray from vanishing.

We illustrate the importance of a vanishing structure factor in two cases[9]:

1. ***Body-Centered Cubic Considered as Simple Cubic with a Basis*** Since the body-centered cubic lattice is a Bravais lattice, we know that Bragg reflections will occur when the change in wave vector $\mathbf{K}$ is a vector of the reciprocal lattice, which is face-centered cubic. Sometimes, however, it is convenient to regard the bcc lattice as a simple cubic lattice generated by primitive vectors $a\hat{\mathbf{x}}$, $a\hat{\mathbf{y}}$, and $a\hat{\mathbf{z}}$, with a two-point basis consisting of $\mathbf{d}_1 = \mathbf{0}$ and $\mathbf{d}_2 = (a/2)(\hat{\mathbf{x}} + \hat{\mathbf{y}} + \hat{\mathbf{z}})$. From this point of view the reciprocal lattice is also simple cubic, with a cubic cell of side $2\pi/a$. However, there will now be a structure factor $S_{\mathbf{K}}$ associated with each Bragg reflection. In the present case, (6.13) gives

$$S_{\mathbf{K}} = 1 + \exp\left[i\mathbf{K}\cdot\tfrac{1}{2}a(\hat{\mathbf{x}} + \hat{\mathbf{y}} + \hat{\mathbf{z}})\right]. \tag{6.14}$$

A general vector in the simple cubic reciprocal lattice has the form

$$\mathbf{K} = \frac{2\pi}{a}(n_1\hat{\mathbf{x}} + n_2\hat{\mathbf{y}} + n_3\hat{\mathbf{z}}). \tag{6.15}$$

Substituting this into (6.14), we find a structure factor

$$S_{\mathbf{K}} = 1 + e^{i\pi(n_1+n_2+n_3)} = 1 + (-1)^{n_1+n_2+n_3}$$
$$= \begin{cases} 2, & n_1 + n_2 + n_3 \quad \text{even}, \\ 0, & n_1 + n_2 + n_3 \quad \text{odd}. \end{cases} \tag{6.16}$$

---

[8] A brief but thorough discussion of the scattering of electromagnetic radiation by crystals, including the derivation of detailed intensity formulas for the various experimental geometries described above, is given by Landau and Lifshitz, *Electrodynamics of Continuous Media*, Chapter 15, Addison-Wesley, Reading, Mass., 1966.

[9] Further examples are given in Problems 2 and 3.

Thus those points in the simple cubic reciprocal lattice, the sum of whose coordinates with respect to the cubic primitive vectors are odd, will actually have no Bragg reflection associated with them. This converts the simple cubic reciprocal lattice into the face-centered cubic structure that we would have had if we had treated the body-centered cubic direct lattice as a Bravais lattice rather than as a lattice with a basis (see Figure 6.11).

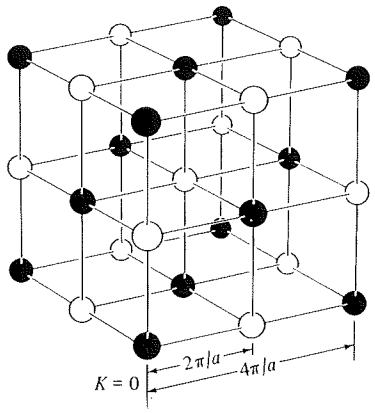

Figure 6.11
Points in the simple cubic reciprocal lattice of side $2\pi/a$, for which the structure factor (6.16) vanishes, are those (white circles) that can be reached from the origin by moving along an odd number of nearest-neighbor bonds. When such sites are eliminated, the remaining sites (black circles) constitute a face-centered cubic lattice with cubic cell of side $4\pi/a$.

Thus if, either inadvertently or for reasons of greater symmetry in description, one chooses to describe a Bravais lattice as a lattice with a basis, one still recovers the correct description of X-ray diffraction, provided that the vanishing of the structure factor is taken into account.

2. ***Monatomic Diamond Lattice*** The monatomic diamond lattice (carbon, silicon, germanium, or grey tin) is not a Bravais lattice and must be described as a lattice with a basis. The underlying Bravais lattice is face-centered cubic, and the basis can be taken to be $\mathbf{d}_1 = \mathbf{0}$, $\mathbf{d}_2 = (a/4)(\hat{\mathbf{x}} + \hat{\mathbf{y}} + \hat{\mathbf{z}})$, where $\hat{\mathbf{x}}$, $\hat{\mathbf{y}}$, and $\hat{\mathbf{z}}$, are along the cubic axes and a is the side of the conventional cubic cell. The reciprocal lattice is body-centered cubic with conventional cubic cell of side $4\pi/a$. If we take as primitive vectors

$$\mathbf{b}_1 = \frac{2\pi}{a}(\hat{\mathbf{y}} + \hat{\mathbf{z}} - \hat{\mathbf{x}}), \quad \mathbf{b}_2 = \frac{2\pi}{a}(\hat{\mathbf{z}} + \hat{\mathbf{x}} - \hat{\mathbf{y}}), \quad \mathbf{b}_3 = \frac{2\pi}{a}(\hat{\mathbf{x}} + \hat{\mathbf{y}} - \hat{\mathbf{z}}), \tag{6.17}$$

then the structure factor (6.13) for $\mathbf{K} = \Sigma n_i \mathbf{b}_i$ is

$$\begin{aligned} S_{\mathbf{K}} &= 1 + \exp\left[\tfrac{1}{2}i\pi(n_1 + n_2 + n_3)\right] \\ &= \begin{cases} 2, & n_1 + n_2 + n_3 \text{ twice an even number}, \\ 1 \pm i, & n_1 + n_2 + n_3 \text{ odd}, \\ 0, & n_1 + n_2 + n_3 \text{ twice an odd number}. \end{cases} \end{aligned} \tag{6.18}$$

To interpret these conditions on Σn_i geometrically, note that if we substitute (6.17) into $\mathbf{K} = \Sigma n_i \mathbf{b}_i$, we can write the general reciprocal lattice vector in the form

$$\mathbf{K} = \frac{4\pi}{a}(\nu_1\hat{\mathbf{x}} + \nu_2\hat{\mathbf{y}} + \nu_3\hat{\mathbf{z}}), \tag{6.19}$$

where

$$v_j = \tfrac{1}{2}(n_1 + n_2 + n_3) - n_j, \quad \sum_{j=1}^{3} v_j = \tfrac{1}{2}(n_1 + n_2 + n_3). \tag{6.20}$$

We know (see Chapter 5) that the reciprocal to the fcc lattice with cubic cell of side a is a bcc lattice with cubic cell of side $4\pi/a$. Let us regard this as composed of two simple cubic lattices of side $4\pi/a$. The first, containing the origin ($\mathbf{K} = 0$), must have all v_i integers (according to (6.19)) and must therefore be given by $\mathbf{K}$ with $n_1 + n_2 + n_3$ even (according to (6.20)). The second, containing the "body-centered point" $(4\pi/a)\frac{1}{2}(\hat{\mathbf{x}} + \hat{\mathbf{y}} + \hat{\mathbf{z}})$, must have all v_i integers $+ \frac{1}{2}$ (according to (6.19)) and must therefore be given by $\mathbf{K}$ with $n_1 + n_2 + n_3$ odd (according to (6.20)).

Comparing this with (6.18), we find that the points with structure factor $1 \pm i$ are those in the simple cubic sublattice of "body-centered" points. Those whose structure factor S is 2 or 0 are in the simple cubic sublattice containing the origin, where Σv_i is even when $S = 2$ and odd when $S = 0$. Thus the points with zero structure factor are again removed by applying the construction illustrated in Figure 6.11 to the simple cubic sublattice containing the origin, converting it to a face-centered cubic structure (Figure 6.12).

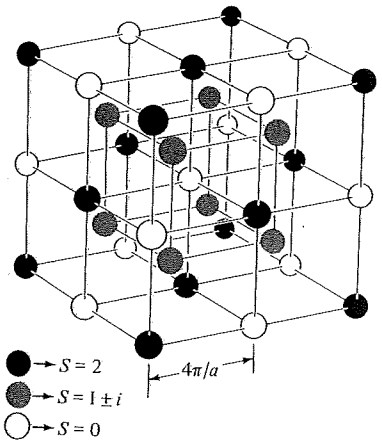

Figure 6.12
The body-centered cubic lattice with cubic cell side $4\pi/a$ that is reciprocal to a face-centered cubic lattice with cubic cell side a. When the fcc lattice is that underlying the diamond structure, then the white circles indicate sites with zero structure factor. (The black circles are sites with structure factor 2, and the gray ones are sites with structure factor $1 \pm i$.)

DIFFRACTION BY A POLYATOMIC CRYSTAL; THE ATOMIC FORM FACTOR

If the ions in the basis are not identical, the structure factor (6.13) assumes the form

$$S_{\mathbf{K}} = \sum_{j=1}^{n} f_j(\mathbf{K}) e^{i\mathbf{K}\cdot\mathbf{d}_j}, \tag{6.21}$$

where f_j, known as the *atomic form factor*, is entirely determined by the internal structure of the ion that occupies position $\mathbf{d}_j$ in the basis. Identical ions have identical form factors (regardless of where they are placed), so (6.21) reduces back to (6.13), multiplied by the common value of the form factors, in the monatomic case.

In elementary treatments the atomic form factor associated with a Bragg reflection

given by the reciprocal lattice vector $\mathbf{K}$ is taken to be proportional to the Fourier transform of the electronic charge distribution of the corresponding ion[10]:

$$f_j(\mathbf{K}) = -\frac{1}{e}\int d\mathbf{r}\, e^{i\mathbf{K}\cdot\mathbf{r}}\,\rho_j(\mathbf{r}). \tag{6.22}$$

Thus the atomic form factor f_j depends on $\mathbf{K}$ and on the detailed features of the charge distribution of the ion that occupies position $\mathbf{d}_j$ in the basis. As a result, one would not expect the structure factor to vanish for any $\mathbf{K}$ unless there is some fortuitous relation between form factors of different types. By making reasonable assumptions about the $\mathbf{K}$ dependence of the different form factors, one can often distinguish quite conclusively between various possible crystal structures on the basis of the variation with $\mathbf{K}$ of the Bragg peak intensities (see, for example, Problem 5).

This concludes our discussion of the Bragg reflection of X rays. Our analysis has exploited no properties of the X rays other than their wave nature.[11] Consequently we shall find many of the concepts and results of this chapter reappearing in subsequent discussions of other wave phenomena in solids, such as electrons (Chapter 9) and neutrons (Chapter 24).[12]

PROBLEMS

1. Powder specimens of three different monatomic cubic crystals are analyzed with a Debye-Scherrer camera. It is known that one sample is face-centered cubic, one is body-centered cubic, and one has the diamond structure. The approximate positions of the first four diffraction rings in each case are (see Figure 6.13):

VALUES OF ϕ FOR SAMPLES

A	B	C
42.2°	28.8°	42.8°
49.2	41.0	73.2
72.0	50.8	89.0
87.3	59.6	115.0

(a) Identify the crystal structures of A, B, and C.

(b) If the wavelength of the incident X-ray beam is 1.5 Å, what is the length of the side of the conventional cubic cell in each case?

(c) If the diamond structure were replaced by a zincblende structure with a cubic unit cell of the same side, at what angles would the first four rings now occur?

---

[10] The electronic charge density $\rho_j(\mathbf{r})$ is that of an ion of type j placed at $\mathbf{r} = \mathbf{0}$; thus the contribution of the ion at $\mathbf{R} + \mathbf{d}_j$ to the electronic charge density of the crystal is $\rho_j(\mathbf{r} - [\mathbf{R} + \mathbf{d}_j])$. (The electronic charge is usually factored out of the atomic form factor to make it dimensionless.)

[11] As a result we have been unable to make precise statements about the absolute intensity of the Bragg peaks, or about the diffuse background of radiation in directions not allowed by the Bragg condition.

[12] Considered quantum mechanically, a particle of momentum p can be viewed as a wave of wavelength $\lambda = h/p$.